

The Cortical and Subcortical Controls of Postural Instability in People with Parkinson's Disease

by  
Jessica Bath

DISSERTATION  
Submitted in partial satisfaction of the requirements for degree of  
DOCTOR OF PHILOSOPHY

in

Rehabilitation Science

in the

GRADUATE DIVISION  
of the  
UNIVERSITY OF CALIFORNIA, SAN FRANCISCO

Approved:

DocuSigned by:

*Erica Pitsch*

Erica Pitsch

E208A49AC4BB4AA...

Chair

DocuSigned by:

*Simon Little*

Simon Little

DocuSigned by:

*Martina Mancini*

Martina Mancini

7B623DCB55F649C...

Committee Members



A huge thank you to my mom, dad, sister, and husband Andy, as well as Mia, the best running buddy and dog ever, and my extended family and friends. Thank you for allowing me to pursue my interests and figure the rest out later; I am so appreciative of your support.

To my fellow members of the Wang Lab (especially esteemed postdoc. Dr. Kenneth Louie) and Dr. Doris Wang, my PI, thank you for teaching me and believing in me. You are all brilliant and I am truly lucky to have worked with and learned from each of you.

To Papa: You fought this disease with courage, stubbornness, and humor. I wish we could have discussed all of this but thank you for always teaching me the importance of education and work ethic.

And, to our patients: Thank you for trusting me and our lab over the course of the study and allowing us to learn from you. This dissertation would not have existed without you.

## Contributions:

1. Bath JE, Wang DD. Unraveling the threads of stability: A review of the neurophysiology of postural control in Parkinson's disease. *Neurotherapeutics*. 2024 Apr;21(3):e00354. doi: 10.1016/j.neurot.2024.e00354. Epub 2024 Apr 4. PMID: 38579454; PMCID: PMC11000188.

The text of this dissertation is a reprint of the material as it appears in *Neurotherapeutics*. The co-author listed in this publication directed and supervised the research that forms the basis for the dissertation.

This article was published in *Neurotherapeutics*, Vol. 21, Issue 3, Bath, JE, Wang, DD, Unraveling the threads of stability: A review of the neurophysiology of postural control in Parkinson's disease, e00354, Copyright Elsevier (2024).

# The Cortical and Subcortical Controls of Postural Instability in People with Parkinson's Disease

Jessica Bath

## Abstract

**Statement of the problem:** Gait initiation and turning are fundamental human motor tasks requiring adept postural control. People with Parkinson's Disease (PD) often exhibit postural control dysfunction during these tasks, which can be quantified using biomechanical tools. A very limited amount of research has characterized these data with the neural circuits underlying postural control in PD. In fact, it is normally not possible to record from the deep structures of the brain while performing motor tasks in humans. However, developments in deep brain stimulation (DBS) now allows the recording of local field potentials from different areas in the brain while performing motor tasks. Further research is needed to decipher the relationships between the circuitry of postural control involved in balance tasks, levodopa's effects, and metrics of task quality because current interventions do not offer a complete resolution for postural instability in PD. This dissertation is the first body of work combine neurophysiological and biomechanical data during gait initiation and turning under varied levodopa medication states to begin to understand these phenomena for implementing effective therapies for these symptoms.

**Methods and procedures:** Five individuals with PD exhibiting gait and balance issues were implanted with an investigational bidirectional neural interface (Summit RC+S, Medtronic Inc) connected to deep brain stimulation (DBS) electrodes at the globus pallidus and cortical paddle electrodes overlying the premotor and primary motor cortices.

Subjects performed multiple gait initiation trials and 180-degree turns under “ON” and “LOW” levodopa states utilizing force plates or body worn sensors for quantifying postural control abilities. The tasks were broken into epochs to examine neural modulation across the task under differing postural control demands, as well as inputted into linear mixed models (gait initiation) or multiple linear regressions (turns) for understanding the respective influences of brain region, medication state, epoch neural data across canonical frequencies, and their relationships to postural control task metrics.

**Summary of findings:** Much individual variation was observed among subject responses to levodopa for both dynamic neural modulation across the task and balance task quality metrics. Neural modulation across the task did not produce consistent effects on the observed task metrics. These results support theories regarding the diversity of the neural circuits underlying different balance components (i.e. they are not dopaminergic-exclusive) and PD’s variable effects. In gait initiation, low frequency power generally decreased globally in a stepwise fashion across the task from quiet standing to weight shift to stepping, where the opposite pattern was seen at higher, pro-kinetic frequencies. Coherence was also dynamically modulated across the task, with significance exhibited in influencing weight shift amplitudes and timing. Turn results were similar, with pronounced modulation between turn preparation and turn itself variably shared among subjects at beta and gamma frequencies among pallidal and cortical locations. These results offer a preliminary framework and methodology for characterizing balance in this population, suggesting its potential application in the future using adaptive and individualized neuromodulatory interventions.

# Table of Contents

<b>Chapter 1. Introduction .....</b>	<b>1</b>
<b>Chapter 2. General Methods .....</b>	<b>19</b>
<b>Chapter 3. Gait initiation (Aim 1) .....</b>	<b>25</b>
<b>Chapter 4. 180-degree turns (Aim 2) .....</b>	<b>70</b>
<b>Chapter 5. Discussion .....</b>	<b>98</b>
<b>References .....</b>	<b>102</b>

## List of Figures

Figure 1.1: Balance domains and Parkinson's effects.....	2
Figure 1.2: Conceptualization of the circuits underlying APA and gait initiation ...	7
Figure 2.2: Aggregated subject lead and ECoG visualization .....	21
Figure 3.1: Gait initiation task epochs and APA metrics .....	29
Figure 3.2: Sample analysis for a gait initiation trial .....	32-33
Figure 3.3: Dynamic power modulation at GPe and M1 during gait initiation ..	39-40
Figure 3.4: Coherence modulation across GPi and M1 during gait initiation .....	45
Figure 3.5: Coherence modulation across GPe and M1 during gait initiation .....	46
Figure 3.6: Subject #2 power modulation across the task .....	58
Figure 3.7: Subject #4 power modulation across the task .....	59
Figure 3.8: Subject #1 power modulation across the task .....	60
Figure 3.9: Subject #3 power modulation across the task .....	61
Figure 3.10: Subject #5 power modulation across the task .....	62
Figure 3.11: Coherence modulation across GPi and PMC during gait initiation ...	63
Figure 3.12: Coherence modulation across GPe and PMC during gait initiation ..	64
Figure 3.13: Coherence modulation across M1 and PMC during gait initiation ...	65
Figure 4.1: Example turn marking schematic using body worn sensors.....	74
Figure 4.2: Subject #1 turn types and power modulation.....	85



<b>Figure 4.3: Subject #2 turn types and power modulation .....</b>	<b>86</b>
<b>Figure 4.4: Subject #3 turn types and power modulation .....</b>	<b>88</b>
<b>Figure 4.5: Subject #4 turn types and power modulation .....</b>	<b>90</b>
<b>Figure 4.6: Subject #5 turn types and power modulation .....</b>	<b>92</b>

## List of Tables

<b>Table 2.1: Baseline subject demographics and motor function.....</b>	<b>20</b>
<b>Table 3.1: Summary of gait initiation trials and APA metrics.....</b>	<b>36</b>
<b>Table 3.2: Summary of significant group power modulation across task.....</b>	<b>41</b>
<b>Table 3.3: Linear mixed model results for APA metrics from “total APA” epoch .</b>	<b>48</b>
<b>Table 3.4: Cumulative APA linear mixed model summary results .....</b>	<b>66</b>
<b>Table 3.5: Peak APA amplitude linear mixed model summary results .....</b>	<b>67</b>
<b>Table 3.6: Net APA amplitude linear mixed model summary results .....</b>	<b>68</b>
<b>Table 3.7: Time to peak APA amplitude linear mixed model summary results .....</b>	<b>69</b>
<b>Table 4.1 Summary of turn trials and turn metrics .....</b>	<b>78</b>
<b>Table 4.2 Subject #1 optimized model comparisons.....</b>	<b>86</b>
<b>Table 4.3 Subject #2 optimized model comparisons.....</b>	<b>87</b>
<b>Table 4.4 Subject #3 optimized model comparisons.....</b>	<b>89</b>
<b>Table 4.5 Subject #4 optimized model comparisons.....</b>	<b>91</b>
<b>Table 4.6 Subject #5 optimized model comparisons.....</b>	<b>93</b>

## List of Symbols

$\theta$ : Theta (4-8 Hertz) frequency band

$\alpha$ : Alpha (8-12 Hertz) frequency band

$\beta$ : Beta (13-30 Hertz) frequency band; analyzed in sub-bands with low  $\beta$  (13-20 Hertz) and high  $\beta$  (20-30 Hertz)

$\gamma$ : Gamma (30-200 Hertz) frequency band; analyzed within sub-bands; low  $\gamma$  (30-50 Hertz) and broadband  $\gamma$  (50-200 Hertz)

# Chapter 1. Introduction

## 1.1 Overview of postural instability in Parkinson's disease

Postural instability (PI) is a common and disabling motor symptom of Parkinson's disease (PD), associated with more severe disease progression and mortality<sup>1-5</sup>. This "cardinal symptom" has been shown to occur in 20% of people at disease onset, increasing to 90% after 15 years of disease<sup>3,5,6</sup>. While many definitions exist, it's generally thought that PI results from alterations in one's static posture and/or postural reflexes, creating abnormal difficulty when an individual's balance is challenged through static and dynamic environmental or task constraints<sup>5,7-11</sup>. These deficits are thought to be caused by the underlying pathophysiology of PD, which includes dopaminergic and cholinergic neuronal dysfunction, leading to deficits in cognitive function and sensory integration, grey matter atrophy and white matter abnormalities, and decreased connectivity at motor cortical and brainstem motor areas<sup>5,10,12-14</sup>. These deficits often are detrimental to one's quality of life, among other negative sequelae, largely due to increased fall risk, loss of autonomy, and fear of falling<sup>5,10</sup>. Despite the significance of these symptoms, existing interventions for PD-PI+ such as medication, deep brain stimulation (DBS), and gait-based rehabilitation do not usually produce wholly-effective or long-term improvements and can even worsen postural responses<sup>5,15-19</sup>. Due to its impact and prevalence, it is imperative that research begin to explore the underlying neurophysiology of postural instability to begin the development of effective therapeutics.

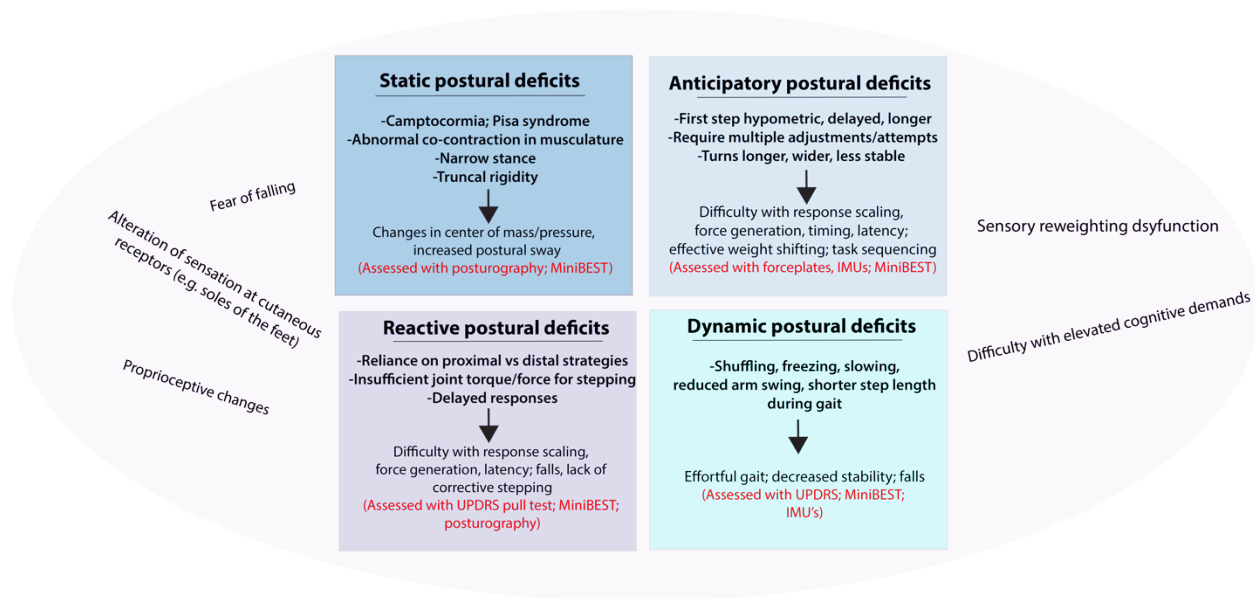


**Figure 1.1 Balance domains and Parkinson's effects**

Figure notes: The different blue boxes represent the domains of postural control: static, reactive, anticipatory, and dynamic (gait). The common findings for each in PD are in bold. Red text indicates common measurement tools in research or clinic. The phrases outside of the boxes are hypothesized or demonstrated findings stemming from the disease's pathophysiology or patient experience which underlie each domain and contribute to postural instability<sup>7-9,20-34</sup>. Abbreviations: IMU = inertial measurement unit, MiniBEST = Mini Balance Evaluation Systems Test, UPDRS = Unified Parkinson's Disease Rating scale (motor subscale, part III).

Balance is often considered to be comprised of static, reactive, and anticipatory domains, in addition to dynamic control throughout movement<sup>32</sup> (Figure 1.1). While PD is thought to affect each domain due to shared underlying basal ganglia-thalamocortical circuits, deficits in *anticipatory* postural control are often exhibited during postural transitions with rapid changes in sensory and motor demands and can result in festination (taking shortened, fast steps) and freezing of gait ("FoG")<sup>5,11,21,35</sup>. FoG is often defined as an episodic, sudden, and unplanned stoppage of walking or decreased forward progression despite the intention to walk, often leading to falls<sup>21</sup>.

One such postural transition occurs during gait initiation, when a person moves from static standing to dynamic locomotion. Successful gait initiation is thought to consist

of anticipatory postural adjustments (APAs), involving a sequence of muscle activations prior to the step when the body's center of mass (CoM) moves forward and over the stance foot while the center of pressure shifts to the stepping foot<sup>20,36</sup>. While APAs are generally thought to be stereotyped in healthy individuals, deviations in APA timing and amplitude are often found in patients with Parkinson's disease (PD)<sup>20,37</sup> and can be a hallmark of postural instability. Much robust biomechanical research utilizing forceplates and body-worn sensors has demonstrated APAs to be variable, prolonged, and hypometric in PD-PI+ individuals compared to healthy subjects, theorized to contribute to problems initiating walking and other negative sequelae including falls<sup>5,20,34,37-39</sup>.

Another prominent and often dysfunctional postural transition seen in people with PD occurs during turning. Performing successful turns while walking involves multiple, sequential APAs to rotate the body and alternate loading and unloading of the stepping limb to change direction<sup>40</sup>. Difficulty with turning is a common symptom and mobility challenge in people with PD, but quantifying kinematic and kinetic changes during APAs in this population while turning has been less explored. Data which currently exists using body-worn sensors has consistently reported turns in people with PD are more variable, less stable, and consist of more steps<sup>5,23,24,41</sup>.

Clinical tests utilizing these tasks are commonly used by neurologists and physical therapists to evaluate for the presence and severity of balance impairments in people with PD. Assessments of balance in PD include the Mini Balance Evaluation Systems Test (Mini-BEST), which tests multiple postural control domains including *anticipatory* (an APA proxy), and Part III of the Movement Disorder Society's (MDS) Unified Parkinson's Disease Rating Scale (UPDRS III)<sup>5,7,10,42</sup>. Scores on the MDS-UPDRS are often used to

classify PD symptoms into motor subtypes, including one called “Postural Instability (and) Gait Difficulty-predominant” disease (PIGD)<sup>5,43</sup>. While the purpose of clustering motor subtypes was to streamline treatment approaches, identifying reliable classifications and effective treatments tailored towards PIGD symptoms remain elusive<sup>5,44</sup>.

## **1.2 The neural substrates underlying postural control**

The cortical-basal ganglia neural activities underlying postural control are complex and not widely understood. Despite theories that dysfunctional APAs are linked to postural instability in people with PD, little research has identified potential neural regions and/or circuits which may be altered in these patients. Much research conceptualizing the neural circuitry of postural control has been done in cats and monkeys due to methodological constraints, despite these species not being bipedal, suggesting unknown transferability to humans. This body of work has offered popular hypotheses, however, suggesting that PD-associated balance impairments stem from increased inhibition from the diseased basal ganglia on various functional centers of gait and posture, rendering the impacts of PD far-reaching and complex<sup>45,46</sup>.

Inferring from these animal studies, gross human postural control is thought to be governed by dopaminergic and non-dopaminergic circuits spanning cortical and subcortical areas with various sensory inputs<sup>5</sup>. A recent review<sup>46</sup> provides an in-depth overview of prevalent theories related to the neural controls of APAs and gait initiation (Figure 1.2). Broadly, sensory input regarding the environment (e.g. proprioceptive, vestibular, and visual inputs) prior to stepping are sent to the supplementary motor area (SMA) and premotor cortex (PMC) for production of a motor program for APA and/or

stepping<sup>5,45,46</sup>. This program is then sent to the basal ganglia, where tonic inhibition is dampened, sending the signal on to downstream targets including the brainstem locomotor centers and reticulospinal tracts<sup>45,46</sup>. For precise stepping, the additional recruitment of primary motor cortex (M1) is presumed to facilitate the selection and execution of a stepping program following the release of basal ganglia inhibition and transmission to downstream corticospinal tracts in the lower extremities<sup>46</sup>. The basal ganglia, particularly relevant to PD, is also thought to serve important roles in postural control besides motor refinement and execution, including somatosensory integration, automatic postural responses, and muscle tone maintenance<sup>5,47</sup>.

While this general schema is thought to be shared among other fundamental human motor tasks such as gait, additional circuits are implicated in postural control<sup>5</sup>. One critical element is the maintenance of appropriate muscle tension and length (“muscle tone”) throughout the body, largely driven by spinal reflexes using inputs from receptors in the soft tissues and joints<sup>5,48,49</sup>. These spinal reflexes also receive input from supraspinal regions including the motor cortical areas, cerebellum, reticular formation, and vestibular nuclei, which contribute to the descending reticulospinal and vestibulospinal tracts in the spinal cord<sup>5,45,46,49</sup>. Prevailing theories suggest that the postural control domains discussed in this review result from dynamic combinations of reflexes, multisensory integration and reweighting, and changes in one’s internal schema of body posture, which are driven by different underlying neuronal populations<sup>5,45,46,48,50</sup>. It is also hypothesized that various postural responses are mediated by different neural circuits, which are automatically selected by factors such as the magnitude and predictability of a perturbation, latency allowed, and/or one’s own capabilities<sup>5,50,51</sup>.



The neuronal circuits underlying these processes are also thought to be diverse and interrelated, which further complicates the study and treatment of postural control impairments<sup>5</sup>. In PD, the loss of dopaminergic neurons in the substantia nigra pars compacta (SNpc) alters their efferent striatal neuronal activities and their subsequent downstream targets in the basal ganglia thalamocortical circuit, which likely results in the characteristic motor symptoms<sup>5,45-47</sup>. Additionally, the basal ganglia have additional downstream GABAergic connections with the thalamus, brainstem, SMA and PMC, as well as the pedunculo pontine nucleus (PPN)<sup>5</sup>. The PPN, in turn, sends cholinergic projections onto the SNpc, with various cholinergic and non-cholinergic synapses at the cortex, thalamus, basal ganglia, cerebellum, and spinal cord locomotive network<sup>5,45-47</sup>. Thus, it is likely that dysfunction among these overlapping circuits contributes to the various postural control deficits seen in PD and complexity of treatment intervention<sup>5</sup>.

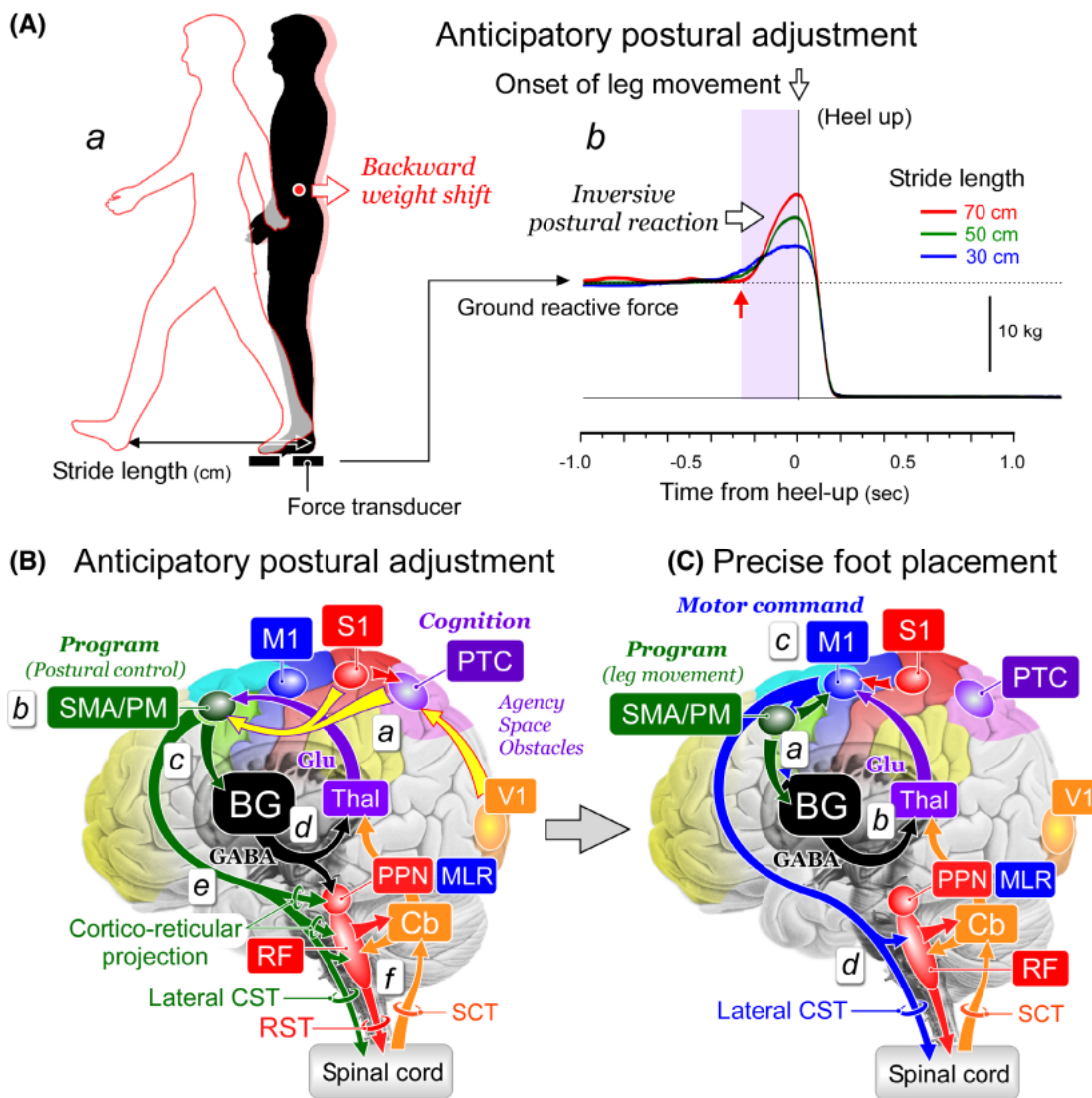


**Figure 1.2 Conceptualization of the circuits underlying APA and gait initiation**

Figure footnotes: Image displaying APA and gait initiation used from Takakusaki et al.<sup>46</sup>: (<https://onlinelibrary.wiley.com/doi/full/10.1111/ncn3.12683>). This work is licensed under the Creative Commons Attribution-Noncommercial-NoDerivs License (<https://creativecommons.org/licenses/by-nc-nd/4.0/>); no modifications were made. PM = premotor cortex, SMA = supplementary motor area, M1 = primary motor cortex, S1 = primary somatosensory cortex, BG = basal ganglia, MLR = mesencephalic locomotor region, Thal = thalamus, RF = reticular formation.

### 1.3 Cortical neurophysiology of postural control in Parkinson's disease

Cortical involvement of human postural control has been predominantly studied using non-invasive electroencephalogram (EEG) recordings and motor tasks eliciting postural responses<sup>5</sup>. Cortical power across multiple frequency bands: delta (1-3 Hz), theta (4-8 Hz), alpha (8-13 Hz), beta (13-30 Hz), and gamma (30-50 Hz), have been shown to exhibit much modulation during bipedal postural responses<sup>5</sup>. EEG data recorded during *static* balancing on foam, theorized to decrease one's ability to use proprioceptive and vestibular input for maintaining balance<sup>52</sup>, reflected much lower theta ( $\theta$ ) power at mid-frontal and cerebellar locations in people with PD exhibiting PI (PD-PI+), compared to those without PI (PD-PI-) and healthy controls<sup>5,53</sup>. Additionally, people with PD were found to have increased postural sway and widespread cortical power differences among alpha ( $\alpha$ ) and beta ( $\beta$ ) bands during a *static*, semi-tandem balance task (decreasing the base of support to increase task difficulty) while "ON" levodopa medication compared to "OFF" periods<sup>5,54</sup>.

In another study comparing EEG changes during *anticipatory* postural responses between healthy young adults and people with PD, movement-related potentials (MRPs) at the central cortical area differed between the two groups for early slope and peak amplitude metrics; furthermore, early slope of the MRP was found to be inversely related to stride length in the PD-PI- sub-group<sup>5,55</sup>. Thus, it was suggested stride length during gait initiation may be coded early in MRPs, with this phase disrupted in PD-PI+ individuals<sup>5,55</sup>.

Another study characterizing EEG activity during gait over planned and unplanned obstacles (requiring both *anticipatory* and *reactive* postural responses, respectively),

found that people with PD “ON” medication exhibited altered  $\theta$  and  $\beta$  cortical modulation compared to age-matched control subjects during multiple phases of the task<sup>5,56</sup>. During the pre-stepping phase,  $\theta$  power was observed to be attenuated in people with PD for steps over unplanned obstacles (*reactive* responses); this contrasted with  $\beta$  power, which remained higher-than-expected in people with PD under both types of obstacles<sup>5,56</sup>. Within the post-stepping phase, the authors also observed a lower-than-expected  $\theta$  and  $\beta$  “rebound” in people with PD during both obstacle types<sup>5,56</sup>. These findings suggest that people with PD may experience dysfunctional cortical modulation, which likely mediates impairments in cognitive-motor control and resulting *anticipatory* and *reactive* postural response deficits<sup>5,56</sup>.

Also examining *reactive* postural responses, a study found that people with PD were shown to display similar architecture of the elicited N1 potential while “OFF” medication during unexpected perturbations compared to healthy older adults, however its correlations with various balance metrics and individuals’ abilities differed<sup>5,57</sup>. In PD, earlier and narrower N1 peak widths correlated with more severe PIGD scores and lower balance abilities and confidence<sup>5,57</sup>. While these findings suggest a potential link between cortical activity and falls in PD, more investigation is warranted to characterize the presumably overlapping domains of cognitive function and balance ability, as well as the effects of dopamine medication and patients’ perceptions of falling and balance ability during such tasks<sup>5,57</sup>.

In summary, PD+PI individuals have been shown to exhibit altered modulation among  $\theta$ ,  $\alpha$ , and  $\beta$  frequencies compared to healthy subjects during *static*, *anticipatory*, and *reactive* postural tasks<sup>5</sup>. This highlights the importance of widespread cortical

network activity in regulating postural control<sup>5</sup> and suggests that postural control is governed via multiple overlapping motor circuit components.

#### **1.4 Invasive neurophysiology recordings associated with balance in Parkinson's disease**

Invasive neurophysiological studies in PD have largely relied on local field potentials (LFPs) recorded from implanted deep brain stimulation (DBS) electrodes in patient who underwent surgery for treatment of their Parkinson's symptoms<sup>5</sup>. While these studies have greatly expanded our understanding of human basal ganglia neurophysiology in different medication and movement states in PD, very little is known about oscillatory changes that occur in the basal ganglia during postural transition tasks, such as gait initiation and turning<sup>5</sup>. In fact, gait initiation and turning are more difficult to measure than straight overground gait and pre-processing from expert skills is needed to characterize these motor tasks. However, since balance is even more impaired in those people with PD who exhibit FoG<sup>58</sup> and since postural transition tasks often elicit FoG<sup>59</sup>, I will review existing studies that have characterized basal ganglia LFP activity associated with FoG in this population<sup>5</sup>.

The subthalamic nucleus (STN) is a primary region in which neurophysiological data during gait and FoG episodes have been examined<sup>5</sup>. Relating to lower frequencies,  $\theta$  and low  $\beta$  modulation may serve as spectral correlates with FoG, as increased STN LFP  $\theta$  and low  $\beta$  power were observed during periods of "vulnerable" gait<sup>5,60</sup>.  $\theta$  modulation was also implicated in comparisons between "effective" gait and FoG periods, with STN LFPs and cortical EEG recordings exhibiting low frequency (4-13 Hz)

synchronization during “effective” walking and FoG associated with cortical-subthalamic decoupling in the hemisphere with less striatal dopaminergic innervation<sup>5,61</sup>. These findings have led to the idea that theta cortical-subthalamic decoupling may be associated with a transition from gait to FoG in this population<sup>5,62</sup>.

For  $\alpha$  and  $\beta$  frequencies, STN LFPs recorded during forward gait, stepping in place, and a turns and barriers course displayed changes in power and entropy between people with PD who experienced FoG (PD-FoG+) and those who did not (PD-FoG-), as well as task-specific modulation in these sub-populations<sup>5,63</sup>. The increased entropy in PD-FoG+ was thought to perhaps serve as a compensatory mechanism for improving FoG in this population<sup>5,63</sup>. Severe akinesia in FoG was also shown by another study to be correlated with increased STN low  $\beta$  power when comparing PD-FoG+ to PD-FoG- individuals during treadmill walking<sup>5,64</sup>; more specifically, an 18 Hz frequency band has gained attention for its potential link to FoG in this population<sup>5,60</sup>. Another neurophysiological signature of FoG is sustained  $\beta$  burst duration, as this feature differentiated between PD-FoG+ and PD-FoG- individuals during forward walking and a stepping in place task<sup>5,65</sup>. The authors found that attenuation of these pathologic bursts using STN-DBS therapy was linked to gait improvements<sup>5,65</sup>.

While not using neurophysiology, it should be noted that some neuroimaging studies have also reported differences in sub-populations of people with PD exhibiting FoG. A functional magnetic resonance imaging (fMRI) study found increased connectivity between the bilateral insulae in PD-FoG- compared to PD-FoG+ during a leg lifting task, which negatively correlated with FoG severity; PD-FoG+ individuals also demonstrated increased SMA reliance during APAs<sup>66</sup>. A recent resting state functional connectivity

study using fMRI suggested deficits in single-task *anticipatory* postural control were associated with increased activation of prefrontal and parietal cortical regions in people with PD when compared to older adults, resembling more of a dual-tasking state; this work also found functional connectivity between frontoparietal and ventral-attention circuits to predict APAs in people with PD<sup>5,67</sup>. These works continue to validate the existence of unique circuits underlying the various domains of postural control and the likely dysfunction present in PD hypothesized to mediate postural instability.

## **1.5 Interventions for balance impairments in Parkinson's disease**

Balance impairments remain difficult to effectively treat, likely due to both their paroxysmal nature and the complex and interrelated nature of multiple motor and sensory circuits underlying the various domains of postural control<sup>5</sup>.

Levodopa is often prescribed as a first-line treatment for the motor symptoms of PD, including PI. Unfortunately, levodopa can often cause problematic secondary symptoms including dyskinesia with continued disease progression<sup>68</sup>. Furthermore, levodopa has often been shown to have a negligible or even worsening effect on various PI symptoms<sup>5,10,18,69-73</sup>, perhaps through compromises to one's postural adaptation and refinement mechanisms<sup>17</sup> or static postural abilities<sup>74</sup>. In people with PD, levodopa has been shown to increase turning speed without affecting dynamic stability<sup>74</sup> and is associated with more consistent turn strategies and taking fewer steps to turn<sup>75</sup>. Levodopa has been shown to improve FoG and akinesia, however<sup>76</sup>. For gait initiation in PD, a recent systematic review and meta-analysis reported levodopa to have no significant pooled effects on various stepping metrics, including amplitude, velocity, and

timing; the sole exception was a small improvement in the velocity of medio-lateral steps<sup>73</sup>.

Another first-line treatment for motor symptoms in PD, including PI, is physical therapy (PT). PT is commonly used in conjunction with levodopa and often neuromodulatory interventions later in the disease. A recent clinical practice guideline released by the American Physical Therapy Association to summarize the quality and strength of existing research to guide PTs in treating PD strongly recommended the use of balance training to improve various domains of postural control in this population, including *static* posture (postural sway), as well as *anticipatory* and *reactive* responses<sup>5,77</sup>. While intervention modalities included by the recommendation were quite varied, supervised, multimodal balance programs, moderate-to-vigorous aerobic treadmill training and the use of novel rehabilitation technologies (sensors, exergaming) were all associated with increased benefit with PT in treating PI<sup>5,77</sup>, however little research exists studying these interventions in combination or the long-term benefit. It is expected that continued research characterizing the neural and biomechanical deficits present among various domains of postural control in this population will also improve the selection of, appropriateness, and effectiveness of PT interventions<sup>5</sup>.

Another often-utilized intervention for severe PI symptoms is DBS applied to the STN (STN-DBS) or globus pallidus internus (GPi-DBS), as these subcortical regions are known to be affected by PD. While DBS technology has been used for over twenty years to treat most of the “cardinal” motor symptoms of PD, controversy remains whether it improves (or worsens) symptoms of PI, especially long-term, and which region and configuration offers the most effective therapeutic benefit<sup>5,16,78</sup>. Research has consistently



shown, however, that medication-responsive PI symptoms will likely have the greatest improvement with DBS regardless of target<sup>5,79,80</sup>.

There is greater data (especially short-term) examining STN-DBS's effects on PIGD symptoms and postural control in people with PD compared to other DBS targets<sup>5</sup>. Specific to *static* postural control, studies have generally suggested that STN-DBS improves most postural sway metrics<sup>5,71,72,81,82</sup>. For *anticipatory* postural control, a review found STN-DBS has a generally positive effect on APAs through amplitude, propulsion, and alignment improvements<sup>79</sup>, with its effects varying with displacement direction, hemisphere stimulated, and frequency of stimulation<sup>5,16</sup>. However, another study suggested medication and STN-DBS together worsened APAs and their responsiveness to levodopa during gait initiation upon 6-month follow-up<sup>5,19</sup>. Similar work also found STN-DBS and medication together had limited benefit on APA metrics compared to medication alone, with both treatment groups continuing to display abnormal lower-extremity muscle activation and co-contraction compared to healthy subjects<sup>5,83</sup>.

Related to the *reactive* postural domain, STN-DBS and medication together have been found to both impair<sup>29</sup>, and partially improve, the speed of postural reflexes and co-contraction ratios compared to healthy subjects<sup>5,83</sup>. Another study found initial improvement with STN-DBS in compensatory stepping abilities, however this benefit was lost and reversed after six months when compared to subjects' "ON" medication function prior to surgery<sup>5,84</sup>. The combined effects of STN-DBS (at least 1-year post-implant) and levodopa during *reactive* balance responses were also found to have a beneficial effect on PI and fall risk, however no treatment combination achieved superior benefit in postural control compared to both "OFF" medication and stimulation conditions<sup>5,69</sup>.

Conversely, other studies found STN-DBS with or without medication to improve PIGD subscores<sup>85</sup>, postural bradykinesia and abnormal sensory aspects of PI following 6 to 12 months of therapy<sup>86</sup>, as well as the ability to improve one's postural strategies<sup>87</sup>, despite them remaining at least partially ineffective compared to controls<sup>5,86,87</sup>.

Longitudinally in people with PD classified into the PIGD subtype (PD-PIGD), STN-DBS's effects on PI symptoms has been mixed, likely complicated by individualized disease progression<sup>5,88,89</sup>. Many studies have reported a loss of therapeutic resolution on axial symptoms, including PI, within one year<sup>90</sup> to ten years after implantation of STN-DBS<sup>5,88,89</sup>. Despite this, others have reported continued benefit during that timeframe<sup>5,85</sup>. Interestingly, STN-DBS in the PD-PIGD population was shown to become less effective in treating "ON" medication PI symptoms over time, while still improving "OFF" medication symptoms<sup>5,85</sup>. Factors such as disease progression, outcomes selected, medication and DBS testing states, and/or pre-surgery PI symptom levodopa responsiveness are all probable sources of variability which could have contributed to the mixed results seen in STN-DBS's effects on PI symptoms<sup>5</sup>.

GPI-DBS is also used to resolve motor symptoms in PD-PIGD individuals. While longitudinal outcomes of PI symptom resolution using GPI-DBS are relatively limited, GPI-DBS with medication was shown to be superior to STN-DBS with medication on PIGD outcomes at six months and two years post-surgery<sup>5,84,91</sup>. Other long-term results using GPI-DBS have suggested that continued therapeutic benefit may be limited to tremor, rigidity, and dyskinesia symptoms only<sup>5,88,92</sup>. GPI-DBS has also been found to have some benefit on *static*<sup>16</sup> and dynamic postural control while counteracting the negative effects levodopa may have<sup>5,93</sup>. In the *reactive* postural domain, GPI-DBS was found to be

superior to STN-DBS in improving compensatory stepping and falls, however GPi-DBS and medication combined were no better than the medication-only state prior to surgery<sup>5,29</sup>. A recent study also suggested GPi-DBS can improve multiple PD-related postural deformities<sup>31</sup>, which may influence postural responses as well<sup>5</sup>.

These findings collectively have led to the suggestion that GPi-DBS may offer greater benefit in people with PI also looking for effective “cardinal symptom” resolution for issues such as tremor, bradykinesia, and rigidity<sup>5,80</sup>. Due to the lack of longitudinal outcomes and limited research exploring the effects of GPi-DBS on various domains of postural control, much work needs to be done in these areas before strong recommendations can be made to guide providers and patients<sup>5</sup>. It is thought that low-frequency (60-80 Hz) stimulation is most effective for targeting axial PD symptoms such as PI<sup>94</sup>, which is much lower than settings often used to treat other “cardinal symptoms” of PD such as tremor and bradykinesia<sup>5</sup>. Thus, commonly used, and continuous high-frequency settings may not be as effective in treating patients also demonstrating PI<sup>5</sup>. Despite the lack of consensus regarding the long-term effects of STN-DBS and GPi-DBS in treating PI, findings showing that targeting these region affects postural responses provides confirmation of their roles in human postural control<sup>5</sup>.

## **1.6 Knowledge gap, rationale, and study aims**

Little is currently known regarding the neurophysiology underlying postural control due to both a lack of research and prior methodological constraints. Currently, no studies have examined cortical and basal ganglia interactions during the postural control mechanisms involved in gait initiation and turning. For this dissertation, I had the unique

opportunity to study neural activities in the form of field potentials using bidirectional neural interfaces in freely moving patients<sup>95,96</sup>.

Analyzing population neural activities in the form of field potentials is a promising method for studying the communication at and between brain regions to elucidate the neural circuits that regulate postural control. By using bidirectional neural implants while “OFF” DBS (recording only), naturalistic neural data can be collected from both the cortical (premotor and motor cortex areas) and subcortical regions (basal ganglia) thought to be implicated in motor circuits affected by PD. This data is also high-fidelity, allowing for robust associations of neural data corresponding to motor activities. Dr. Wang’s laboratory is one of the few laboratories in the world that currently is using this set-up to characterize gait and balance in people with PD. Specifically, we observed low-frequency modulation across the M1 and STN during specific phases of the gait cycle in people with PD<sup>96</sup>. These neurophysiological data have been linked to dysfunctional gait symptoms experienced by people with PD and are now successfully being studied by researchers (including the Wang laboratory) for the development of adaptive neuromodulatory therapies to improve gait function and safety and overcome limitations currently present with continuous DBS and levodopa.

Using similar methods, my dissertation combines human ambulatory neural recordings with corresponding biomechanical data collected during a Phase I clinical trial under principal investigator (PI) and primary mentor, Dr. Doris Wang, MD, PhD to assess neural oscillatory changes during gait initiation (**Aim 1**) and 180-degree turning (**Aim 2**) and relates these neural changes to the quality of these movements, quantified with force plates and wearable sensors.

This study is the first of its kind to collect and analyze neural data from people with PD while they perform salient motor tasks designed to characterize postural transitions and probe levodopa's effects on such phenomena. It is hypothesized that prior to the start of the postural transition (either APA onset or turn), low frequency pallidal oscillations and pallidal-premotor coherences will dynamically change to produce a motor program that will then engage M1 for task execution.

The overarching goals of this study were to start to build a conceptual framework regarding the neurophysiological changes underlying bipedal postural control, and shed light on the pathophysiology of impaired postural transitions in PD. These results may contribute important information for developing novel, individualized neuromodulation strategies to improve postural transitions in this population.

## **Chapter 2. General Methods**

### **2.1 Study Participants**

Five subjects with idiopathic PD undergoing evaluation for DBS surgery were enrolled in the clinical trial (ClinicalTrials.gov ID: NCT-03582891) at the University of California, San Francisco (Table 2.1). Study inclusion criteria included subjects who were: candidates for DBS for motor fluctuations, could walk without an assistive device, and experienced fewer than 4 falls per month. Study exclusion criteria included: subjects with “ON” medication freezing of gait. All subjects provided written informed consent according to the Declaration of Helsinki and the study was administered under institutional review board approval.

**Table 2.1 Baseline subject demographics and motor function**

Table notes: <sup>a</sup>Values taken from closest visit prior to DBS implantation; <sup>b</sup>Test performed virtually by neurologist so rigidity and pull-test not examined. Abbreviations: MDS-UPDRS-III = Movement Disorders Society's Unified Parkinson's Disease Rating Scale, Part III - motor domain; PIGD = Posture Instability Gait Disorder (subscores from items 3.9: arising from chair, 3.10: gait, 3.11: freezing, 3.12: postural stability and 3.13: posture); LEDD = L-dopa equivalent daily dose; MiniBEST = Mini Balance Evaluation Systems Test.

<b>Patient Demographics</b>	<b>Subject 1</b>	<b>Subject 2</b>	<b>Subject 3</b>	<b>Subject 4</b>	<b>Subject 5</b>
Age (years)	68	64	62	68	68
Male/Female	Male	Male	Female	Male	Female
Disease duration (years)	21	12	10	8	4
<b>Baseline Motor Function<sup>a</sup></b>					
MDS-UPDRS III score OFF MED (PIGD subscore)	42 (7)	42 (10) <sup>b</sup>	57 (3) <sup>b</sup>	31 (3) <sup>b</sup>	21 (2) <sup>b</sup>
MDS-UPDRS III score ON MED (PIGD subscore)	25 (5) <sup>b</sup>	19 (3) <sup>b</sup>	29 (1) <sup>b</sup>	17 (2) <sup>b</sup>	9 (2) <sup>b</sup>
Baseline LEDD (mg) <sup>a</sup>	2590	1514	1099	1025	618
MiniBEST score LOW MED (Anticipatory subscore)	13 (3)	-	3 (1)	21 (4)	19 (4)
MiniBEST score ON MED (Anticipatory subscore)	17 (3)	19 (4)	7 (2)	20 (6)	21 (4)

## 2.2 Surgery and electrode localization

All subjects underwent implantation of quadripolar DBS leads implanted in the pallidum (model 3387, Medtronic Inc.), as well as subdural cortical paddle electrodes (model 0913025, Medtronic Inc.) overlying the PMC and M1 areas. Electrodes were connected to an investigational bidirectional neural stimulation device which allows chronic sensing of local field potentials in ambulatory subjects (Summit RC+S, model B35300R, Medtronic Inc.)<sup>95,96</sup>.

Precise electrode localization was performed using established image analysis pipelines for depth and cortical electrodes by fusing preoperative MRI images with a

postoperative computed tomography scan (CT)<sup>97</sup>. For group analyses, electrode locations were normalized into Montreal Neurological Institute space and visualized either on the FreeSurfer average cortical surface or a standardized subcortical atlas (Figure 2.2). Electrode localization figures provided courtesy of Dr. Thomas Wozny, MD.

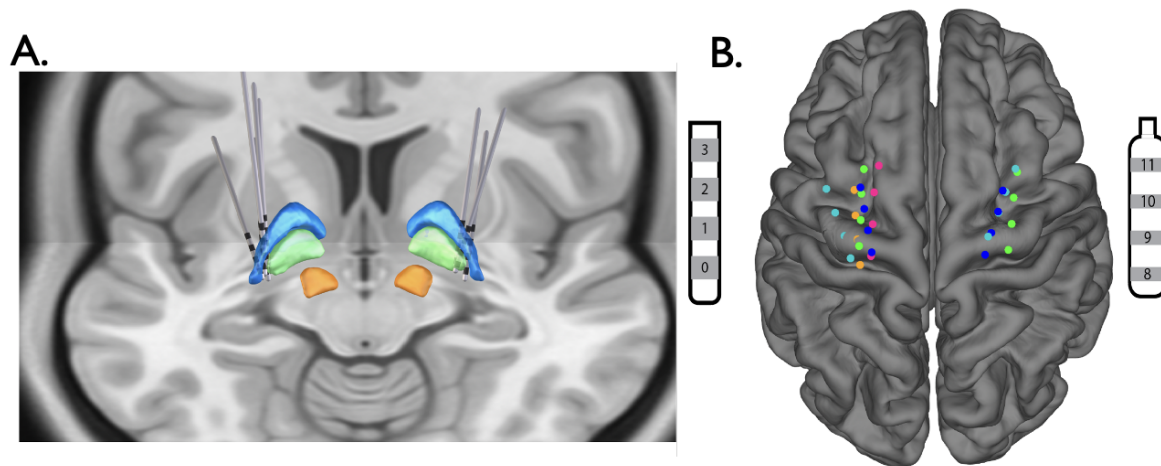


**Figure 2.2 Aggregated subject lead and ECoG visualization**

Figure notes. 2.2A: Aggregated subject DBS leads targeting the globus pallidus internus (green) and globus pallidus externus (blue); 2.2B: Aggregated subject ECoG contacts targeting the premotor cortex and primary motor cortex (hand-knob region).

### 2.3 Motor Symptom Outcome Measures

Subjects received baseline gait and balance assessments 1-2 months prior to DBS surgery, including the Movement Disorders Society’s Unified Parkinson’s Disease Rating Scale (MDS-UPDRS) Part III subscore assessed by a movement disorders neurologist, as well as the Mini Balance Evaluation Systems Test (Mini-BESTest) performed by a physical therapist (this author) (Table 2.1). These tests were administered during both “ON” and “LOW” medication states; the “ON” medication state was tested after the subject took their typical dose(s) of Parkinsonian-medication(s). This period was usually 20-30 minutes after medication was taken, with the individual (and often their partner), and study



PT, confirming that their present motor functioning was comparable to the expected or usual optimized “ON” medication functioning. Subjects were also given “warm-up” time prior to testing if experiencing residual stiffness or other persistent “LOW” medication motor symptoms. The “LOW” medication state was defined as the subject withholding one or more scheduled doses of medication; this spanned overnight for one subject to multiple hours for other patients depending on symptom tolerance, “LOW” medication function, and dosing regimen. Baseline UPDRS-III and MiniBEST data including *anticipatory* balance subscores are provided in Table 2.1.

## 2.4 Neural data collection and processing

**All neural and biomechanical data for this study were collected after the subjects had been implanted with the bidirectional neural RC+S device, but prior to DBS ever being turned “ON” (recording in a completely “OFF” DBS state).** The time between DBS surgery and data collection varied among subjects from 14-44 days.

Local field potentials (LFPs) were recorded in a sandwich configuration from the following two electrode pairs: +2-0 (more ventral, primarily targeting the GPi) and +3-1 (more dorsal, targeting the GPe and striatum). Bilateral cortical data was recorded using two pairs of contacts: +9-8 (over M1) and +11-10, over PMC. LFPs were sampled at 500 Hz and initially preprocessed using a preamplifier high-pass filter of 0.85 Hz and a two-staged low-pass filter at 1700 Hz and 450 Hz. Accelerometry data from the Summit RC+S device was sampled at 64 Hz. All data were extracted using open-source code (<https://github.com/openmind-consortium/Analysis-rCS-data>)<sup>98</sup>.

Kinematic data were also collected using a wireless surface electromyography (EMG) system (Trigno, Delsys Inc., Natick, MA) and a wireless inertial measurement unit (IMU) system (Xsens, Movella, Netherlands). Accelerometer sensors were placed on top of subjects' RC+S implants for synchronization between EMG and neural LFP. Trial-by-trial LFP data were aligned prior to further processing with biomechanical data collected using peaks in accelerometer data from the Xsens and Delsys systems and RC+S device. Alignments were verified visually, with a 3-sample difference allowed between accelerometry peaks in the final alignments. Dropped neural data packets in the RC+S recordings were also identified and noted (0.01s threshold).

All neural data for the included gait initiation trials (Aim 1) or turn intervals (Aim 2) were concatenated under similar conditions (e.g. medication state, contact) and presumable artifacts were identified and labeled with 50 sample buffers on each end using "NaN" values prior to analysis using MATLAB scripts authored by Kara Presbrey, BS. Broadly, data was processed using a multitaper spectral transform (filter parameters: 16 voices per octave, 75-150 Hz gamma filter limits, 60 time bandwidth)<sup>99,100</sup>, then normalized using median-based z-scoring. Data was blanked over time intervals where gamma power surpassed a set threshold of deviations which was tailored to each subject following visualization. Specific artifact thresholds used for each subject are further detailed in the methods section for both aims. All localized artifacts and artifact-labeled spectrograms were visualized to ensure appropriate inclusion and labeling.

All neural data for each gait initiation trial or turn were analyzed using a built-in MATLAB signal processing function for short-time Fourier transform ("spectrogram" function) with a 1s window, 90% window overlap, and a transform length of 512 data

points. Data ran through the spectrogram function were also filtered beforehand through a high pass, 4<sup>th</sup>-order Butterworth filter with 2 Hz cutoff to remove low frequency noise. Average epoch neural power were calculated over time and averaged for the canonical frequencies. The canonical frequencies analyzed included theta (4-8 Hz), alpha (8-12 Hz), low beta (13-20 Hz), high beta (20-30 Hz), low gamma (30-50 Hz), and broadband gamma (50-200 Hz).

## **2.5 Statistical analysis**

Each subjects' postural task quality metrics were compared between "ON" and "LOW" medication states using Wilcoxon rank sum tests in R/R Studio to assess medication-related differences. Group data comparing the neural modulation during each task and the relationship to task metrics are detailed in the methods for each aim.

## **Chapter 3. Gait initiation (Aim 1)**

### **3.1 Task rationale and hypothesis**

People with PD often demonstrate gait initiation impairments, thought to be caused by the presence of one or more dysfunctional APAs stemming from the disease's effects on basal-ganglia-thalamocortical circuits underlying these processes. While much literature has characterized various amplitude and timing deviations (APAs are generally thought to be more variable, hypometric, and/or delayed in people with PD),<sup>20,37</sup> it is less-known which specific neural regions and circuits underlie this fundamental motor task, how neural modulation changes with levodopa during varying postural control requirements, and whether relationships exist between dynamic task-related neural modulation and resulting APA timing and amplitude metrics. This work is a likely important first step to begin to answer these important questions prior to development of future neuromodulatory interventions which could effectively treat gait initiation dysfunction (and potentially, related sequelae such as FoG) in this population.

This project combined forceplate data quantifying subject APAs with neural data collected during repeated gait initiation trials under both "LOW" and "ON" levodopa medication states utilizing a simple cueing paradigm. Our hypothesis for Aim 1 (in addition to the general hypothesis above) is that "ON" medication, APAs would display larger amplitudes, and be associated with greater overall beta desynchronization across the task.

## **3.2 Gait initiation methods**

### **3.2.1 Gait initiation task overview**

Subjects performed repeated gait initiation trials in both the “ON” and “LOW” medication states on embedded twin AMTI force plates (1000 Hz sampling rates) using a self-selected stepping foot in response to a visual cue. Each trial began with the patient settling on the force plates (choosing their weight distribution with a foot on each force plate without feedback), with readiness confirmed prior to initiation of cueing paradigm. Subjects were instructed to begin walking with display of a green “go” screen; no other feedback was provided for cueing to maximize naturalistic performance. Gait initiation trials were performed in 5-10 trial bouts depending on patient tolerance, with seated breaks between sets and as requested. Trials were excluded if patient was unable to perform a period of quiet standing due to dyskinesia, lacked an APA, or had multiple APAs with no quiet standing interval between.

### **3.2.2 Biomechanical data collection and processing**

All ground reaction force data from the force plates’ z-axes (GRFz) were processed using a low-pass, 4<sup>th</sup>-order Butterworth filter with 50 Hz cutoff frequency<sup>25,39</sup>. Kinematic data were also collected using the Trigno Delsys EMG and Xsens IMU systems. Accelerometer sensors were placed on top of subjects’ RC+S implants for synchronization between EMG and neural LFP. The IMU system consisted of 15 units placed in a standard configuration<sup>101</sup> over the subjects’ body and limbs and were used for data synchronization with an automatic force plate trigger.

### 3.2.3 Task analysis

Force plate data were separated into epochs during the gait initiation using custom MATLAB scripts to demarcate a period of quiet standing, pre-APA onset, APA onset, peak APA amplitude, and when the stepping foot completely came off the force plate (Figure 3.1A). These points were chosen to gain insight into the differing postural control requirements of the task, including *static* (quiet standing), *anticipatory* postural demands (APA execution), and motor execution (stepping)<sup>102,103</sup>.

**Quiet standing:** The period prior to cue when subjects stood as quietly as possible on the force plates. Quiet Standing start (trial start) was defined as the last GRFz crossing of the subjects' feet on the force plate prior to the "Quiet Standing End" mark; the "Quiet Standing End" mark was defined as exactly 1.5s before the subjects' stepping foot completely left the force plate. (This "rule" was established as patients generally took 0.5-0.75s to execute the APA and step, creating a 0.75-1s *preparatory APA* period prior.) Trials were required to have a minimum of 3s of quiet standing. (For one subject, two trials were included with 2.5s of quiet standing, to utilize as many trials as possible despite difficulty with quiet standing.)

**APA preparation:** The period from "Quiet Standing End to APA Onset" was designed to be a *preparatory APA* proxy with the "go" cue; its length and reasoning is above. APA onset was defined as the instance at which the stepping foot GRFz slope exceeded 3.5 times the standard deviation of its slope averaged during the quiet standing epoch, which was adapted from previous methods<sup>37,104,105</sup>. APA onset was manually marked on occasion if a subject's APA did not cross this threshold.

**APA:** The period from APA onset to when the stepping foot completely left the force plate (GRFz crossed 0N) was included as a *total APA* proxy. Note: if a GRFz value did not fully cross 0 N due to calibration, but approached and plateaued or increased again, the time at which the local minimum closest to 0 N was used.) Another epoch (“*early APA*”) consisted of the interval between APA onset to APA peak amplitude and did not include stepping.

### 3.2.4 APA metrics

APA metrics used to assess task quality and performance were: 1) Cumulative APA area, calculated using the built-in MATLAB “trapz” function (GRFz were integrated under the curve from APA onset to APA peak amplitude); this was normalized to subjects’ bodyweight in kilograms as a *combined* length and amplitude APA metric; 2) APA peak amplitude, also normalized to subject bodyweight and used as a proxy for APA vigor; 3) APA amplitude  $\Delta$  (“Net” APA; the difference between peak and initial APA amplitudes), also normalized to subject bodyweight and used as a proxy for APA scaling; and 4) Time to peak APA amplitude, defined as the time between APA onset and APA peak amplitude (Figure 3.1B).

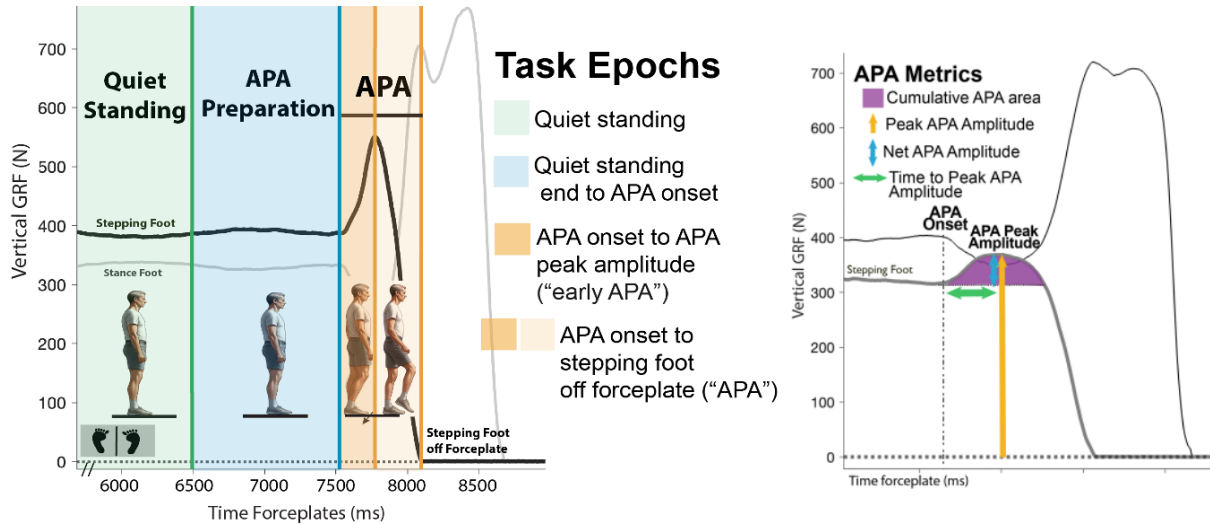


**Figure 3.1 Gait initiation task epochs and APA metrics**

Figure notes: Task epochs (3.1A) marked for each gait initiation trial featuring varying postural control strategies: “Quiet standing,” “Quiet standing end to APA Onset,” “APA Onset to APA Peak Amplitude,” and “APA Onset to Stepping Foot off the Forceplate.” The task’s APA metrics (3.1B) assessed by the study both “ON” and “LOW” medication included cumulative APA, peak and net APA amplitudes, and time to peak APA amplitude. Abbreviations: GRF = ground reaction force; ms = milliseconds; APA = anticipatory postural adjustment.

### 3.2.5 Data analysis

All task markings and epochs for each trial were visually inspected, with inappropriate markings manually corrected. **To facilitate consistency of the results and to include subjects who were unilaterally implanted, all gait initiation trials analyzed used neural data recorded from the contralateral hemisphere to the stepping leg.** This resulted in minimal trials being excluded due to stepping with the ipsilateral foot. There were also a few trials excluded from analysis due to subjects performing multiple, subsequent APAs with no quiet standing (thus eliminating normalization of data at subsequent epochs). For Subjects #1, 2, 4, and 5, 89% (74/83) of trials met these criteria and were analyzed; for Subject #3 37% (24/65) of trials were used, due to difficulties performing the task.



**Artifact rejection:** Artifacts were identified and localized as detailed above in the general methods section for all included trials. Subject-specific median-based z-score thresholds were set under both medication states following visualization of the transformed and normalized neural data. Thresholds were initially set very high (so no data were blanked prior to visualization), then lowered as appropriate following consideration of the overall data and the waveform and regularity of potential artifacts. Subject #1's set median-based z-scores were 32 while "LOW" medication and 42 "ON" medication, with no artifacts identified using these thresholds. Subject #2's median-based z-scores were 87 while "LOW" medication and 60 "ON" medication, with no artifacts identified. Subject #5's median-based z-scores were 25 while "LOW" medication and 42 "ON" medication, with no artifacts identified. Subject #4's median-based z-scores were 85 while "LOW" medication and 100 "ON" medication (with additional blanking added following visualization); three artifacts were identified which were at least 1300 samples apart. Subject #3's thresholds were 45 while "LOW" medication and 30 "ON" medication; no artifacts were identified. However, additional blanking was performed for all this subject's data, due to the presence of continuous artifact-appearing bands across all time points. These bands were present at GPi (68 Hz, 131 Hz, and 200 Hz), and M1 (75 Hz) while "ON" medication, and at GPi (66 Hz, 70 Hz, 131 Hz, 200 Hz), and M1 (74 Hz) while "LOW" medication. Blanking was performed at the frequencies listed for this subject, and 2 additional frequencies above and below for all trials for power and coherence analyses. All localized artifacts and artifact-labeled spectrograms were visualized to ensure appropriate inclusion and labeling.

**Signal processing:** Corresponding neural data for each trial were analyzed as detailed in the general methods using MATLAB's "mscohere" for magnitude-squared coherence (32 segment hamming window, 256 nfft, 90% overlap) and "spectrogram" functions (spectrogram parameters detailed above). Average absolute epoch neural power and coherence were calculated over time and averaged for the canonical frequencies, with data also normalized to the "Quiet Standing" epoch for each trial for input into the linear mixed model analyses. Subject #4's trials with artifacts were not included in coherence analyses for the implicated contacts due to scaling of these data. An illustration of these methods using a sample "LOW" and "ON" medication trial is in Figure 3.2. Additional plots (Figure 3.3) also reflect the median power spectral density (PSDs) and median absolute deviations of grouped subject trials using filtered neural data as detailed above using MATLAB function "pwelch" with segment length 128 samples and 90% overlap; these were included for improved visualization for data presentation. Subject #3's data were notch filtered for PSD visualization only at the frequencies above.

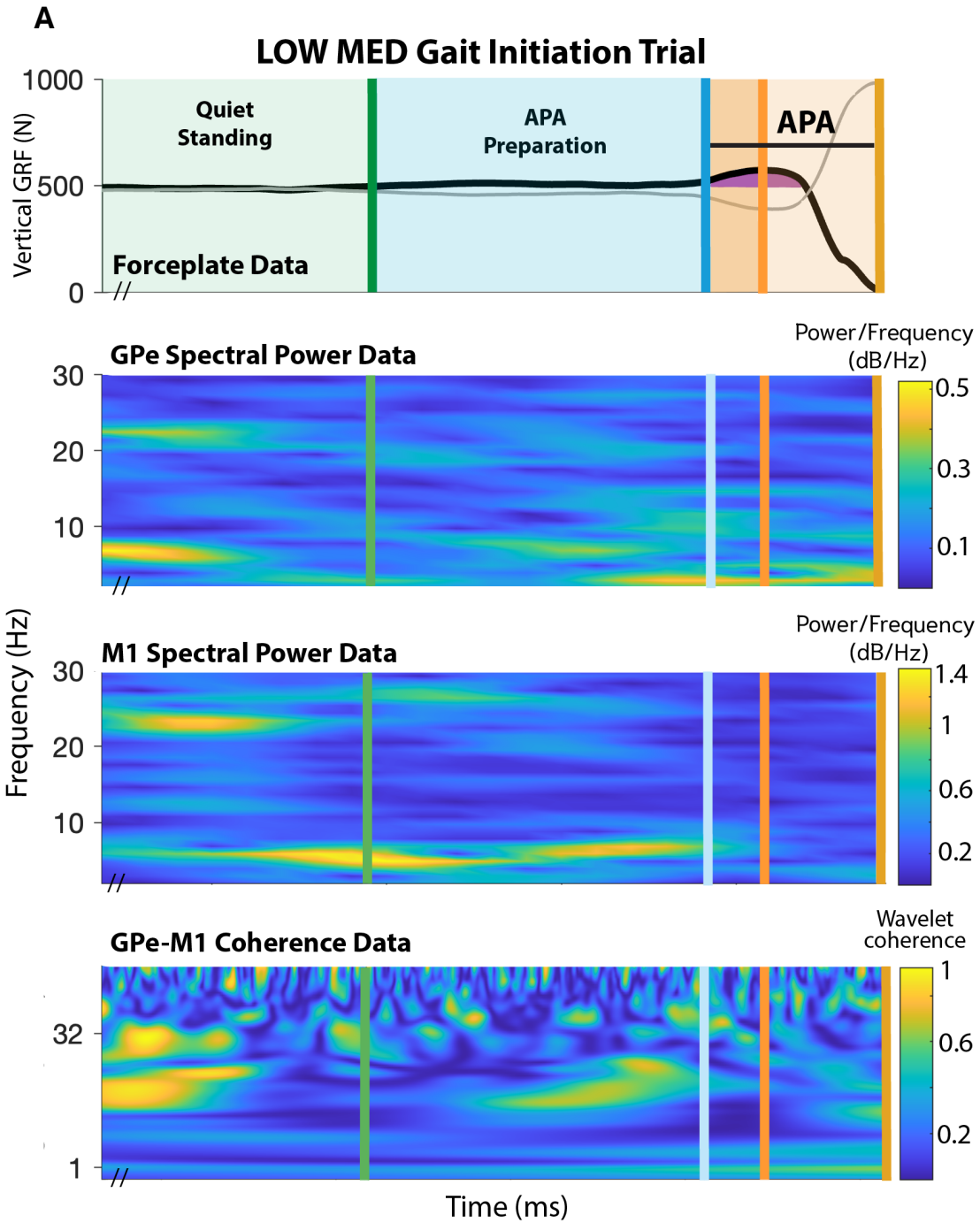


**Figure 3.2A** Sample analysis for a gait initiation trial

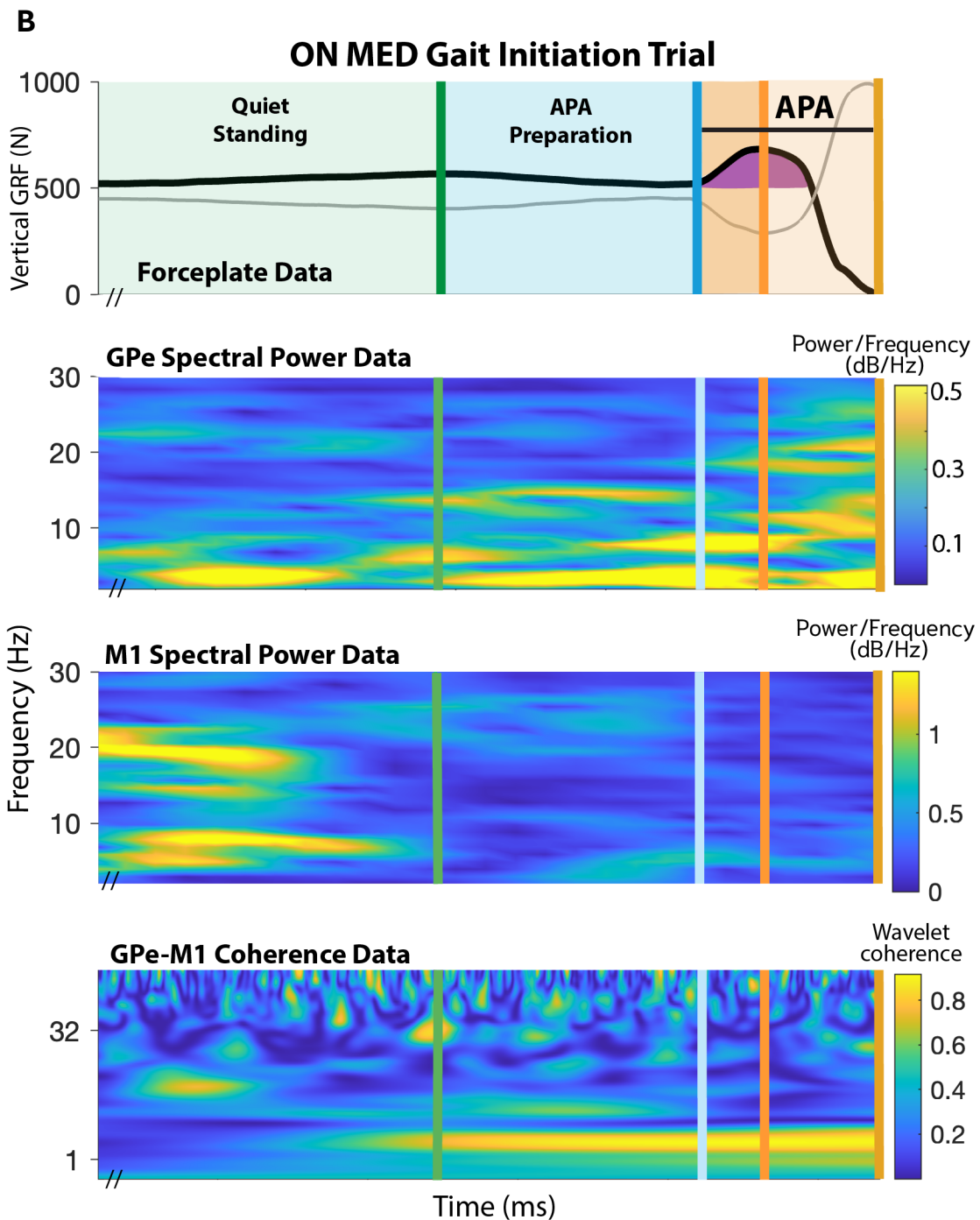


**Figure 3.2B Sample analysis for a gait initiation trial**

Figure notes: Sample subject's "LOW" vs "ON" forceplate data with task epochs, neural power (middle plot) via spectrogram, and wavelet coherence via coherogram during single gait initiation trial. Neural power and coherence were averaged within each epoch for all trials and contacts.

### 3.2.6 Statistical analysis

Averaged neural data were compared between four gait initiation task epochs featuring varying postural control requirements (quiet standing, APA preparation, early APA, and APA) using Kruskal-Wallis and post-hoc Dunn's tests, with multiple corrections via the Benjamini-Hochberg method. Linear mixed models (LMMs) were constructed using group data for all subjects in R/RStudio using the "lme4" package<sup>106</sup>. LMMs were built using backwards model selection with the package's "step" function and APA metrics as outcomes; all neural data and medication predictors for a single epoch were ran at a time, thus comparing model performance and relative predictor significance between different task epochs. Fixed predictors inputted into the LMM included averaged, normalized neural data for all frequency bands at each recording contact, under both medication states; subjects were inputted as random effects. Due to trial numbers and increasing model complexity with greater random effects, only subjects were included as random effects in this analysis; all final models reached suitable convergence.

LMMs were assessed for quality using Akaike Information Criterion (AIC) and likelihood ratio tests, with model residuals visualized in Q-Q plots. All fixed effects in the final models were evaluated for multicollinearity using variance inflation factor (VIF). Models presented in the main results include all significant predictors resulting from backwards selection for the "APA" epoch, with additional epochs and corresponding model performance in the supplemental figures.

### 3.3 Gait initiation results

#### 3.3.1 APA metrics during gait initiation are inconsistently affected by levodopa in people with Parkinson's Disease

Five subjects (3 male and 2 females) with PD participated in the study. Patient baseline clinical characteristics are summarized in Table 2.1. Ninety-eight unique gait initiation trials were included for analysis which met criteria (Table 3.1). Neural data were analyzed from the brain hemisphere contralateral to the stepping foot, which was the left hemisphere in 3 subjects (#1, #2, and #5) and right hemisphere in 2 subjects (#3 and #4).

Trials performed in the "LOW" and "ON" medication states were relatively matched within subjects and two subjects (#2 and #4, characterized as "APA levodopa responders") demonstrated significantly decreased APA amplitudes in the "LOW" medication state. Average cumulative APA across subjects was 333.1 N-ms/kg +/- 188.0 N-ms/kg (mean +/- std) in the "LOW" medication state and 410.8 N-ms/kg +/- 190.7 N-ms/kg in the "ON" state, which was a significant difference ( $p=0.03$ ; Wilcoxon rank sum test). Average APA peak amplitude across subjects was 6.139 N/kg +/- 1.306 N/kg while "LOW" medication and 6.397 N/kg +/- 1.445 N/kg in the "ON" state ( $p = 0.19$ ). Average  $\Delta$  APA amplitude across patients was 1.524 N/kg +/- 0.925 N/kg in the "LOW" medication state and 1.744 N/kg +/- 0.790 N/kg while "ON" ( $p = 0.12$ ). Average time to peak APA across patients was 261 ms +/- 7.6 ms in the "LOW" state and 270 +/- 83 ms while "ON" medication ( $p = 0.46$ ).

**Table 3.1 Summary of gait initiation trials and APA metrics**

Table notes: <sup>a</sup>Metric normalized to subject body weight in kilograms (kg); \* “LOW” vs “ON” medication **APA metrics significantly different ( $p \leq 0.05$ )**. Abbreviations: GI = gait initiation; APA = anticipatory postural adjustment; N-ms = Newton-milliseconds; ms = milliseconds; std = standard deviation.

<b>Gait Initiation Data</b>	<b>Subject 1</b>	<b>Subject 2</b>	<b>Subject 3</b>	<b>Subject 4</b>	<b>Subject 5</b>
Stepping foot for all GI trials	Right	Right	Left	Left	Right
Neural hemisphere analyzed	Left	Left	Right	Right	Left
Number of trials analyzed ON MED/LOW MED	4/3	5/6	13/11	13/14	14/15
Average cumulative APA (std) LOW MED/ON MED <sup>a</sup> (N-ms/kg)	490.3 (467.6)/ 636.8 (309.6)	<b>324.9 (66.2)/ 446.7 (77.9)*</b>	406.6 (212.4)/ 432.2 (207.1)	<b>187.8 (111.7)/ 344.8 (209.5)*</b>	386.4 (104.1)/ 374.9 (88.5)
Average peak APA amplitude (std) LOW MED/ON MED <sup>a</sup> (N/kg)	6.45 (3.0)/ 6.96 (0.9)	<b>6.86 (0.2)/ 7.96 (0.5)*</b>	6.13 (1.6)/ 5.43 (1.8)	5.10 (0.9)/ 6.14 (1.5)	6.77 (0.4)/ 6.82 (0.1)
Average $\Delta$ APA amplitude (std) LOW MED/ON MED <sup>a</sup> (N/kg)	2.53 (2.3)/ 2.04 (0.7)	<b>1.74 (0.3)/ 2.23 (0.3)*</b>	2.18 (0.9)/ 2.18 (1.0)	<b>0.73 (0.4)/ 1.39 (0.8)*</b>	1.49 (0.4)/ 1.40 (0.4)
Average time to peak APA (std) LOW MED/ON MED (ms)	229 (48)/ 318 (174)	<b>227 (34)/ 277 (21)*</b>	240 (74)/ 279 (95)	283 (106)/ 247 (84)	275 (56)/ 269 (47)

### 3.3.2 Pallidal and cortical oscillatory amplitudes dynamically change during gait initiation and are variably affected by levodopa

To evaluate signals from the pallidal and motor cortical areas during gait initiation, we analyzed their mean spectral power across the following epochs of the gait initiation task: quiet standing, APA preparation, early APA (not included in figure illustrations to improve clarity), and APA, using grouped subject data and Kruskal-Wallis and Dunn’s post-hoc testing with Benjamini-Hochberg corrections (Figure 3.3).

In the “LOW” medication state, dynamic power modulation was observed across the task in the subcortical regions for beta ( $\beta$ ) and broad gamma ( $\gamma$ ) frequencies. At GPi, median low  $\beta$  power was significantly higher during quiet standing (low  $\beta$  power: 0.181 mV) and APA preparation (0.178 mV) compared to the APA epoch (0.152 mV;  $p < 0.01$ ). GPi high  $\beta$  power significantly decreased in a stepwise fashion between quiet standing (median high  $\beta$  power: 0.144 mV), early APA (0.119 mV;  $p < 0.01$ ) and APA (0.115 mV;

$p < 0.01$ ). High  $\beta$  power at GPe was also significantly elevated during quiet standing (median high  $\beta$  power: 0.102 mV) compared to APA preparation (0.092 mV), early APA (0.089 mV) and APA (0.085 mV;  $p < 0.0001-0.01$ ). GPe broadband gamma ( $\gamma$ ) power was significantly higher during early APA (median broad  $\gamma$  power: 0.031 mV) and APA (0.030 mV), compared to quiet standing (0.028 mV;  $p < 0.001-0.01$ ). GPe broadband  $\gamma$  power displayed stepwise power increases with task progression.

While “ON” medication, GPi exhibited differing significant power modulation across the task. At GPi and GPe, broadband  $\gamma$  power again increased in a stepwise fashion, with significant differences between both quiet standing and APA preparation (median GPi broad  $\gamma$  power: 0.030 mV, GPe broad  $\gamma$  power 0.028 mV) compared to the APA epoch (GPi: 0.033 mV; GPe: 0.031 mV) ( $p < 0.01-0.05$ ). GPe high  $\beta$  power “ON” medication also exhibited significant task-related decreases between quiet standing (median high  $\beta$  power: 0.089 mV) to the early APA (0.079 mV), and APA epochs (0.078;  $p < 0.05$ ).

At the cortex, task-related dynamic power modulation was significant regardless of medication state. While in the “LOW” medication state, M1 alpha ( $\alpha$ ) power significantly incrementally decreased from quiet standing (median  $\alpha$  power: 0.345 mV) to the early APA (0.281 mV) and APA (0.269 mV;  $p < 0.001-0.01$ ) epochs. “ON” medication similarly demonstrated  $\alpha$  power decreases there between quiet standing (median  $\alpha$  power: 0.353 mV) and total APA (0.287 mV;  $p < 0.01$ ). While “LOW” medication, M1 low  $\beta$  power significantly decreased from quiet standing (median low  $\beta$  power: 0.288 mV) to early APA (0.247;  $p < 0.01$ ) and APA epochs (0.223 mV;  $p < 0.01$ ). The “ON” medication state demonstrated similar modulation, with low  $\beta$  power significantly decreasing from quiet standing (median low  $\beta$  power: 0.334 mV) to APA preparation (0.277 mV;  $p < 0.05$ ) and



then APA (0.231;  $p < 0.0001-0.05$ ). For M1 high  $\beta$  power, both medication states exhibited similar trends, with quiet standing and APA preparation displaying significantly higher power than APA epochs. As a representative example, M1 high  $\beta$  median power while “LOW” medication was 0.334 mV during quiet standing, 0.292 mV in APA preparation, 0.226 mV during early APA, and 0.251 mV during APA ( $p < 0.001-0.05$ ).

Comparable task modulation was also observed at PMC under both medication states. Theta ( $\theta$ ) power significantly decreased while “LOW” and “ON” medication between quiet standing (median “LOW” power: 0.775 mV, “ON” power: 0.730 mV) and APA (median “LOW” power: 0.535 mV, “ON” power 0.545 mV;  $p < 0.01-0.05$ ). This trend was similarly exhibited at  $\alpha$  frequencies between quiet standing (median “LOW” power: 0.504 mV, “ON”: 0.536 mV) compared to early APA (median “LOW” power: 0.380 mV,  $p < 0.01$ ; “ON”: 0.353 mV,  $p < 0.05$ ), and APA (median “LOW” power: 0.369 mV, “ON”: 0.348 mV;  $p < 0.01-0.05$ ).

For both medication states, PMC demonstrated pronounced beta modulation across the task epochs. Low  $\beta$  power significantly decreased between quiet standing (median “LOW” power: 0.441 mV, “ON”: 0.464 mV) to APA preparation (median “LOW” power: 0.339 mV,  $p < 0.01$ ; “ON”: 0.324 mV,  $p < 0.01$ ), early APA (median “LOW” power: 0.294 mV,  $p < 0.001$ ; “ON”: 0.304 mV,  $p < 0.001$ ), and APA (“LOW” power: 0.286 mV,  $p < 0.0001$ ; “ON”: 0.307 mV,  $p < 0.001$ ). High  $\beta$  power under both medication states also significantly decreased here between quiet standing (median “LOW” and “ON” power: 0.431 mV) to early APA (median “LOW” and “ON” power: 0.292 mV,  $p < 0.001$ ) and APA (median “LOW” power: 0.284 mV,  $p < 0.001$ ; “ON”: 0.289,  $p < 0.001$ ). High  $\beta$  power was also significantly different between APA preparation (median “LOW” power: 0.341 mV,

“ON”: 0.385 mV) to APA ( $p < 0.01-0.05$ ). In the “ON” medication state only, PMC low  $\gamma$  power significantly decreased from quiet standing (median power: 0.185 mV) to early APA (0.158 mV;  $p < 0.05$ ).

Trends among dynamic power modulation across the task in the “APA levodopa responders” (Subjects #2 and 4) vs “non-responders” (Subjects #1, 3, 5) subgroups reflected much similarity. Both subgroups exhibited greater power modulation overall at the cortical regions vs pallidal, with  $\beta$  power decreasing across the task and increasing for broadband  $\gamma$ , regardless of medication state or contact. Both subgroups also exhibited inconsistent  $\theta$  and  $\alpha$  dynamic power modulation across the task under both medication states. Trends regarding group power modulation are summarized in Table 3.2, and individual subject power data is provided in Figures 3.6-3.10.

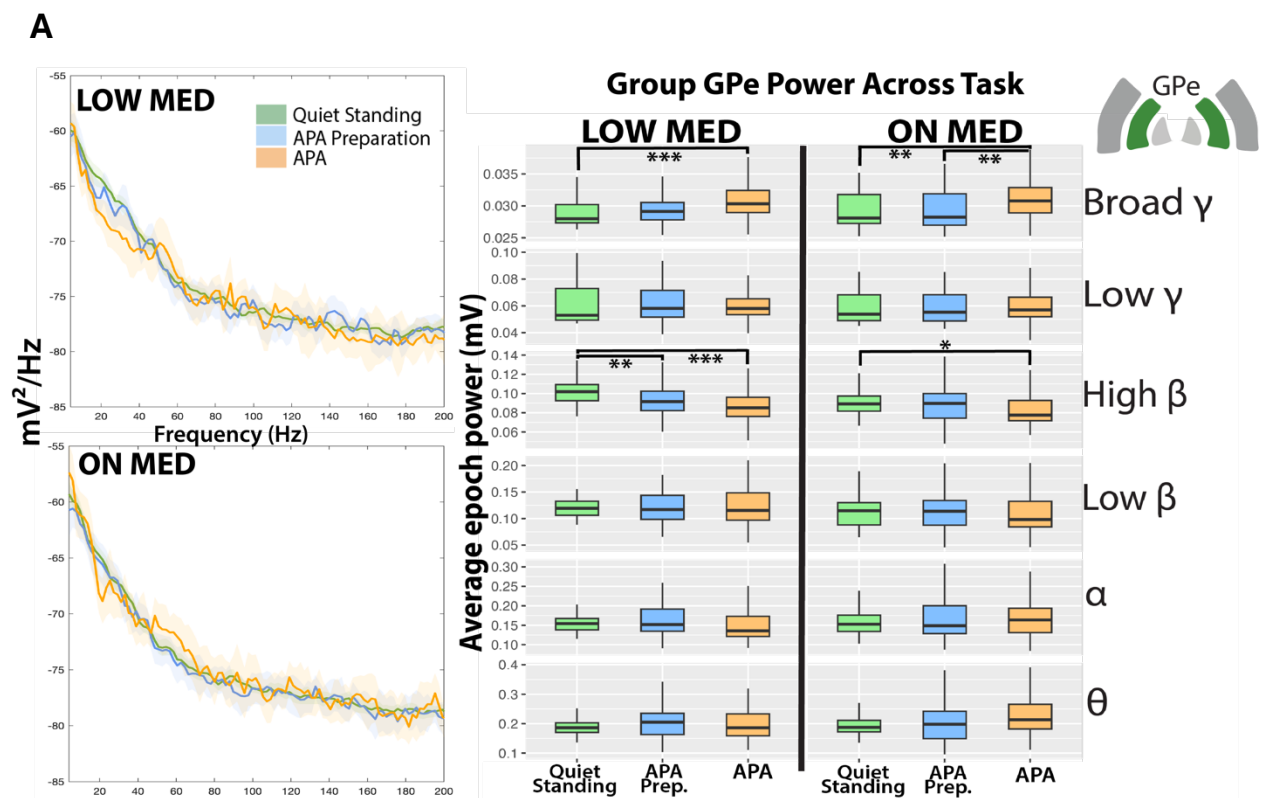


**Figure 3.3A Dynamic group power modulation at GPe and M1 during gait initiation**

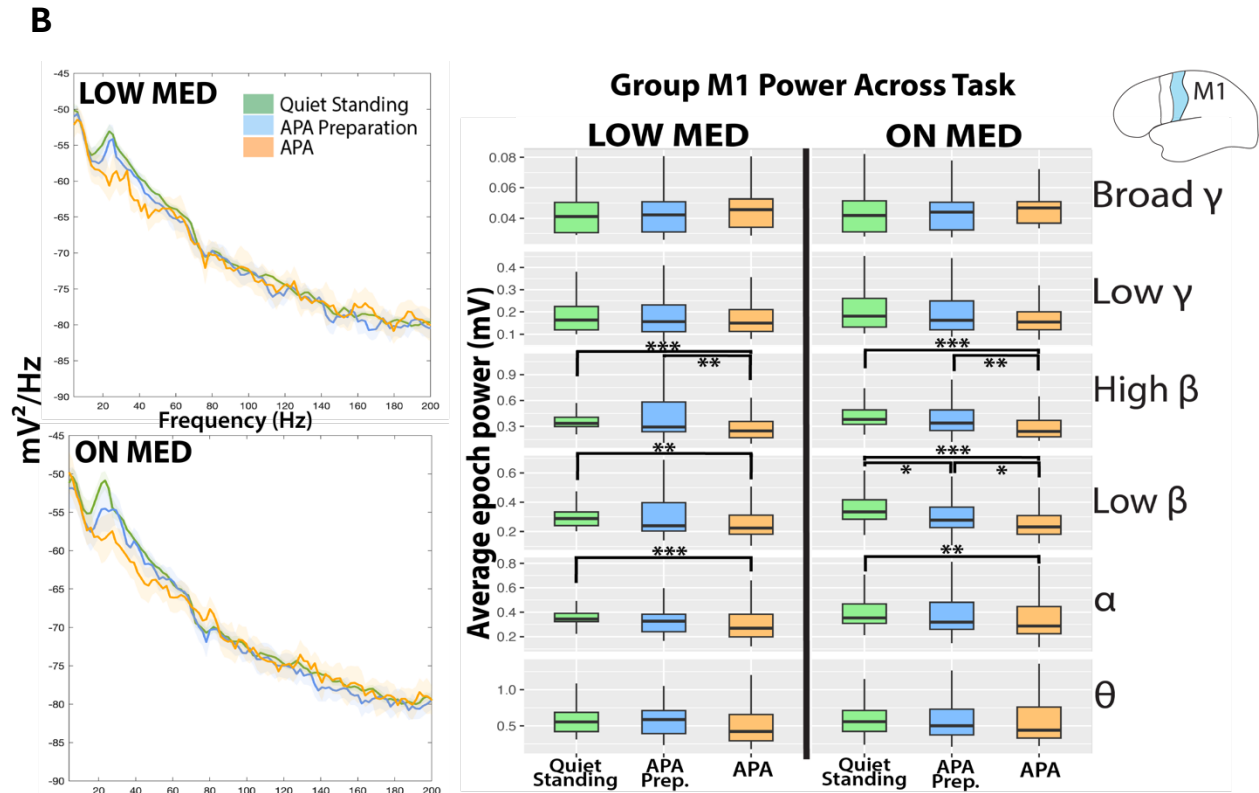















**Figure 3.3B Dynamic group power modulation at GPe and M1 during gait initiation**

Figure footnotes: Grouped subject data at GPe (A) and M1 (B) PSDs for “LOW” and “ON” medication states during the three primary task epochs: “Quiet standing,” “APA preparation” and “APA”. Boxplots demonstrate group average power from all subjects from the “spectrogram” function during each epoch across the canonical frequencies. Significance between epochs is denoted with \*  $p < 0.05$ , \*\*  $p < 0.01$ , \*\*\* $p < 0.001$  following Kruskal-Wallis and Dunns testing with multiple corrections. Boxplots created with upper whisker representing  $1.5 \times$  interquartile ratio (IQR) past the 3<sup>rd</sup> quartile and lower whisker representing  $1.5 \times$  the IQR below the 1<sup>st</sup> quartile. Significance is seen among power modulation at  $\alpha$ ,  $\beta$ , and  $\gamma$  frequencies depending on contact location under both medication states. Abbreviations: GPe = globus pallidus externus, M1 = primary motor cortex; Hz = Hertz; mV = millivolts; APA = anticipatory postural adjustment;  $\theta$  = theta,  $\alpha$  = alpha,  $\beta$  = beta,  $\gamma$  = gamma.

**Table 3.2 Summary of significant group power modulation across task**

Table notes: Significant group power modulation displayed across task epochs using Kruskal-Wallis tests with post-hoc Dunn’s testing and multiple corrections ( $p < 0.05$ ). Results shown for the significant frequency bands, respective contact and medication state, as well as the overall direction of the significant power modulation across the task (either decreased, as represented with the purple arrow, or increased, represented with the blue arrow). Abbreviations:  $\theta$  = theta,  $\alpha$  = alpha,  $\beta$  = beta,  $\gamma$  = gamma; GPi= globus pallidus internus, GPe = globus pallidus externus, M1 = primary motor cortex, PMC = premotor cortex. “Both” for medication = both “ON” and “LOW” medication states were significant.

Frequency Band	Contact	Medication State	General modulation across task
Low $\beta$	GPi	“LOW”	
High $\beta$	GPi & GPe	“LOW”	
Broadband $\gamma$	GPe	“LOW”	
Broadband $\gamma$	GPi & GPe	“ON”	
High $\beta$	GPe	“ON”	
$\alpha$	M1	Both	
Low $\beta$	M1	Both	
High $\beta$	M1	Both	
$\theta$	PMC	Both	
$\alpha$	PMC	Both	
Low $\beta$	PMC	Both	
High $\beta$	PMC	Both	
Low $\gamma$	PMC	“ON”	

**3.3.3 Gait initiation in Parkinson’s disease involves significant, widespread coherence increases across pallidal and cortical regions**

To evaluate signal transfer between pallidal and cortical areas during gait initiation, we analyzed their mean magnitude-squared coherence across the following epochs of the gait initiation task: quiet standing, APA preparation, early APA, and APA using group

subject data and Kruskal-Wallis and Dunn's post-hoc testing with Benjamini-Hochberg corrections (Figures 3.4-3.5; 3.11-3.13).

Across the task, widespread and consistent coherence modulation was seen between pallidal-cortical regions, regardless of medication state. For GPi-M1, GPi-PMC, GPe-M1, and GPe-PMC, coherence generally significantly increased between quiet standing and APA preparation, further increased between APA preparation and early APA, then decreased between the early APA and APA epochs while "LOW" and "ON" medication. This pattern was seen for all canonical frequency bands at the epochs as described, with GPe-cortical  $\theta$  coherence between the early APA and APA epochs the exceptions (some did not reach significance). As a representative lower-frequency example of this modulation, GPi-PMC low  $\beta$  coherence increased from quiet standing (median "LOW" medication coherence: 0.007, "ON": 0.017) to APA preparation (median "LOW" medication coherence: 0.041, "ON": 0.049), further upon early APA (median "LOW" and "ON" medication coherence: 0.175), then decreased (but remained elevated compared to earlier task epochs) during the APA epoch (median "LOW" coherence: 0.082, "ON": 0.063);  $p < 0.01-0.0001$ ). Similarly, for a higher-frequency example, broadband  $\gamma$  coherence there increased from quiet standing (median "LOW" medication coherence: 0.005, "ON": 0.006), to APA preparation (median "LOW" medication coherence: 0.042, "ON": 0.035), further increased at early APA (median "LOW" medication coherence: 0.155, "ON": 0.133), then significantly decreased, yet remained elevated compared to earlier task epochs at the APA epoch (median "LOW" medication coherence: 0.059, "ON": 0.055);  $p < 0.0001$ .

Modulation differed somewhat in these trends for inter-regional cortical coherence. While the same general trend was displayed while “LOW” medication (coherence increased across the task until the APA epoch, where it decreased), much less significance was observed between epochs and at fewer frequency bands. For example,  $\theta$  coherence was significant in its increases between quiet standing and subsequent epochs only (early APA;  $p < 0.0001$ , and APA;  $p < 0.01$ ). While  $\alpha$ ,  $\beta$ , and low  $\gamma$  coherence still increased between various epochs, these trends were significant and shared between the quiet standing to early APA ( $p < 0.0001-0.05$ ), then to the total APA ( $p < 0.0001-0.01$ ) only. Broadband  $\gamma$  coherence continued to display widespread and consistent significant modulation here between all task epochs ( $p < 0.01-0.0001$ ).

The “ON” medication state was especially different in coherence modulation across the task between the inter-cortical areas. There, the canonical frequencies excepting  $\beta$  exhibited the trends as discussed, with limited significance seen consistently across intermediate task epochs; broadband  $\gamma$  coherence was again the exception, which continued to display widespread and significant modulation ( $p < 0.0001$ ). As a representative example of non- $\beta$  modulation here,  $\alpha$  coherence changes were significant between the early APA and APA epochs only, with coherence significantly decreasing (median  $\alpha$  coherence at early APA: 0.160, APA: 0.067;  $p < 0.01$ ). Interestingly, low  $\beta$  displayed an initial coherence increase from quiet standing (median low  $\beta$  coherence: 0.122) and peaked at APA preparation (0.132, an epoch sooner than the other results discussed), then decreased upon early APA (0.126) and APA (0.065); these changes were significant for the earlier epochs to the terminal APA epoch only ( $p < 0.01$ ). Differing trends regarding significance were also seen for high  $\beta$ , with coherence decreasing

across the task after peaking in quiet standing. (Median low  $\beta$  coherence in quiet standing: 0.167, APA preparation: 0.154, early APA: 0.144, and APA: 0.085;  $p < 0.001-0.01$ ); again, these changes were significant for all earlier epochs to the terminal APA epoch only ( $p < 0.001-0.01$ ).

Within the “APA levodopa responsive” and “non-responsive” subject subgroups, there were no appreciable, consistent differences in coherence modulation between the subgroups across the task.

To summarize, coherence data reflected widespread increases across the task between pallidal-cortical regions under both medication states across most canonical frequency bands, with a decrease often observed between early APA and APA epochs (while remaining elevated compared to quiet standing).

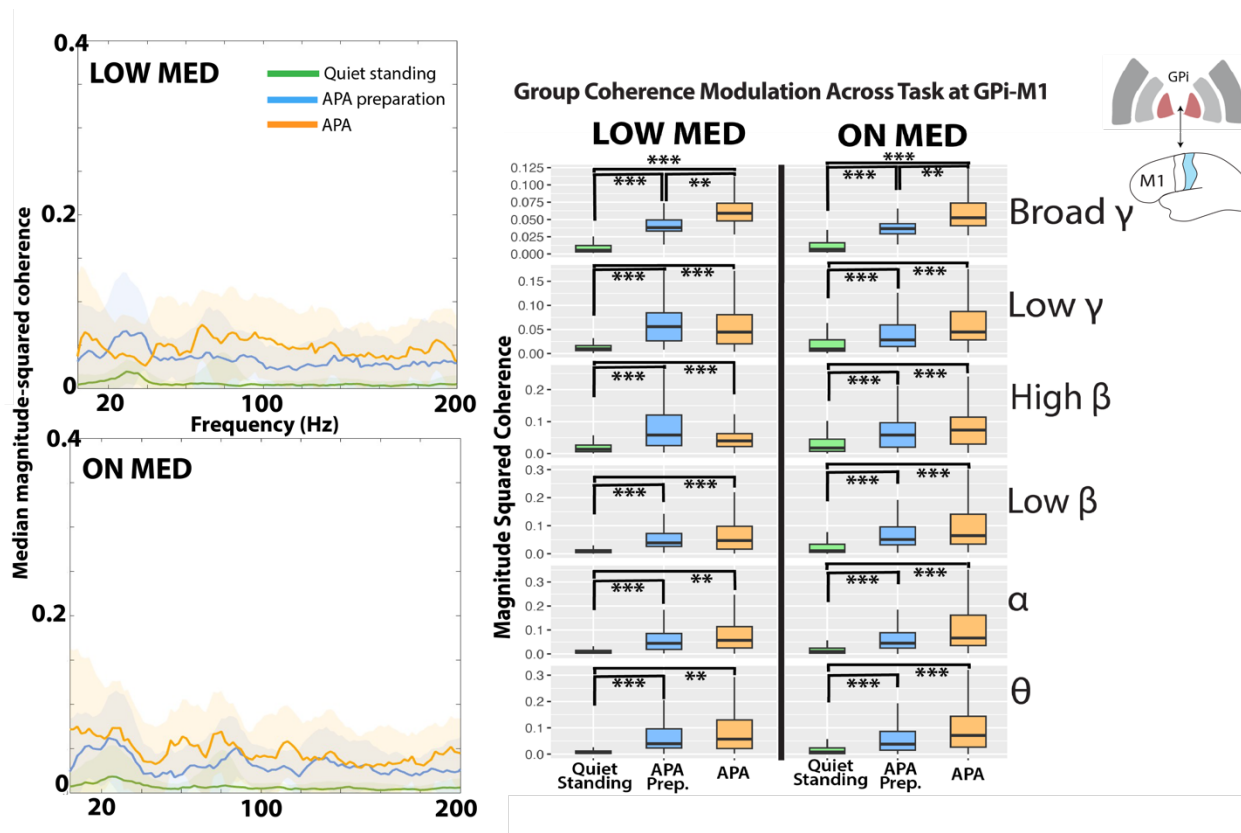


**Figure 3.4 Coherence modulation across GPI and M1 during gait initiation**

Figure footnotes: Group GPI-M1 magnitude-squared coherence data for “LOW” and “ON” medication states during the three primary task epochs: “Quiet standing,” “APA preparation” and “APA”. Plots represent median magnitude-squared coherence and median absolute deviations from all included trials and subjects. Boxplots represent averaged magnitude-squared coherence from each epoch within the canonical frequency bands and were created with the upper whisker representing  $1.5 \times$  the interquartile ratio (IQR) past the 3<sup>rd</sup> quartile and the lower whisker representing  $1.5 \times$  IQR below the 1<sup>st</sup> quartile. Significance between epochs is denoted with \*  $p < 0.05$ , \*\*  $p < 0.01$ , \*\*\*  $p < 0.001$  following Kruskal-Wallis testing and multiple corrections. Significant task-related coherence modulation is demonstrated under both medication states and frequencies. Abbreviations: GPI = globus pallidus internus, M1 = primary motor cortex; APA = anticipatory postural adjustment;  $\theta$  = theta,  $\alpha$  = alpha,  $\beta$  = beta,  $\gamma$  = gamma.



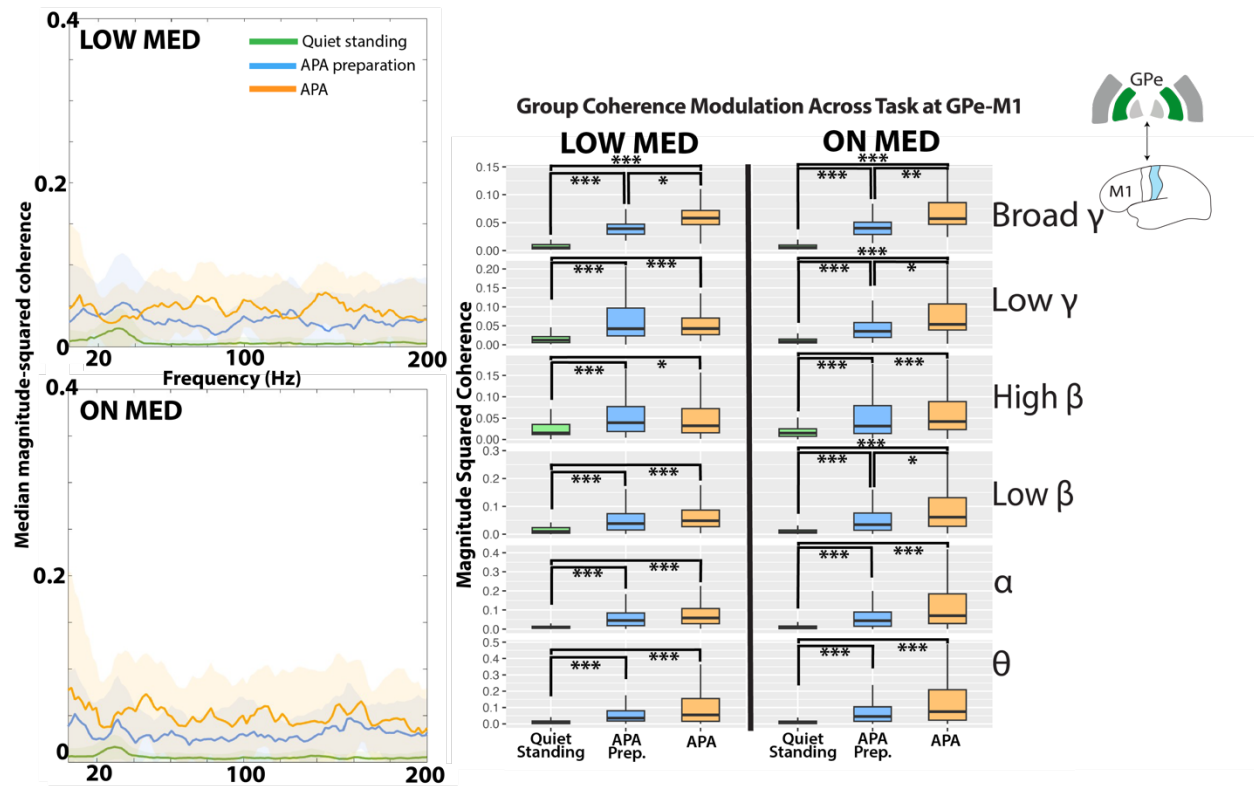


**Figure 3.5 Coherence modulation across GPe and M1 during gait initiation**

Figure footnotes: Group GPe-M1 magnitude-squared coherence data for “LOW” and “ON” medication states during the three primary task epochs: “Quiet standing,” “APA preparation” and “APA”. Plots represent median magnitude-squared coherence and median absolute deviations from all included trials and subjects. Boxplots represent averaged magnitude-squared coherence from each epoch within the canonical frequency bands and were created with the upper whisker representing 1.5 \* the interquartile ratio (IQR) past the 3<sup>rd</sup> quartile and the lower whisker representing 1.5 \* IQR below the 1<sup>st</sup> quartile. Significant task-related coherence modulation is demonstrated under both medication states and frequencies. Abbreviations: GPe = globus pallidus externus, M1 = primary motor cortex; APA = anticipatory postural adjustment;  $\theta$  = theta,  $\alpha$  = alpha,  $\beta$  = beta,  $\gamma$  = gamma.

### 3.3.4 Subcortical coherence modulation during APA is highly influential in determining APA amplitudes and timing, relative to neural power

Optimized LMMs built separately using normalized neural power and magnitude-squared coherence from the APA epoch are presented in Table 3.3 with significant predictors included for each APA metric; additional LMMs using data from other epochs and all model statistics are presented in supplemental Figures 3.8-3.11.

Cumulative APA was found to be largely, positively influenced by levodopa medication (estimate = 0.093,  $t = 2.43$ ,  $p < 0.05$ ), and negatively by M1 broadband  $\gamma$  power (estimate = -0.004,  $t = -2.24$ ,  $p < 0.05$ ) following backwards model selection for significant outcome predictors. PMC  $\theta$  power (estimate = -0.011,  $t = -2.36$ ,  $p < 0.05$ ) was shown to negatively impact peak APA amplitude; the random effects of subject variability were also significant in this LMM. For APA “net” amplitude, GPi broadband  $\gamma$  power (estimate = 0.018,  $t = 2.46$ ,  $p < 0.05$ ) was found to positively influence, while GPe low  $\gamma$  power (estimate = -0.014,  $t = -2.64$ ,  $p < 0.01$ ) was found to negatively influence amplitudes during gait initiation. The model with neural power and medication inputs during APA did not have any significant predictors following backwards selection for the time to peak APA amplitude metric.

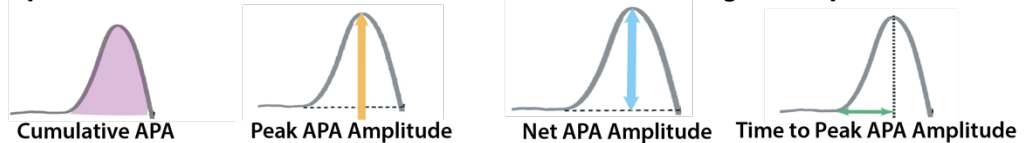
Using normalized coherence as input from the APA epoch, pallidal-cortical predictors of GPi-M1  $\theta$  (estimate =  $1.97 \times 10^{-5}$ ,  $t = -3.24$ ;  $p < 0.01$ ) and GPe-M1  $\alpha$  (estimate =  $-1.76 \times 10^{-6}$ ,  $t = -2.46$ ;  $p < 0.05$ ) coherence were found to negatively affect cumulative APA, and levodopa medication (estimate = 0.09,  $t = 2.64$ ,  $p < 0.01$ ), GPi-M1  $\alpha$  (estimate =  $2.38 \times 10^{-5}$ ,  $t = 2.30$ ;  $p < 0.05$ ), and GPe-PMC low  $\beta$  (estimate =  $6.89 \times 10^{-6}$ ,  $t = 2.52$ ;  $p < 0.05$ ) coherence were found to positively affect this metric. The random effects of subject variability were also significant in this LMM. For peak APA amplitudes, GPe-M1 low  $\beta$  coherence (estimate =  $-4.72 \times 10^{-5}$ ,  $t = -3.02$ ;  $p < 0.01$ ) was found to negatively affect this metric. The random effects of subject variability were again significant in this LMM. For “net” APA amplitudes, GPi-M1  $\theta$  (estimate =  $-7.81 \times 10^{-5}$ ,  $t = -2.93$ ;  $p < 0.01$ ) and GPe-M1 low  $\beta$  (estimate =  $-2.13 \times 10^{-5}$ ,  $t = -2.23$ ;  $p < 0.05$ ) coherence were found to negatively affect this metric. GPi-M1  $\alpha$  coherence (estimate =  $1.11 \times 10^{-4}$ ,  $t = 2.45$ ;  $p < 0.05$ ) was the sole

positive predictor in this model. The random effects of subject variability were again significant in this LMM. Lastly, the time to peak APA amplitude metric model included predictors of GPe-M1  $\alpha$  (estimate =  $-1.08 \times 10^{-6}$ ,  $t = -3.35$ ;  $p < 0.01$ ) and low  $\beta$  coherence (estimate =  $2.2 \times 10^{-6}$ ,  $t = 2.25$ ;  $p < 0.05$ ). If GPi-GPe coherence was a significance predictor in any of these optimized models, these data were not described, due to the likelihood of having artificially elevated coherence between these contacts due to shared signal proximity while recording from pallidal DBS leads in a sandwich configuration.

**Table 3.3 Linear mixed model results for APA metrics from “APA” epoch**

Table Footnotes: Linear mixed model results using normalized epoch power and coherence to predict APA metrics of amplitude and timing. The table provides significant model predictors and their relationship to each APA outcome following backwards model selection from the “APA” epoch. + : positive relationship between APA outcome and neural data; - : negative (inverse) relationship. Note: GPi-GPe coherence results were not included due to the likelihood of signal bias due to the sandwich recording configuration. Abbreviations: APA = anticipatory postural adjustments; GPi = globus pallidus internus, GPe = globus pallidus externus, M1 = primary motor cortex, PMC = premotor cortex;  $\theta$  = theta,  $\alpha$  = alpha,  $\beta$  = beta,  $\gamma$  = gamma.

**Optimized Linear Mixed Model Results for APA Metrics with a Single Task Epoch**



Linear Mixed Model Results for APAs using Normalized Power				
Medication +	Random (patient) effects	Broad $\gamma$ power +		
Broad $\gamma$ power -	$\theta$ power -	Low $\gamma$ power -		
Linear Mixed Model Results for APAs using Normalized Coherence				
Medication +				
$\theta$ - , $\alpha$ +			$\theta$ - , $\alpha$ +	
Low $\beta$ +				
$\alpha$ -		Low $\beta$ -	Low $\beta$ -	$\alpha$ - , Low $\beta$ +
Random (patient) effects	Random (patient) effects	Random (patient) effects		

### **3.4 Gait initiation discussion:**

This study combined biomechanical data assessing timing and amplitude metrics of APA performance and quality with neural recordings from cortical and subcortical areas during a bipedal gait initiation task. The goals of this work were to advance our understanding of how neural power, coherence, and levodopa medication at various regions implicated in human motor circuits interact during gait initiation and their respective influences on APA performance. It is expected that results from this work and others can be applied for the eventual development of individualized neuromodulatory therapeutics to improve treatment effectiveness for people with PD experiencing difficulties with gait initiation.

First, we demonstrate that APAs and neural modulation during gait initiation are individualized and subjects appear to vary in their responsiveness to levodopa medication despite similar baseline motor function. Second, we provide additional characterization of this modulation at the canonical frequencies relative to different epochs of the task featuring varying postural responses. Notably, power generally decreased incrementally across the task at lower frequencies, with broadband  $\gamma$  the opposite. Conversely, coherence generally increased at all canonical frequencies from quiet standing to early APA, before decreasing (but remaining elevated compared to quiet standing) during APA. Lastly, we suggest that coherence may be highly influential in predicting APA amplitudes and timing, relative to neural power, at these regions.

### **3.4.1 APAs and neurophysiology responsiveness to levodopa during gait initiation is subject-specific**

A main finding of this work is that subject responses to levodopa are highly variable based on the individual, observable both through APA performance as well as neurophysiology data. Subjects #2 and #4 had a marked motor response to levodopa in our study, exhibiting significant changes between medication states in APA amplitudes and timing, as well as in absolute power and coherence data across many epochs of the task and contacts, while Subjects #1 and #3 did not reach significance among their APA differences and displayed much less neural modulation across task epochs under both medication states. Subject #5 demonstrated much significant neural modulation under both medication states during the task, however accompanying medication-related differences were not observed in the APA metrics. Complicating things further, the subjects' baseline motor function, levodopa daily equivalent dosages (LEDD), and response to medication on clinical metrics were comparable to each other. More specifically, in the "APA levodopa responsive" subgroup, Subject #2 and #4's LEDD and UPDRS III scores were within the range of the subjects' in the "non-responsive" subgroup.

This finding is consistent with literature investigating the effects that both levodopa and DBS may have on APA performance, as well as suggesting a potential reason for why identifying effective therapeutics to treat gait initiation dysfunction is so difficult. Much research characterizing APAs in people with PD during gait initiation have suggested levodopa has either no effect, variable amplitude benefit, or a worsening effect on postural control (e.g. postural sway, latency of first step, etc.). We suggest that this variation in responses to levodopa may be due to the task's varying motor demands, requiring an individual to perform quiet standing (static postural control), an anticipatory postural

response under strict timing and scaling constraints, then stepping (motor execution), with each part critical for overall effectiveness. The differences seen across subjects in their APAs, neural modulation during the task, and levodopa responsiveness suggest each task component may be governed by somewhat disparate parts of the cortico-basal ganglia-thalamo-cortical loop, with individual disease progression and neural neurodegeneration affecting which circuits are more implicated and how levodopa-responsive they may be. These results are consistent with much literature suggesting that APAs (anticipatory postural control) may be coordinated via different circuits than other balance domains, as well as skilled gait<sup>45,107</sup>. Our results across the task and LMMs also exhibited much significance relating to neural modulation at the PMC and M1 during APA, suggesting validity of these theories. Continued validation of the potential diversity in postural-related circuits offer both a continued therapeutic challenge as well as reminder to clinicians of the importance of testing and treating dysfunction among these domains uniquely, as they may not respond to similar interventions equally.

Interestingly, all subjects, whether they demonstrated significant levodopa responsiveness, exhibited unique trends of APA timing and scaling under both medication states. For example, “ON” medication data shows Subject #2 had increased APA amplitude and time to peak amplitude, while Subject #3 had increased cumulative APA and time to peak amplitude, with lower peak and net APA amplitudes. This constellation of findings suggests there may also be an interplay between the temporal and amplitude aspects of APAs, such as a longer APA allows for appropriate force or movement generation, which levodopa may facilitate. For all subjects, cumulative APA (a combined time and amplitude APA proxy) and peak APA amplitudes were generally elevated while

“ON” medication, further suggesting the role that levodopa may have in non-specifically increasing APA amplitudes while perhaps having an unchanged, variable, or detrimental effect on the resulting timing and scaling metrics. These preliminary findings warrant further investigation regarding the effects of therapeutic intervention (e.g. physical therapy, DBS, levodopa) on various APA components, and whether influencing one aspect of APA has any effect on other APA aspects.

### **3.4.2 Gait initiation in Parkinson’s disease features stepwise decreases in power across lower frequencies**

Group power data across the task suggests that as subjects progressed through gait initiation, power at  $\alpha$ ,  $\beta$ , and low  $\gamma$  frequencies decreased, while simultaneously increased at broadband  $\gamma$  frequencies in subcortical and cortical circuits. These findings are consistent with theories regarding the roles that these oscillations may have in human movement, especially when considering the presumable incremental changes in motor activity during gait initiation as the task progresses from no movement (quiet standing) to small muscle activations with changing base of support (APA) and stepping.

In motor-related cortical regions, broadband  $\gamma$  power is thought to be a pro-kinetic signal which may exhibit modulation relative to task scaling or force requirements, thus the finding of increased contralateral broadband cortical  $\gamma$  power as the motor vigor of the task increases is consistent with these results<sup>108</sup>. Increased STN broadband  $\gamma$  power has also been reported during motor activities, with maximal activity at peak movement velocity compared to onset and amplitude during voluntary hand movements<sup>109</sup>. These results all suggest gamma modulation at both cortical and subcortical regions to be

dynamically affected by motor task parameters and unique task time windows, as well as potentially mediating different processes besides pure movement.

Similar studies<sup>108-110</sup> have also consistently reported contralateral  $\beta$  desynchronization to accompany physiological movement initiation at the cortex and basal ganglia, thought to facilitate movement via subcortical de-inhibition. Our results are consistent with this and complementary findings linking gait initiation errors to less-intense event-related desynchronizations at the sensorimotor cortex,<sup>111</sup> suggesting that effective gait initiation may be mediated by stepwise  $\beta$  oscillatory decreases at the cortex and pallidum following quiet standing to APA and stepping. Previous EEG and ECoG work<sup>110</sup> have also linked movement initiation to  $\alpha$  desynchronization, thought to mediate greater attentional control or sensorimotor integration. In our study, task-related  $\alpha$  modulation seems probable due to the subject watching the screen for a cue and preparing to step in response (significantly utilizing these processes) during quiet standing and APA preparation, before displaying decreased power during APA if the motor program was already selected and integrated.

### **3.4.3 Gait initiation in Parkinson's disease features widespread, stepwise increases in coherence prior to decreasing with APA across pallidal-cortical circuits**

Our group results offering novel characterization of cortical and pallidal coherence modulation during gait initiation suggests circuit connectivity may differ from power modulation across the task. Under both medication states, both subcortical-cortical and cortical coherence generally increased for  $\theta$ ,  $\alpha$ ,  $\beta$ , and  $\gamma$  frequencies as the task progressed from quiet standing to early APA, before decreasing during the APA execution



and stepping epoch. These results are mostly complementary to research linking dynamic changes in coherence during gait in PD, as previous work showed STN  $\beta$  coherence and power to decrease during movement (relative to resting and standing) in people with PD<sup>112</sup>, with elevated cortical coherence across  $\alpha$ ,  $\beta$ , and  $\gamma$  frequencies linked to postural control issues such as FoG in PD<sup>113</sup>. Additionally, consistent with our results of elevated broadband  $\gamma$  coherence across the task relative to quiet standing, prior work has documented the presence of increased broadband  $\gamma$  coherence between basal ganglia-M1 during a button pressing task, theorized to represent physiological drive to M1 around movement onset<sup>108</sup>. Broadly, these results suggest that perhaps the increased coherence through the early part of the task (APA and its preparation) facilitates gross motor drive from the pallidum to the cortex, with the stepping component of the gait initiation task representing a switch in motor plans and circuitry or more automatic control coinciding with a decrease in coherence. An alternative explanation to these data however, is that perhaps this widespread, elevated coherence is mediating gait initiation difficulties and represents more pathological vs physiological neural activity.

As our results are in individuals with gait initiation difficulties, it is unclear whether the modulation observed in coherence and power across the task are reflective of physiological phenomenon or dysfunctional processes. These results do reinforce the importance of circuit connectivity and neural modulation in mediating PD-related motor symptoms, however further investigation is required to untangle under which task conditions, across which regions, and in which types of patient presentations coherence switches from being “elevated and pathologic” (causing detrimental effects such as FoG) to “beneficial and/or compensatory” (improving motor vigor and metrics including speed,

stride length, or APAs). Regardless, these findings validate ideas that coherence does not remain fixed throughout the preparation and execution of a motor task.

### **3.4.3 APA timing in PD is significantly influenced by coherence, relative to power**

A primary finding through this work from grouped subject data using normalized epoch data and LMMs is the relative significance of neural coherence during APAs in influencing gait initiation quality and safety (especially in APA timing) as measured with amplitude and timing metrics.

For cumulative APA, lower-frequency pallidal-cortical coherence was particularly influential, with a mix of predictors which were shown to both positively and negatively affect the metric. This supports the idea that there are likely various neural phenomena underlying APA, which are reflected across multiple regions and frequencies. With the findings above suggesting that decreased coherence may benefit postural control (FoG) in people with PD, our results suggest that perhaps this may be true for some regions (e.g. GPe-M1) but not true for others (e.g. GPe-PMC). Interestingly,  $\alpha$  coherence across GPi-M1 was shown to positively affect cumulative APA, while  $\alpha$  coherence across GPe-M1 negatively affected this metric; thus, this band may represent a useful therapeutic target to explore with neuromodulatory interventions in the future. The cumulative APA metric was also the only instance levodopa was significant in the optimized LMMs. While evidence of levodopa's effects on increased force production exists in the literature<sup>114</sup>, the magnitude of its effects on the metric compared to the neural modulation predictors suggests that it may non-specifically predominate or override physiological modulation occurring during APA, with unknown consequence.

While our group results exhibited stepwise M1 broadband  $\gamma$  power increases across the task, the finding that this may not benefit cumulative APA size is surprising. Perhaps this is due to a necessary “scaling” period which occurs for effective APA execution, where cortical broadband  $\gamma$  power is transiently decreased at the cortex to facilitate execution of the postural response. Similarly, the LMM results for the time to peak APA amplitude metric may also support this theory, as one of its significant predictors was GPe-M1 low  $\beta$  coherence, which increased the time to peak APA amplitude. Thus, perhaps the window for effective APA scaling is mediated by dynamic pallidal-cortical  $\beta$  and broadband  $\gamma$  modulation, through preventing a change in motor program or movement vigor to maintain “status quo” until task scaling is completed.

Conversely, both peak APA and “net” APA amplitudes were negatively affected by low  $\beta$  pallidal-cortical coherence. This suggests that perhaps these metrics rely less on a critical “scaling” window, or simply that decreased  $\beta$  synchrony may be necessary for physiological refinement or integration of a different motor program (e.g. for APA or stepping, from quiet standing). The sole power predictor for increased peak APA amplitude (a proxy for movement vigor) was decreased cortical  $\theta$  power, which is consistent with the likelihood that the attentional focus demands decreased following cue and response.

#### **3.4.4 Limitations to the gait initiation task**

One significant limitation for this task was the varied number of gait initiation trials analyzed for each subject due to individuals’ motor function and symptoms or fatigue, as well as some trial elimination due to stepping with the opposite (non-dominant) foot and/or

lacking APA or the presence of multiple APAs prior to stepping. Every attempt was made to utilize all trials wherever possible. Neural data analyzed in this study all utilized the subject's contralateral hemisphere to their stepping foot; this methodology does not account for potential motor-related ipsilateral neural activation which is not yet as well conceptualized. Another limitation for this analysis is that the trials where subjects demonstrated severe gait initiation impairments were not included, due to the lack of quiet standing, multiple APAs with no quiet standing between, etc. which made compiling the data into discrete and consistent epochs difficult. However, these data likely offer great insights into the dysfunction relating to circuit breakdown, suggesting future work analyze these trials and compare them to these results as well.

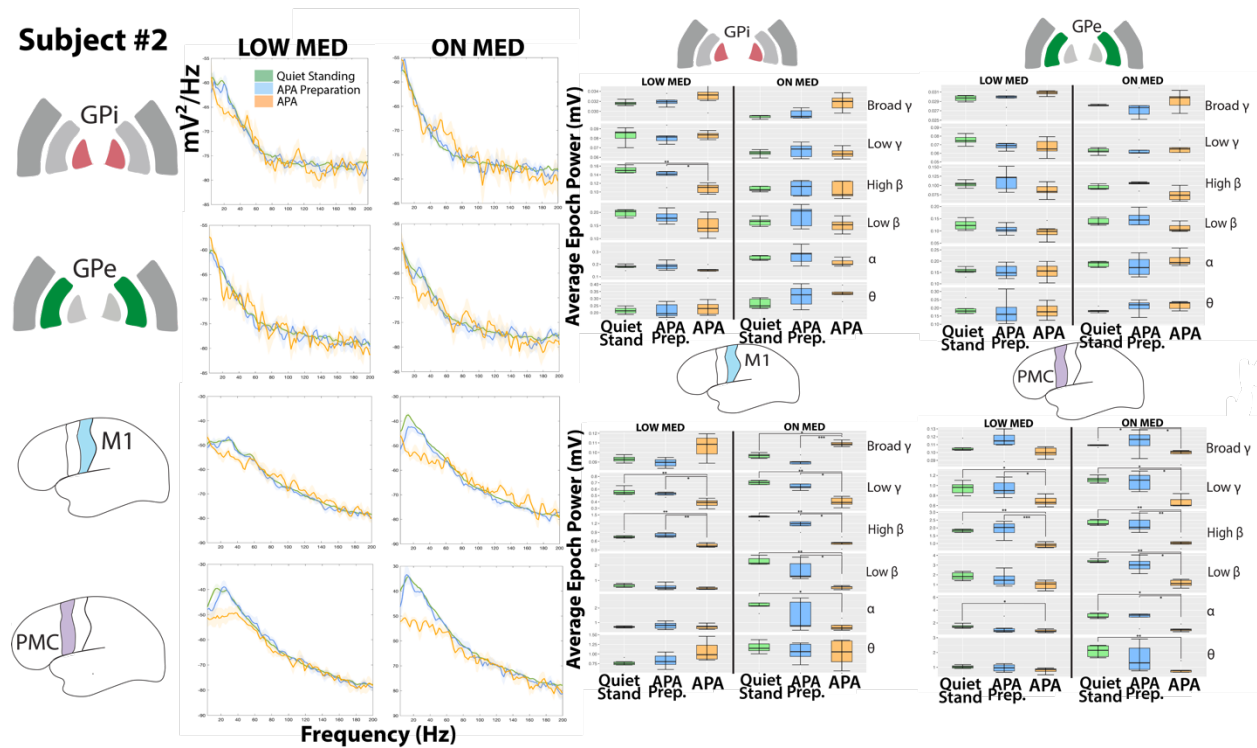
### **3.5 Gait initiation conclusions:**

Gait initiation is a highly individualized and complex motor task typically requiring an APA for effective performance. APA metrics and the circuits governing these processes appear to be variably affected by levodopa depending on the subject's underlying pathophysiology and neural location. Furthermore, it appears APA quality (especially timing) may be preferentially influenced by dynamic cortical-subcortical coherence at motor-related neural regions across various canonical frequencies regardless of levodopa state. These findings offer greater insight into power and coherence modulation associated with the varying postural responses in PD exhibited during gait initiation, with the goal of assisting in the development of effective interventions for treating dysfunction in this fundamental motor task.

### 3.6 Gait initiation supplemental materials:

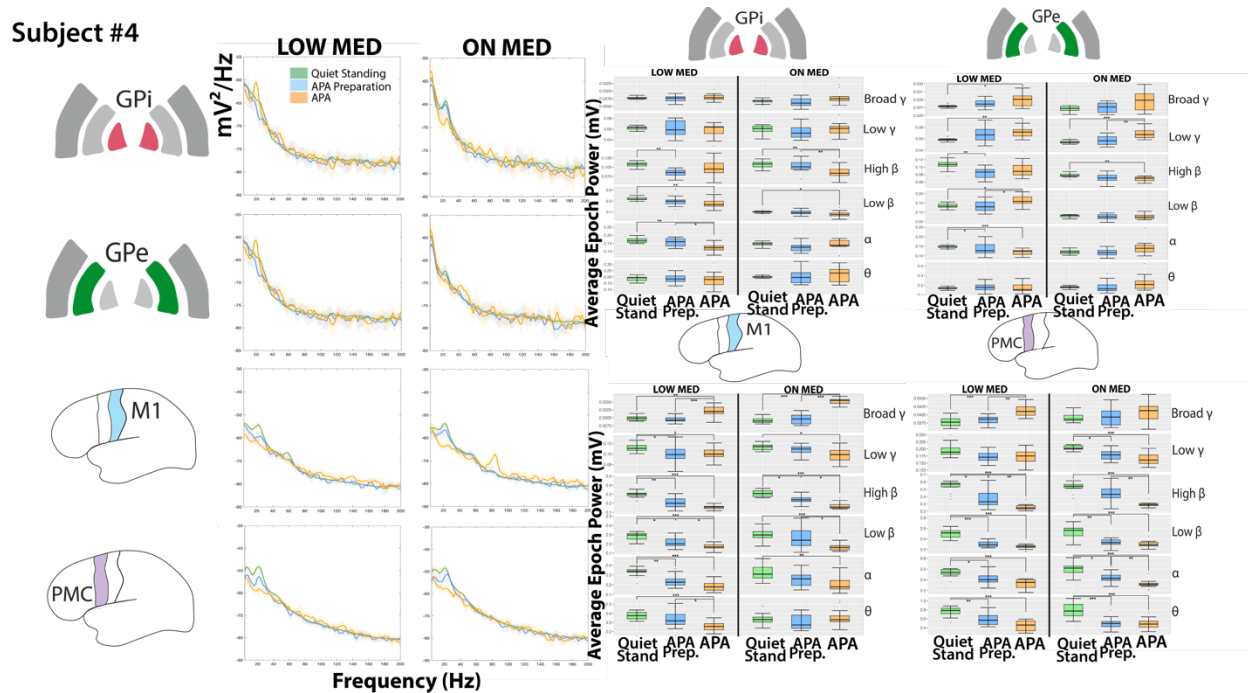
Individual subject power modulation across the task (Figures 3.6-3.10):

Subjects #2 and 4 are grouped together for ease of comparison, as they were categorized as “APA levodopa responders”, whereas Subjects #1, 3, and 5 as “non-responders.”



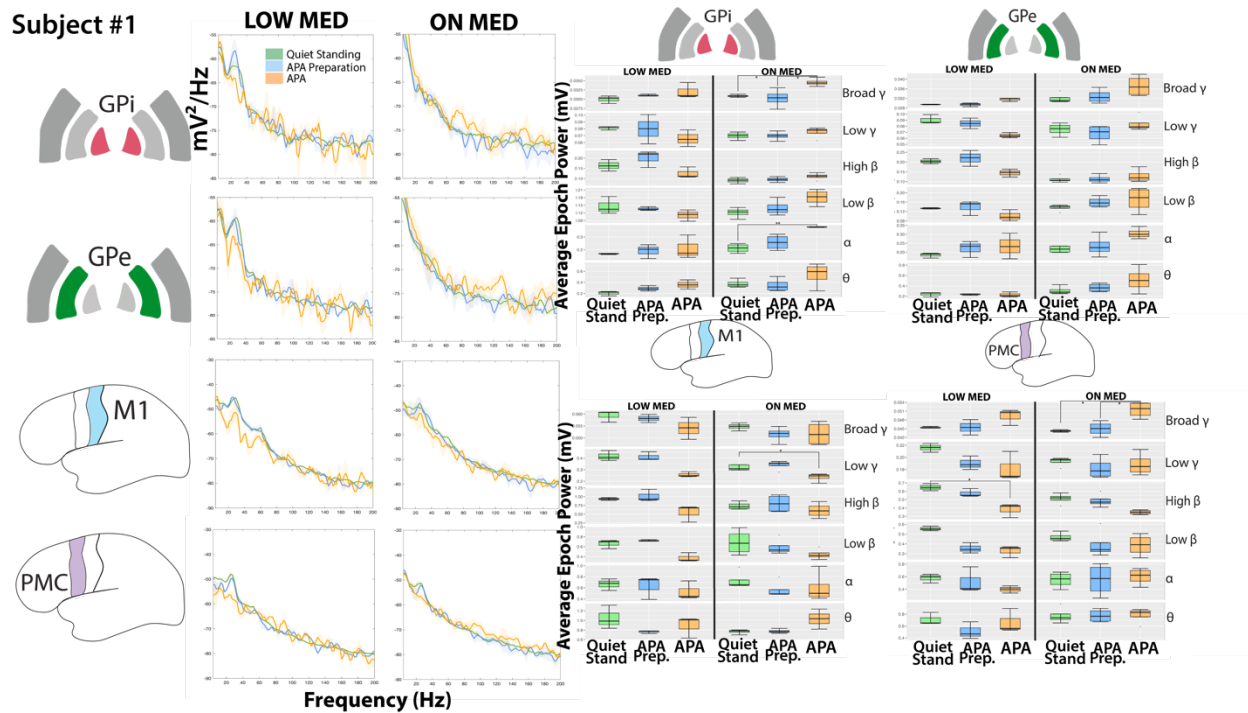
**Figure 3.6: Subject #2 power modulation across the task**

Figure footnotes: Subject #2’s median PSDs and median absolute deviations for “LOW” and “ON” medication states during the three primary task epochs: “Quiet standing,” “APA preparation” and “APA” at all contacts. Boxplots demonstrate average power from the “spectrogram” function during each epoch across the canonical frequencies created with the “geom\_boxplot” and “stat\_boxplot” functions in R/RStudio. Significance between epochs is denoted with \*  $p < 0.05$  and \*\*  $p < 0.01$  following Kruskal-Wallis testing and multiple corrections. GPi = globus pallidus internus, GPe = globus pallidus externus, M1 = primary motor cortex, PMC = premotor cortex.  $\theta$  = theta,  $\alpha$  = alpha,  $\beta$  = beta,  $\gamma$  = gamma. Significance in task-related power modulation was seen for GPi  $\beta$  power while “LOW” medication, as well as M1 and PMC  $\beta$  and  $\gamma$  under both medication states; M1 while “ON” medication and PMC under both medication states also displayed significant modulation for  $\alpha$  frequencies as well as PMC for  $\theta$  while “ON” medication.



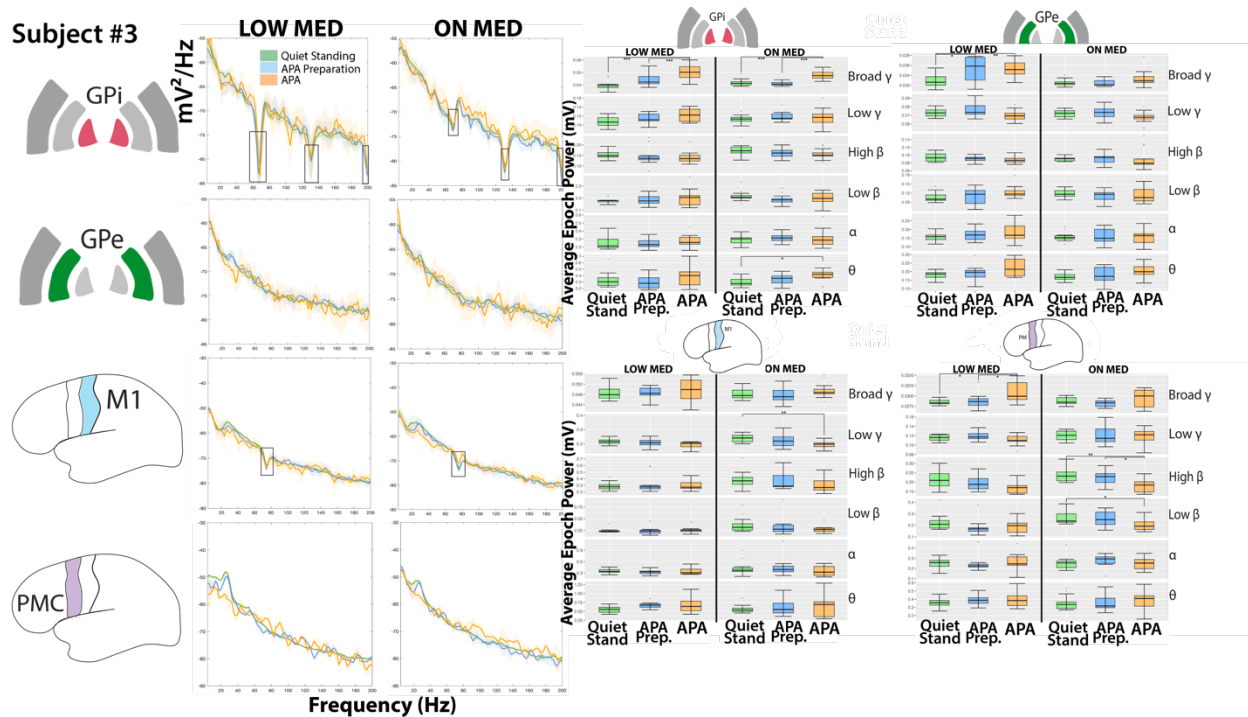
**Figure 3.7: Subject #4 power modulation across the task**

Figure footnotes: Subject #4's median PSDs and median absolute deviations for "LOW" and "ON" medication states during the three primary task epochs: "Quiet standing," "APA preparation" and "APA" at all contacts. Boxplots demonstrate average power from the "spectrogram" function during each epoch across the canonical frequencies and were created with the "geom\_boxplot" and "stat\_boxplot" functions in R/RStudio. Significance between epochs is denoted with \*  $p < 0.05$ , \*\*  $p < 0.01$ , \*\*\*  $p < 0.001$  following Kruskal-Wallis testing and multiple corrections. GPi = globus pallidus internus, GPe = globus pallidus externus, M1 = primary motor cortex, PMC = premotor cortex.  $\theta$  = theta,  $\alpha$  = alpha,  $\beta$  = beta,  $\gamma$  = gamma. Task-related power modulation was significant for this individual for pallidal  $\beta$  frequencies under both medication states, as well as  $\alpha$  while "LOW" medication; other significance was observed at  $\gamma$  for GPe. Cortical power modulation exhibited significance across all canonical frequency bands and medication states.



**Figure 3.8: Subject #1 power modulation across the task**

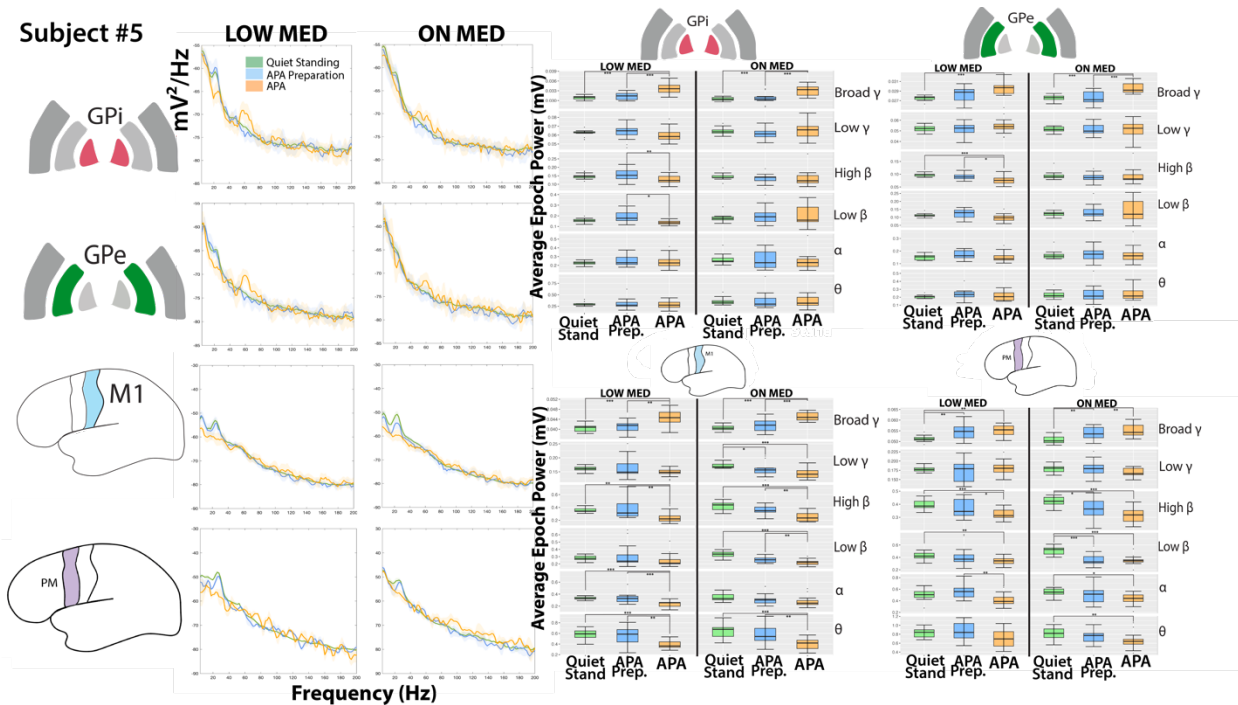
Figure footnotes: Subject #1's median PSDs and median absolute deviations for "LOW" and "ON" medication states during the three primary task epochs: "Quiet standing," "APA preparation" and "APA" at all contacts. Boxplots demonstrate average power from the "spectrogram" function during each epoch across the canonical frequencies and were created with the "geom\_boxplot" and "stat\_boxplot" functions in R/RStudio. Significance between epochs is denoted with \*  $p < 0.05$  following Kruskal-Wallis testing and multiple corrections. GPi = globus pallidus internus, GPe = globus pallidus externus, M1 = primary motor cortex, PMC = premotor cortex.  $\theta$  = theta,  $\alpha$  = alpha,  $\beta$  = beta,  $\gamma$  = gamma. Significance was seen in task-related power modulation for this individual while "ON" medication for GPi  $\alpha$  and broadband  $\gamma$  frequencies, M1 "ON" medication low  $\gamma$ , and PMC high  $\beta$  ("LOW" medication) and broadband  $\gamma$  "ON" medication.



**Figure 3.9: Subject #3 power modulation across the task**

Figure footnotes: Subject #3's median PSDs and median absolute deviations for "LOW" and "ON" medication states during the three primary task epochs: "Quiet standing," "APA preparation" and "APA" at all contacts. Boxplots demonstrate average power from the "spectrogram" function during each epoch across the canonical frequencies and were created with the "geom\_boxplot" and "stat\_boxplot" functions in R/RStudio. Significance between epochs is denoted with \*  $p < 0.05$ , \*\*  $p < 0.01$ , \*\*\*  $p < 0.001$  following Kruskal-Wallis testing and multiple corrections. GPI = globus pallidus internus, GPe = globus pallidus externus, M1 = primary motor cortex, PMC = premotor cortex.  $\theta$  = theta,  $\alpha$  = alpha,  $\beta$  = beta,  $\gamma$  = gamma. Significance in task-related power modulation was observed in this individual for GPI broadband  $\gamma$  (both medication states), and  $\theta$  while "ON" medication, as well as GPe and PMC broadband  $\gamma$  ("LOW" medication only), M1 "ON" medication low  $\gamma$ , and PMC  $\beta$  while "ON" medication. Subject's data were notch filtered at the frequencies in black boxes for improved data visualization and PSD generation (further reasoning and parameters detailed in Aim 1 methods).

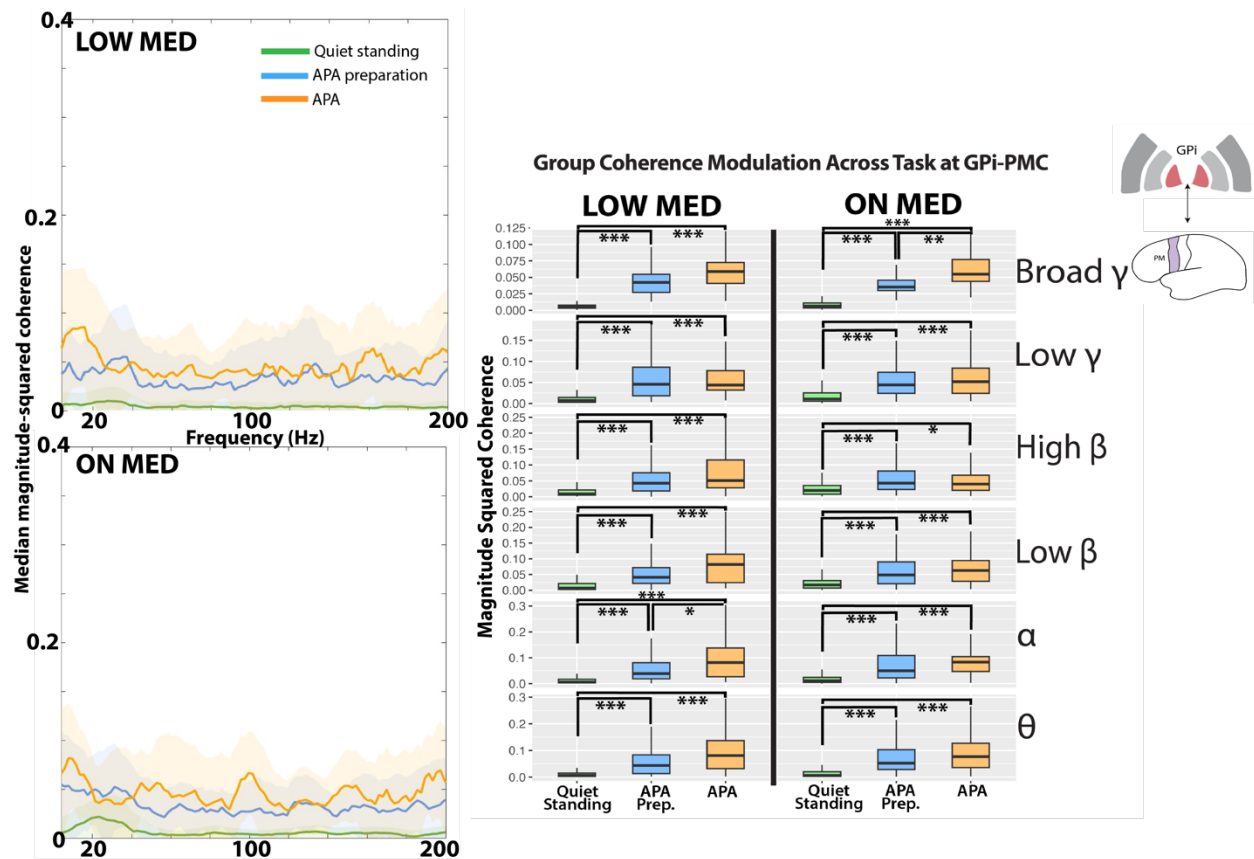




**Figure 3.10: Subject #5 power modulation across the task**

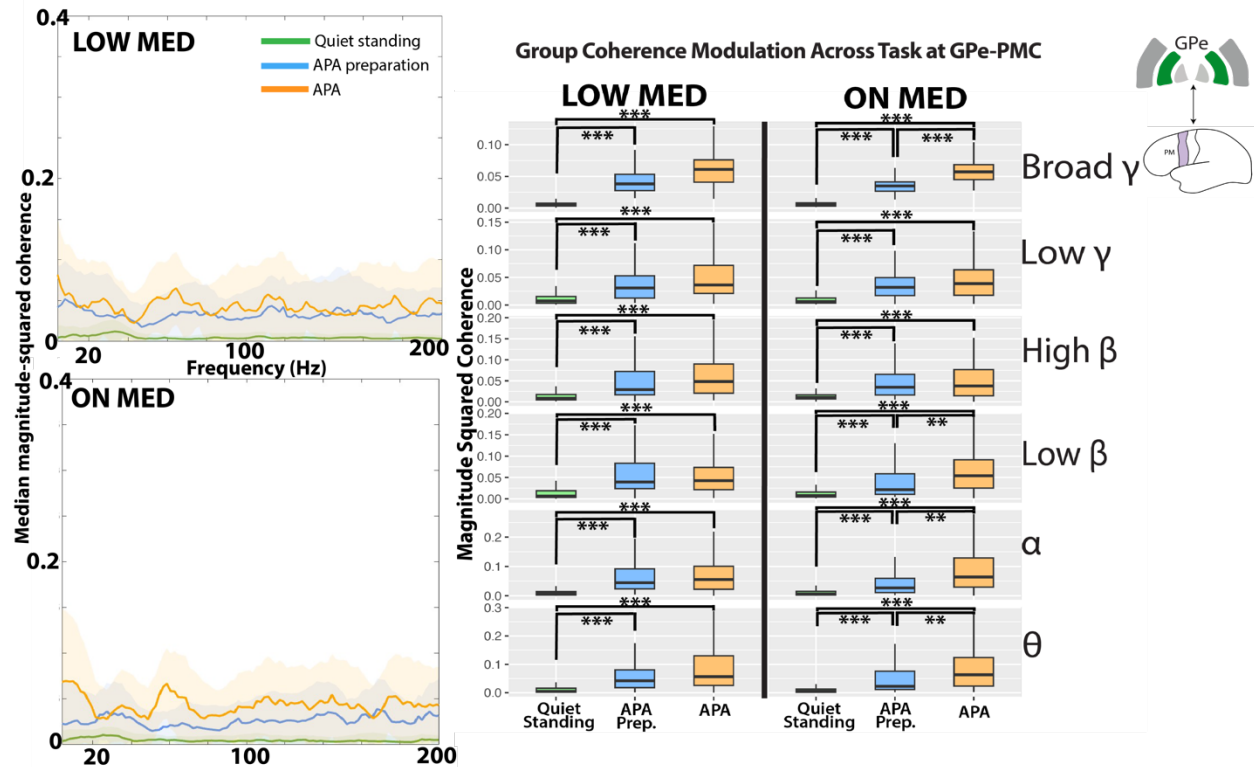
Figure footnotes: Subject #5's median PSDs and median absolute deviations for "LOW" and "ON" medication states during the three primary task epochs: "Quiet standing," "APA preparation" and "APA" at all contacts. Boxplots demonstrate average power from the "spectrogram" function during each epoch across the canonical frequencies and were created with the "geom\_boxplot" and "stat\_boxplot" functions in R/RStudio. Significance between epochs is denoted with \*  $p < 0.05$ , \*\*  $p < 0.01$ , \*\*\*  $p < 0.001$  following Kruskal-Wallis testing and multiple corrections. GPi = globus pallidus internus, GPe = globus pallidus externus, M1 = primary motor cortex, PMC = premotor cortex.  $\theta$  = theta,  $\alpha$  = alpha,  $\beta$  = beta,  $\gamma$  = gamma. Significance in task-related power modulation was observed in this individual for GPi, GPe, M1, and PMC broadband  $\gamma$  (both medication states), and GPi and GPe  $\beta$  while "LOW" medication only. M1 and PMC featured much additional  $\theta$ ,  $\alpha$ ,  $\beta$  and low  $\gamma$  significant power modulation under both medication states.

Group coherence modulation across the task (Figures 3.11-3.13)



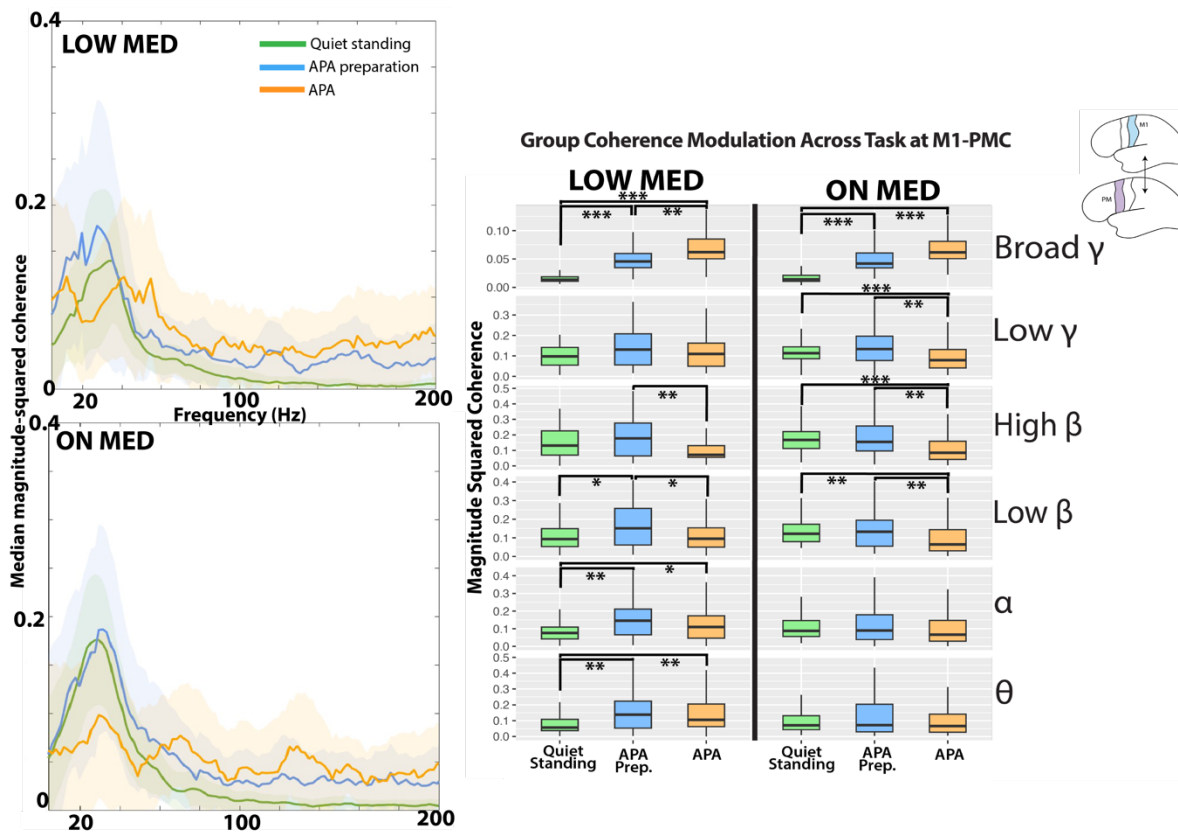
**Figure 3.11 Coherence modulation across GPI and PMC during gait initiation**

Figure footnotes: Group GPI-PMC magnitude-squared coherence for “LOW” and “ON” medication states during the three primary task epochs: “Quiet standing,” “APA preparation” and “APA”. Plots represent median magnitude-squared coherence and median absolute deviations from all included trials and subjects. Boxplots represent averaged magnitude-squared coherence from each epoch within the canonical frequency bands and were created with the upper whisker representing 1.5 \* the interquartile ratio (IQR) past the 3<sup>rd</sup> quartile and the lower whisker representing 1.5 \* IQR below the 1<sup>st</sup> quartile. Significant task-related coherence modulation is demonstrated under both medication states at all canonical frequencies. Abbreviations: GPI = globus pallidus internus, PMC = premotor cortex; APA = anticipatory postural adjustment;  $\theta$  = theta,  $\alpha$  = alpha,  $\beta$  = beta,  $\gamma$  = gamma.



**Figure 3.12 Coherence modulation across GPe and PMC during gait initiation**

Figure footnotes: Group GPe-PMC magnitude-squared coherence for “LOW” and “ON” medication states during the three primary task epochs: “Quiet standing,” “APA preparation” and “APA”. Plots represent median magnitude-squared coherence and median absolute deviations from all included trials and subjects. Boxplots represent averaged magnitude-squared coherence from each epoch within the canonical frequency bands and were created with the upper whisker representing 1.5 \* the interquartile ratio (IQR) past the 3<sup>rd</sup> quartile and the lower whisker representing 1.5 \* IQR below the 1<sup>st</sup> quartile. Significant task-related coherence modulation is demonstrated under both medication states and frequencies. Abbreviations: GPe = globus pallidus externus, PMC = premotor cortex; APA = anticipatory postural adjustment;  $\theta$  = theta,  $\alpha$  = alpha,  $\beta$  = beta,  $\gamma$  = gamma.

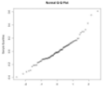
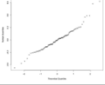
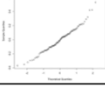
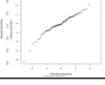
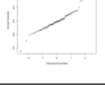
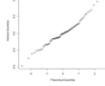


**Figure 3.13 Coherence modulation across M1 and PMC during gait initiation**

Figure footnotes: Group M1-PMC magnitude-squared coherence for “LOW” and “ON” medication states during the three primary task epochs: “Quiet standing,” “APA preparation” and “APA”. Plots represent median magnitude-squared coherence and median absolute deviations from all included trials and subjects. Boxplots represent averaged magnitude-squared coherence from each epoch within the canonical frequency bands and were created with the upper whisker representing 1.5 \* the interquartile ratio (IQR) past the 3<sup>rd</sup> quartile and the lower whisker representing 1.5 \* IQR below the 1<sup>st</sup> quartile. Significant task-related coherence modulation is demonstrated under both medication states and frequencies. Abbreviations: M1 = primary motor cortex, PMC = premotor cortex; APA = anticipatory postural adjustment;  $\theta$  = theta,  $\alpha$  = alpha,  $\beta$  = beta,  $\gamma$  = gamma.

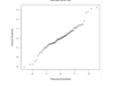
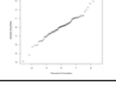
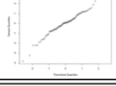
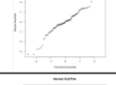
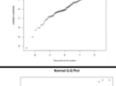
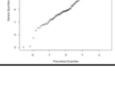
**Table 3.4 Cumulative APA linear mixed model summary results**

Table footnotes: Summary statistics from the LMMs for this metric from the three primary task epochs, which were normalized to quiet standing. AIC = Akaike Information Criterion; VIF = variance inflation factor. Random effects presented as the variance (standard deviation); if “N/A” this indicates the optimized model did not include this as a significant predictor. Note: GPI-GPe coherence predictors are included here if part of the optimized model, however, were not discussed in the main results and should be interpreted with caution due to the presence of potentially inflated values due to presumable signal overlap from recording in a sandwich configuration within the pallidum. APA = anticipatory postural adjustment, GPI = globus pallidus internus, GPe = globus pallidus externus, M1 = primary motor cortex, PMC = premotor cortex.

Epoch	Normalized data input	AIC	VIFs	Significant predictors (t-statistic)	Q-Q plot	Random effects: variance (std)
APA Preparation	Power	-55.987	1.00-1.01	GPI low $\gamma$ (2.93) & GPe low $\gamma$ (-2.19), GPe $\theta$ (2.50); medication (2.19)		N/A
Early APA	Power	-49.304	1.00-1.01	GPe low $\gamma$ (-2.14), PMC $\alpha$ (2.13); medication (2.38)		N/A
<b>Total APA</b>	<b>Power</b>	<b>-47.293</b>	<b>1.03</b>	<b>MI broadband <math>\gamma</math> (-2.28); medication (2.45)</b>		<b>N/A</b>
APA Preparation	Coherence	-53.112	1.01-1.02	GPI-GPe low $\beta$ (2.64), GPe-MI $\alpha$ (-2.41), medication (2.09)		N/A
Early APA	Coherence	24.126	1.02-1.07	GPI-GPe $\theta$ (-3.27), GPe-MI low $\beta$ (-2.11), GPe-PMC broadband $\gamma$ (-3.27); MI-PMC broadband $\gamma$ (-3.07); medication (2.80)		Patient ID: 0.01 (0.11) Residual: 0.02 (0.15)
<b>Total APA</b>	<b>Coherence</b>	<b>78.257</b>	<b>1.03-4.6</b>	<b>GPI-GPe low <math>\gamma</math> (-2.39) &amp; broadband <math>\gamma</math> (-2.73), GPI-MI <math>\theta</math> (-3.24) &amp; <math>\alpha</math> (2.30), GPe-MI <math>\alpha</math> (-2.46), GPe-PMC low <math>\beta</math> (2.52); medication (2.64)</b>		<b>Patient ID: 0.01 (0.11) Residual: 0.02 (0.15)</b>

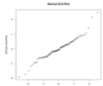
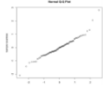
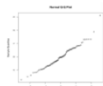
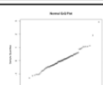
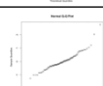
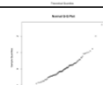
**Table 3.5 Peak APA amplitude linear mixed model summary results**

Table footnotes: Summary statistics from the LMMs for this metric from the three primary task epochs, which were normalized to quiet standing. AIC = Akaike Information Criterion; VIF = variance inflation factor. Random effects presented as the variance (standard deviation); if “N/A” this indicates the optimized model did not include this as a significant predictor. Note: GPI-GPe coherence predictors are included here if part of the optimized model, however, were not discussed in the main results and should be interpreted with caution due to the presence of potentially inflated values due to presumable signal overlap from recording in a sandwich configuration within the pallidum. APA = anticipatory postural adjustment, GPI = globus pallidus internus, GPe = globus pallidus externus, M1 = primary motor cortex, PMC = premotor cortex.

Epoch	Normalized data input	AIC	VIFs	Significant predictors (t-statistic)	Q-Q plot	Random effects: variance (std)
APA Preparation	Power	355.683	1.04-1.28	GPI $\theta$ (-2.80), GPe $\theta$ (2.56), GPe high $\beta$ (1.92)		Patient ID: 0.40 (0.63) Residual: 1.41 (1.19)
Early APA	Power	339.567	N/A	PMC $\theta$ (-2.58)		Patient ID: 0.47 (0.69) Residual: 1.45 (1.20)
<b>Total APA</b>	<b>Power</b>	<b>340.132</b>	<b>N/A</b>	<b>PMC <math>\theta</math> (-2.36)</b>		<b>Patient ID: 0.47 (0.68)</b> <b>Residual: 1.46 (1.21)</b>
APA Preparation	Coherence	340.522	N/A	GPe-PMC broadband $\gamma$ (-2.31)		Patient ID: 0.45 (0.67) Residual: 1.48 (1.22)
Early APA	Coherence	369.096	1.01-1.02	GPI-GPe $\theta$ (-3.38), GPI-M1 $\alpha$ (2.12), GPe-PMC broadband $\gamma$ (-2.91)		Patient ID: 0.50 (0.71) Residual: 1.27 (1.13)
<b>Total APA</b>	<b>Coherence</b>	<b>377.062</b>	<b>1.02-1.20</b>	<b>GPI-GPe <math>\theta</math> (-2.38) &amp; low <math>\gamma</math> (-2.90) &amp; broadband <math>\gamma</math> (-2.80), GPe-M1 low <math>\beta</math> (-3.02)</b>		<b>Patient ID: 0.45 (0.67)</b> <b>Residual: 1.22 (1.10)</b>

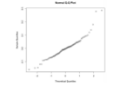
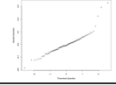
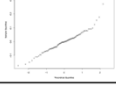
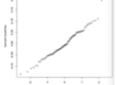
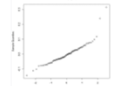
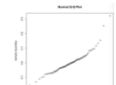
**Table 3.6 Net APA amplitude linear mixed model summary results**

Table footnotes: Summary statistics from the LMMs for this metric from the three primary task epochs, which were normalized to quiet standing. AIC = Akaike Information Criterion; VIF = variance inflation factor. Random effects presented as the variance (standard deviation); if “N/A” this indicates the optimized model did not include this as a significant predictor. Note: GPI-GPe coherence predictors are included here if part of the optimized model, however, were not discussed in the main results and should be interpreted with caution due to the presence of potentially inflated values due to presumable signal overlap from recording in a sandwich configuration within the pallidum. APA = anticipatory postural adjustment, GPI = globus pallidus internus, GPe = globus pallidus externus, M1 = primary motor cortex, PMC = premotor cortex.

Epoch	Normalized data input	AIC	VIFs	Significant predictors (t-statistic)	Q-Q plot	Random effects: variance (std)
APA Preparation	Power	256.999	1.01-1.08	GPI low $\beta$ (-2.31), GPe $\theta$ (2.80), GPe high $\beta$ (2.35)		Patient ID: 0.17 (0.41) Residual: 0.49 (0.70)
Early APA	Power	241.669	N/A	PMC $\theta$ (-2.64)		Patient ID: 0.34 (0.59) Residual: 0.51 (0.71)
<b>Total APA</b>	<b>Power</b>	<b>241.954</b>	<b>1.01</b>	<b>GPI broadband <math>\gamma</math> (2.47), GPe low <math>\gamma</math> (-2.64)</b>		<b>N/A</b>
APA Preparation	Coherence	276.070	1.40-3.28	GPI-GPe high $\beta$ (2.05) & low $\gamma$ (-2.77), GPe-PMC broadband $\gamma$ (-2.68)		Patient ID: 0.23 (0.48) Residual: 0.51 (0.71)
Early APA	Coherence	253.984	1.00	GPI-GPe low $\gamma$ (-2.75), GPe-PMC broadband $\gamma$ (-3.74)		Patient ID: 0.38 (0.62) Residual: 0.48 (0.69)
<b>Total APA</b>	<b>Coherence</b>	<b>308.384</b>	<b>1.03-4.69</b>	<b>GPI-GPe low <math>\gamma</math> (-2.56) &amp; broadband <math>\gamma</math> (-2.13), GPI-M1 <math>\theta</math> (-2.93) &amp; <math>\alpha</math> (2.45), GPe-M1 low <math>\beta</math> (-2.23)</b>		<b>Patient ID: 0.38 (0.61) Residual: 0.44 (0.66)</b>

**Table 3.7 Time to peak APA amplitude linear mixed model summary results**

Table footnotes: Summary statistics from the LMMs for this metric from the three primary task epochs, which were normalized to quiet standing. AIC = Akaike Information Criterion; VIF = variance inflation factor. Random effects presented as the variance (standard deviation); if “N/A” this indicates the optimized model did not include this as a significant predictor. N/A in the VIF column indicates there was 1 predictor only in the optimized LMM so VIFs were not generated. APA = anticipatory postural adjustment. Note: GPi-GPe coherence predictors are included here if part of the optimized model, however, were not discussed in the main results and should be interpreted with caution due to the presence of potentially inflated values due to recording in a sandwich configuration within the pallidum.

Epoch	Normalized data input	AIC	VIFs	Significant predictors (t-statistic)	Q-Q plot	Random effects: variance (std)
APA Preparation	Power	-221.914	1.2-1.4	GPi high $\beta$ (-2.51), M1 $\theta$ (-2.75), M1 low $\beta$ (2.55)		N/A
Early APA	Power	-219.913	1.08	M1 high $\beta$ (2.29), PMC $\theta$ (-2.43)		N/A
<b>Total APA</b>	<b>Power</b>	<b>-215.230</b>	<b>N/A</b>	<b>N/A</b>		<b>N/A</b>
APA Preparation	Coherence	-244.749	1.04-1.14	GPi-GPe $\alpha$ (2.81), GPe-M1 $\alpha$ (-2.62) & low $\beta$ (2.56) & broadband $\gamma$ (4.94), M1-PMC broadband $\gamma$ (2.66)		N/A
Early APA	Coherence	-241.470	1.07-1.16	GPi-GPe broadband $\gamma$ (-3.32), GPi-M1 $\theta$ (2.21), GPe-PMC broadband $\gamma$ (-2.08), M1-PMC broadband $\gamma$ (-4.46)		N/A
<b>Total APA</b>	<b>Coherence</b>	<b>-225.959</b>	<b>1.02-1.03</b>	<b>GPi-GPe broadband <math>\gamma</math> (-3.56), GPe-M1 <math>\alpha</math> (-3.35) &amp; low <math>\beta</math> (2.25)</b>		<b>N/A</b>



## Chapter 4. 180-degree turns (Aim 2)

### 4.1 Task rationale and hypothesis

Turning is another fundamental motor task in bipedal humans requiring adept postural control. Like gait initiation, turning requires a series of sequential, APA-like weight shifts as an individual rotates their body and alternates loading and unloading of the stepping limb to change direction<sup>40</sup>. Much biomechanical research has characterized turning dysfunction in people with PD (turns are often longer and variable, less stable, and consist of more steps compared to healthy controls) and connected these dysfunctions to the anticipatory phase of the turn<sup>41,115,116</sup>.

Unfortunately, postural instability which manifests as turning dysfunction often is a refractory symptom in PD, especially in the long-term. Likely contributing to this, it remains relatively unknown how various turning issues stem from the disease's effects on cortico-basal ganglia-thalamo-cortical motor circuits and neural modulation, as well as levodopa's effects, across phases of the turn. Similarly, no studies have assessed for potential correlations between this neural modulation and turning metrics reflecting quality, safety, and performance. This work hopes to also begin to improve the characterization of neural modulation during 180-degree turns in people with PD, with the promise of someday being incorporated into neuromodulatory interventions which target turning in this population.

The proposed project combines IMU data from sensors placed throughout the trunk and limbs in a standard configuration<sup>101</sup> with neural data collected while the subjects performed 180-degree turns during overground walking. The turns were performed under

both “LOW” and “ON” levodopa medication states, and both turn duration and the number of steps taken to complete the turn were assessed.

Our hypothesis for Aim 2 is that  $\beta$  power will decrease at pallidal locations prior to turn onset, with the opposite modulation demonstrated at cortical broadband  $\gamma$  frequencies coinciding with turning, suggesting engagement and execution of a turning motor program. It is also hypothesized that turn duration will be longer and feature more steps to complete the turn while in the “LOW” medication state, due to the prevalence of existing literature describing levodopa’s effects on turning performance.

## **4.2 180-degree turning methods**

### **4.2.1 180-degree turning task overview**

Subjects performed bouts of overground walking in a biomechanics laboratory for 200 steps at a time (step counts excluded turns) while alternating left and right-sided turn directions. Subjects were encouraged to turn 180-degrees when they wanted to, while allowing enough space to complete a “normal” turn (i.e. one that was not altered due to space constraints.) No external markers (tape on the floor, cues, etc.) were provided to the subject to facilitate as naturalistic an environment as possible. Overground walking bouts were performed under both medication states with exceptions as detailed below.

### **4.2.2 Biomechanical data collection and processing**

Xsens’ IMUs were used to characterize the turn itself (e.g. turn start and end, and inter-turn steps) and resulting turn metrics. All sensor data were initially processed using a low-pass, 4<sup>th</sup> order Butterworth filter with 1.5 Hz cutoff frequency as detailed in Aim 1.

To demarcate turn starts and ends, the pelvis (bony landmark: L5) IMU's angular velocity data from the z-axis (angVz) were plotted, converted to degrees from radians, and either a 30 or 38-degree-per-second threshold was used, depending on the subject's motor function and appropriateness of the data. Turns were marked using these thresholds so turn start was defined as occurring when the angVz data exceeded this threshold and turn end when the pelvis IMU data dropped below this threshold<sup>23,41</sup>. Turns where the threshold initially was exceeded then dropped before exceeding and remaining over the threshold were counted as beginning from the initial exceeding point, so long as it was within 0.5s of the subsequent exceeding point<sup>23,41</sup>. Similarly, turns were marked at the final point that the angVz dropped below the threshold of a turn, so long as the earlier points where the data dropped below the threshold were within 0.5s of each other (Figure 4.1).

To determine the gait events leading into and within the turn, the angVz in degrees recorded from the bilateral shanks was used as adapted from existing methods<sup>41</sup>. These sensors were located on the lateral, lower legs approximately midway between the lateral malleolus and lateral epicondyle of the tibia. Custom MATLAB scripts were authored by this author and Poojan Shukla, BS to identify peaks in the angVz data at the shanks surrounding and within the turns, which corresponded to midswing<sup>41</sup>. The number of peaks were summed for both shanks within the turn and used to calculate the "number of steps to turn" metric. Inter-turn shank angVz peaks were required to be at least 30% of the amplitude of the maximal shank angVz amplitude during the turn to be counted as a "step;" this rule was added following close video corroboration of each subject's turns with the biomechanical data.

Shank angVz data were also used to determine where the “turn preparation” epoch began prior to each turn. This epoch was consistently defined as beginning at the earlier of the pair of bilateral shank zero-crossings following the last midswing (corresponding to terminal contact) prior to turn start<sup>41</sup>. This point was chosen as it was consistently about 500ms prior to turn start (or more) across subjects and both medication states, creating a good proxy interval for which to assess potential preparation and planning neural modulation for the turn which was also consistent with previous literature regarding this timeframe.

#### **4.2.3 Task analysis**

Turns were processed initially by turn direction. Turns which were not 180-degrees (i.e. they proceeded to turn in a different direction), or the subject stopped mid-turn, were not included in analysis. Each turn was divided into two epochs: “turn preparation” and the turn itself (between turn start and turn end as described above). Absolute neural power was averaged within these two epochs as detailed for Aim 1, for each turn, at each recording contact under both medication states (Figure 4.1).

#### **4.2.4 Turn metrics**

To assess overall turn quality and performance as it may relate to neural modulation across the task, two metrics covering different aspects of the task were chosen for analysis. Turn metrics included: 1) Number of steps to complete the turn (explained in 4.2.2) and 2) Turn duration (calculated as the time difference between turn end and turn start).

### Turn Markings Schematic Example Subject Trial

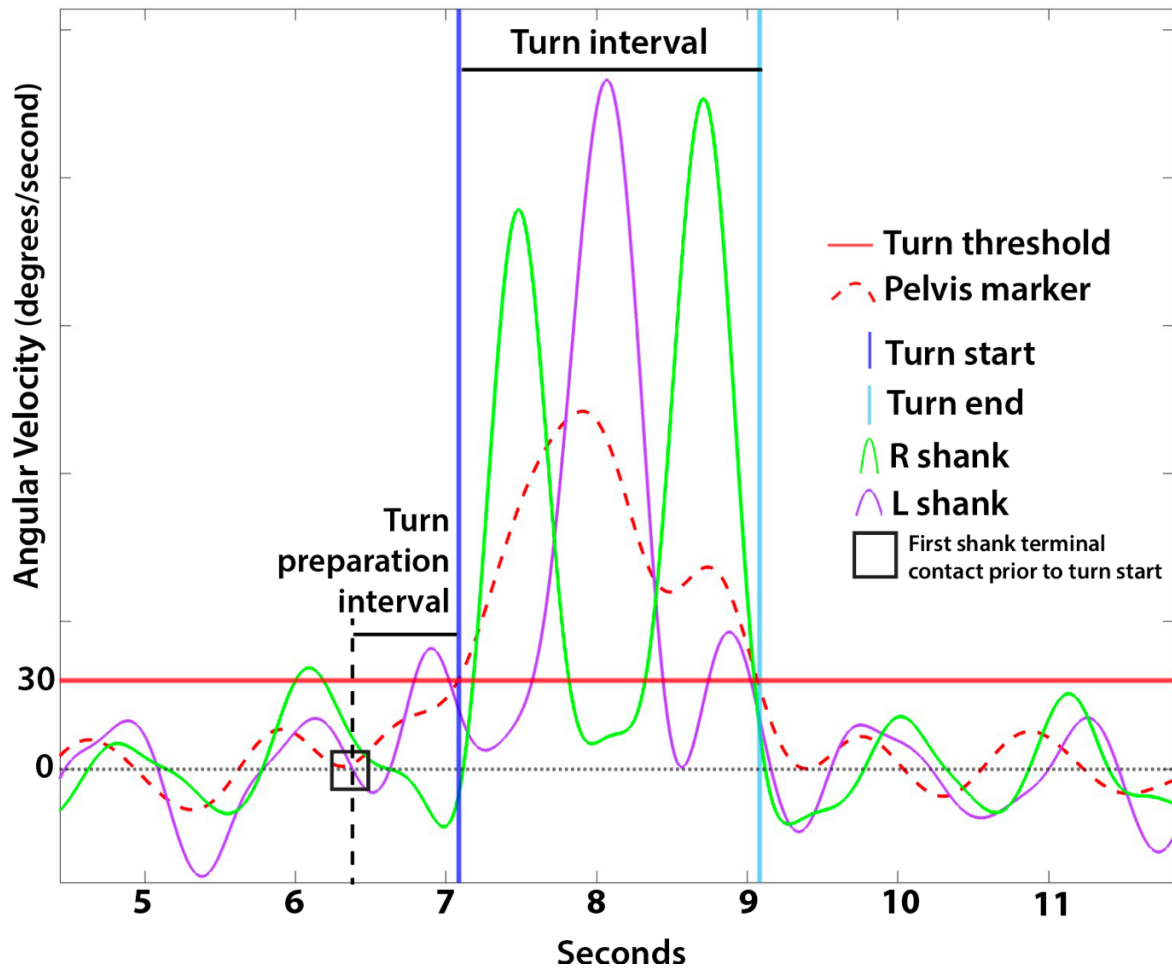


**Figure 4.1 Example turn marking schematic using body worn sensors**

Figure footnotes: Turn marking methods using shank and pelvis angular velocity data from the z-axis. Turns began and ended relative to a 30-degree per second threshold using the pelvis sensor. Average power data from the “spectrogram” function in MATLAB were compared both within the turn interval, as well as in the “turn preparation” epoch. The “turn preparation” epoch was formed by the first of the last pair of shank terminal contacts prior to the turn start (as recorded from the body worn sensors), spanning to the start of the turn.

#### 4.2.5 Data analysis

All neural data included in this analysis were recorded from the left hemisphere while “OFF” DBS. This was chosen to maintain generalizability of the results due to two subjects being implanted only on the L-side. While turns were initially intended to be analyzed separately in both directions, data were ultimately combined

within each patient across both turn directions, due to various limitations regarding data quality and a lack of subject data. To provide examples, Subject #1 did not have any R-sided turns data across either medication state, Subject #2 had no R-sided turns data while “LOW” medication, and Subject #4 displayed cardiac artifacts within the GPe recording contact during all turns while “ON” medication. The included trials, direction, and summary statistics of the turns data are in Table 4.1.

Turns were classified by the author into “few-step” or “multi-step” turns depending on how many steps were taken to turn and the overall strategy used with application of previous approaches in this population<sup>75</sup>. (Few-step turns featured < 3 steps, with multi-step turns using greater)<sup>75</sup>. Turns were classified asynchronously during data processing using Xsens’ video 3D reconstructions of IMU data, with corroboration using video camera footage where necessary.

**Artifact rejection:** Artifacts were handled as detailed above in the general methods section. Subject-specific median-based z-score thresholds were set under both medication states following visualization of the transformed and normalized neural data. Thresholds were initially set very high (so no data were blanked prior to visualization), then lowered as appropriate following consideration of the overall data and the waveform and regularity of potential artifacts. Subject #1’s set median-based z-scores were 50 while “LOW” medication and 110 “ON” medication, with 1 artifact identified using these thresholds. Subject #2’s median-based z-scores were 120 while “LOW” medication and 100 “ON” medication, with no artifacts identified. Subject #5’s median-based z-scores were 20 while “LOW” medication and 25 “ON” medication, with no artifacts identified. Subject #4’s median-based z-scores were 60 while “LOW” and “ON” medication; 2

artifacts were identified. However, this subject's GPe contacts also had cardiac-appearing artifacts throughout, so they were not included in further analyses due to the limited presumable consistency with data that did not have cardiac artifacts present. Subject #3's median-based z-score thresholds were 65 while "LOW" medication and 30 "ON" medication; no artifacts were identified. However, notch filtering was performed for all this subject's data, due to the presence again of continuous artifact-appearing bands across all time points. This filtering was performed for M1 (76 Hz) while "ON" medication and 74 Hz while "LOW" medication. All localized artifacts and artifact-labeled spectrograms were visualized to ensure appropriate inclusion and labeling.

#### **4.2.6 Statistical Analysis**

Subject data were collectively analyzed under each medication state across bilateral turn directions (rationale in 4.2.5). Due to the discrepancies between turn number, direction, and data quality and artifacts present for individual subjects, data were kept separate for analysis for each subject versus combining it together using LMMs such as in Aim 1. This was also done due to the highly individualized turning strategies exhibited by our subjects, with unknown relevance and/or generalizability relating to the underlying neurophysiology.

To better conceptualize these phenomena, average neural power prior to and during the turn were compared for each subject using non-parametric Wilcoxon rank sum tests with Benjamini-Hochberg corrections. Wilcoxon rank sum testing was also used to compare "LOW" vs "ON" medication state turn metrics data for each subject (Table 4.2).

To examine the relationships between neural data and turning metrics, multiple linear regressions were chosen for analysis. This method was chosen as turn duration is a continuous outcome, and “number of steps to turn” is a discrete variable with equal intervals between values<sup>117</sup>. Scatter plots were also used to visualize the data and appropriateness for this method. The “lm” function was used (base package in R/R Studio) with the “step” feature, allowing all neural predictors for a single epoch (i.e. “turn preparation” or “turn”) and medication state to be inputted with the final output a most-parsimonious model for both turn metrics. VIF values were assessed for all models following optimization to account for potential multicollinearity and Shapiro-Wilk’s testing was performed on all models to assess normality of the residuals, suggesting appropriateness of linear modeling. Models were produced for each subject separately using both “turn preparation” and “turn” epoch data for both turn metrics (4 total models for each subject), with the primary model described in the results section reflective of the “most” representative model to describe the turn metrics (assessed using the highest adjusted R<sup>2</sup> value).

## **4.3 180-degree turning results**

### **4.3.1 Turn metrics and levodopa’s effects**

Similar to Aim 1, Subjects #2 and #4 demonstrated much medication-related differences between the turning metrics of turn duration and number of steps to complete a turn. For both subjects, turn duration decreased while “ON” medication and each took less steps to complete the turn ( $p < 0.05$ ). Subject #3 also displayed significant medication-related effects for L-direction number of steps to complete the turn; the individual took a



greater number of steps while “ON” medication ( $p < 0.05$ ). Subjects #1 and #5 did not exhibit any medication-related differences in their turn metrics (Table 4.1). Additional figures characterizing each subjects’ turn types and neural power modulation are located in figures 4.2-4.6.

**Table 4.1 Summary of turn trials and turn metrics**

Table footnotes: Subject turns data for all included trials. \***bold** indicates a significant difference in the turn metric ( $p < 0.05$ ) between medication states using Wilcoxon rank sum testing. Abbreviations: L = left, R = right; s = seconds, avg = average, std = standard deviation. Subjects #2 and #4 had significant medication-related differences for various task metrics and turn directions, as well as Subject #3 for L-sided number of steps to complete the turn.

	Subject #1	Subject #2	Subject #3	Subject #4	Subject #5
Number of trials: L direction (LOW/ON medication)	25/28	16/15	12/11	15/15	13/14
Number of trials: R direction (LOW/ON medication)	-	-/15	11/10	10/13	13/13
Turn duration avg. (std): L direction (s) (LOW/ON medication)	2.23 (0.4)/ 2.15 (0.5)	<b>2.95 (0.3)/ 2.21 (0.2)*</b>	2.36 (0.4)/ 2.17 (0.2)	<b>3.85 (0.8)/ 2.83 (0.5)*</b>	2.49 (0.4)/ 2.37 (0.4)
Turn duration avg. (std): R direction (s) (LOW/ON medication)	-	-/2.04 (0.1)	1.87 (0.3)/ 2.06 (0.3)	3.82 (0.9)/ 3.29 (0.4)	2.43 (0.4)/ 2.86 (0.8)
Avg. (std) number of steps to turn: L direction (LOW/ON medication)	4 (0.6)/ 4 (0.8)	<b>4.8 (0.8)/ 3.6 (0.5)*</b>	<b>3.9 (0.5)/ 4.5 (0.5)*</b>	<b>6.9 (1.8)/ 4.1 (0.7)*</b>	5.5 (1.1)/ 5.4 (0.9)
Avg. (std) number of steps to turn: R direction (LOW/ON medication)	-	-/3.6 (0.5)	3.64 (0.5)/ 4 (0.5)	<b>6 (2.1)/ 4.4 (0.5)*</b>	5.2 (0.9)/ 6 (1.3)

### 4.3.2 Turning is highly individualized, with varying levodopa-responsiveness and neuromodulation at cortex and pallidum for $\beta$ and broadband $\gamma$ frequencies

#### Subject #1:

For Subject #1, all turns data were from turns performed in the L-direction under both medication states. The subject’s dominant turn type while “LOW” medication was “sideways,” classified as a few-step turn with  $\leq 3$  steps where a sideways step is taken

with one foot during the turn, and “forward” while “ON medication (a type of multistep turn with > 3 steps where the subject moves in a “U” shape).

Wilcoxon rank sum tests with Benjamini-Hochberg corrections reflected dynamic power modulation at various neural regions between the “turn preparation” and “turn” epochs while in the “LOW” medication state only. Pallidal high  $\beta$  and broadband  $\gamma$  power demonstrated significant decreases between the “turn preparation” and “turn” epochs (median turn preparation GPi high  $\beta$  power: 0.114 mV, turn power: 0.094 mV,  $p < 0.001$ ; median turn preparation GPi broadband  $\gamma$  power: 0.033 mV, turn power: 0.031 mV,  $p < 0.001$ .) At the cortex, M1 also demonstrated significant power differences between the epochs for high  $\beta$  and broadband  $\gamma$  frequencies. Broadband  $\gamma$  power again exhibited decreased power within the turn (median turn preparation power: 0.051 mV, turn power: 0.049;  $p < 0.05$ ), however M1 high  $\beta$  power increased during the turn compared to prior (median turn preparation power: 0.510 mV, turn power: 0.638 mV,  $p < 0.05$ ).

The multiple linear regression model which produced the highest adjusted  $R^2$  value ( $R^2 = 0.51$ ) used neural data from the “turn preparation” epoch to describe turn duration (Table 4.2). Here, the optimized model consisted of predictors including: levodopa (estimate = 0.21,  $t = 1.83$ ), GPi broadband  $\gamma$  power (estimate = -22.87  $t = -1.46$ ), and GPe  $\theta$  (estimate = -0.40,  $t = -1.43$ ),  $\alpha$  (estimate = -1.56,  $t = -3.4$ ), low  $\beta$  (estimate = 2.49,  $t = 2.5$ ), and broadband  $\gamma$  power (estimate = 21.08,  $t = 1.7$ ), as well as M1 low  $\beta$  (estimate = 0.37,  $t = 1.8$ ), low  $\gamma$  (estimate = 2.18,  $t = 2.9$ ), and broadband  $\gamma$  power (-21.40,  $t = -2.0$ ); significant PMC predictors included  $\theta$  (estimate = 0.23,  $t = 1.6$ ),  $\alpha$  (estimate = 0.37,  $t = 2.0$ ), and high  $\beta$  (estimate = 0.65,  $t = 1.4$ ), and low  $\gamma$  power (estimate = 1.94,  $t = 1.4$ ). This model’s VIF values ranged from 1.4-4.3, suggesting low to moderate multicollinearity

between predictors. The Shapiro-Wilk's test was used to assess normality of model residuals ( $p = 0.63$ ), suggesting model residuals were approximately normally distributed. Multiple linear regression models assembled from both epochs to describe the "number of steps to turn metric" had adjusted  $R^2$  values of 0.24-0.30, suggesting the models did not explain much of the variability present in this metric.

To summarize, this subject demonstrated marginal or worsening benefit of levodopa on turn metrics, with power significantly decreasing at pallidal and cortical areas for broadband  $\gamma$  power across the task (and pallidal  $\beta$ ). This modulation was likely most influential on turning quality and performance during the "turn preparation" window.

### **Subject #2:**

For Subject #2, combined turns data were analyzed for both medication states and turn directions besides R-sided "LOW" medication turns. The subject's dominant turn type while "LOW" medication was "backwards," a type of multistep turn with  $> 3$  steps where the subject takes a full step or weight shift backwards prior to advancing. While "ON" medication, the subject's dominant turn type was "sideways," as defined above.

Wilcoxon rank sum tests with corrections reflected much significant pallidal and cortical task-related power modulation under both medication states. Pallidal locations exhibited significant power decreases between epochs at broadband  $\gamma$  frequencies (GPi median turn preparation power: 0.034 mV, turn: 0.032 mV;  $p < 0.05$ ; GPe median broadband  $\gamma$  turn preparation power: 0.124 mV, turn: 0.118 mV,  $p < 0.05$ ); GPe high  $\beta$  power decreased, however ( $p < 0.05$ ). At M1, significant power differences were seen between epochs for  $\alpha$  (median turn preparation power: 0.650 mV, turn: 0.537 mV;  $p < 0.05$ )

and high  $\beta$  frequencies (median turn preparation power: 0.602 mV, turn: 0.724 mV;  $p < 0.05$ ). While “LOW” medication, PMC also exhibited broadband  $\gamma$  power increases around the turn (median turn preparation power: 0.092 mV, turn: 0.099 mV ( $p < 0.01$ )).

The multiple linear regression model which produced the highest adjusted  $R^2$  value used data from the turn itself (adjusted  $R^2 = 0.85$ ) to describe turn duration (Table 4.3). Here, the model consisted of predictors including levodopa (estimate = -1.038,  $t = 5.5$ ), GPi  $\theta$  (estimate = 1.06,  $t = 1.7$ ),  $\alpha$  (estimate = 2.29,  $t = 2.6$ ) and high  $\beta$  (estimate = -5.82,  $t = -2.7$ ) power, as well as GPe low  $\beta$  (estimate = -4.53,  $t = -2.4$ ) and broadband  $\gamma$  power (estimate = 33.81,  $t = 1.79$ ). Cortical model predictors included high  $\beta$  (estimate = -0.322,  $t = -1.3$ ), low  $\gamma$  (estimate = 1.67,  $t = 2.3$ ), and broadband  $\gamma$  (estimate = -14.30,  $t = -2.8$ ), as well as PMC  $\alpha$  (estimate = -0.26,  $t = -2.3$ ), low  $\beta$  (estimate = 0.42,  $t = 3.7$ ), high  $\beta$  (estimate = -0.19,  $t = -1.4$ ), low  $\gamma$  (estimate = 0.68,  $t = 2.1$ ), and broadband  $\gamma$  power (estimate = -8.51,  $t = -1.76$ ). VIF values ranged from 2.2-11.6 (this single outlier was for medication), suggesting significant multicollinearity for the predictor. The Shapiro-Wilk's test suggested model residuals were approximately normally distributed ( $p = 0.14$ ).

To summarize, this subject demonstrated significant changes among the turning metrics with levodopa, as turn duration was shorter and less steps were taken to turn. Neural modulation exhibited decreased pallidal broadband  $\gamma$  power, with increased cortical power at  $\beta$  and broadband  $\gamma$  across the task. This modulation appeared most influential on task quality and performance during the turn itself, compared to earlier.

### **Subject #3:**

For Subject #3, turns data included an approximately even split of L- and R-direction turns under both medication states. The subject demonstrated “wheeling” turns under both medication states, which is a multi-step turn via a series of steps around a central point. No significant turn-related power modulation was observed following significance testing for any contacts or frequency bands under either medication state.

The model with the overall highest adjusted  $R^2$  value (adjusted  $R^2$  value 0.54) for this subject described the “number of steps to turn” metric with data from the “turn preparation” epoch (Table 4.4). Predictors in this model included levodopa (estimate = 0.55,  $t = -3.9$ ), GPi high  $\beta$  (estimate = 9.60,  $t = 2.4$ ) and low  $\gamma$  power (estimate = 24.85,  $t = 3.1$ ), as well as GPe  $\theta$  (estimate = 2.47,  $t = 2.2$ ),  $\alpha$  (estimate = -2.67,  $t = -1.5$ ), low  $\gamma$  (estimate = -25.32,  $t = -4.3$ ), and broadband  $\gamma$  power (estimate = 58.34,  $t = 2.7$ ). Cortical predictors included M1  $\theta$  (estimate = 1.19,  $t = 2.3$ ) and  $\alpha$  power (estimate = -1.81,  $t = -2.3$ ), and PM  $\theta$  (estimate = 2.22,  $t = 3.1$ ),  $\alpha$  (estimate = -1.65,  $t = -1.8$ ), low  $\beta$  (estimate = 1.55,  $t = 1.3$ ), high  $\beta$  (estimate = -2.67,  $t = -1.4$ ) and broadband  $\gamma$  power (estimate = -84.3,  $t = -3.3$ ). VIF values ranged from 1.3-3.5, suggesting low-moderate multicollinearity, and the residuals were approximately normal, using Shapiro-Wilk’s testing ( $p = 0.79$ ).

To summarize, this subject did not demonstrate significant levodopa-related effects on turn type, as well as statistically significant neural modulation between the turn epochs. Model results suggest the “turn preparation epoch” was the most influential for affecting overall turn metrics.

#### **Subject #4:**

Subject #4's data exhibited widespread cardiac artifacts within the GPe channels. While template subtraction methods were used for further processing, it likely remains incompatible for combination alongside data without cardiac artifacts. Thus, Subject #4's data were not included in GPe power modulation calculations across the task, as well as in the multiple linear regression models. While "LOW" medication, the subject demonstrated "festination" turn types (a multi-step turn involving small, shuffling steps to complete the turn), and largely "forward" turns while "ON" medication, as defined above.

Dynamic, turn-related power modulation exhibited no significant differences across the turn for any contacts or canonical frequencies under either medication state. The models which produced the highest adjusted  $R^2$  values (adjusted  $R^2 = 0.45$  and  $0.49$ ) used data from the "turn preparation" and "turn" epochs, respectively, to describe the "number of steps to turn" metric (Table 3.5). However, Shapiro-Wilk's results for the "turn" epoch model's residuals suggest a non-normal distribution ( $p = 0.03$ ), suggesting the model violates assumptions of the distribution of data and presents questionable validity of representation; thus, the model from the "turn epoch" is summarized here as its residuals suggest normal distribution ( $p = 0.34$ ). In this model, significant predictors included levodopa (estimate =  $-2.59$ ,  $t = -6.0$ ), GPi low  $\gamma$  power (estimate =  $31.33$ ,  $t = 1.5$ ), and M1 high  $\beta$  power (estimate =  $6.34$ ,  $t = 2.0$ ). VIF values ranged from  $1.1$ - $1.4$ , suggesting very low multicollinearity.

To summarize, this subject demonstrated a change in turn type and various turn metrics with levodopa but no significant changes in power modulation across the task.

Model results from this individual suggest both turn epochs may have similar importance in affecting their turning metrics.

### **Subject #5:**

For Subject #5, combined turns data was present and analyzed for all medication states and turn directions. The subject's dominant turn type while "LOW" and "ON" medication was "forward," as described above.

Wilcoxon rank sum tests reflected minor dynamic task-related power modulation at M1 under both medication states. While "LOW" medication, broadband  $\gamma$  power decreased from turn preparation to the turn (median turn preparation power: 0.045 mV, turn: 0.043 mV;  $p < 0.05$ ), and  $\theta$  power increased while "ON" medication across those epochs (median turn preparation power: 0.385 mV, turn: 0.481 mV;  $p < 0.01$ ). No other frequencies or contacts exhibited significant task-related power modulation.

The multiple linear regression model which produced the highest adjusted  $R^2$  value ( $R^2 = 0.63$ ) used data from the turn itself to describe turn duration (Table 3.6). Significant predictors included levodopa (estimate = 0.19,  $t = 1.7$ ), GPi  $\theta$  (estimate = 3.34,  $t = 3.1$ ), high  $\beta$  (estimate = 5.01,  $t = 2.1$ ), and low  $\gamma$  power (estimate = -23.29,  $t = -2.3$ ), as well as GPe  $\theta$  (estimate = -6.57,  $t = -3.9$ ),  $\alpha$  (estimate = 5.32,  $t = 2.4$ ), high  $\beta$  (estimate = -21.28,  $t = -4.0$ ), low  $\gamma$  (estimate = -19.09,  $t = -1.9$ ) and broadband  $\gamma$  power (estimate = -109.50,  $t = -1.9$ ). Cortical predictors included M1 low  $\beta$  (estimate = 7.73,  $t = 5.7$ ) and broadband  $\gamma$  power (estimate = 73.85,  $t = 2.7$ ), as well as PMC  $\alpha$  (estimate = 1.44,  $t = 2.9$ ), low  $\beta$  (estimate = -2.62,  $t = -3.4$ ), high  $\beta$  (estimate = -5.18,  $t = -4.7$ ), and broadband  $\gamma$  power

(estimate = -118.65,  $t = -5.4$ ). VIF values ranged from 1.1-3.3, suggesting low-moderate multicollinearity, and model residuals were normally distributed ( $p = 0.44$ ).

To summarize, this subject demonstrated no change in turn type due to levodopa, with significant cortical broadband  $\gamma$  power decreases across the task. Model results suggest the turn may have provided greater influence on overall turning metrics.

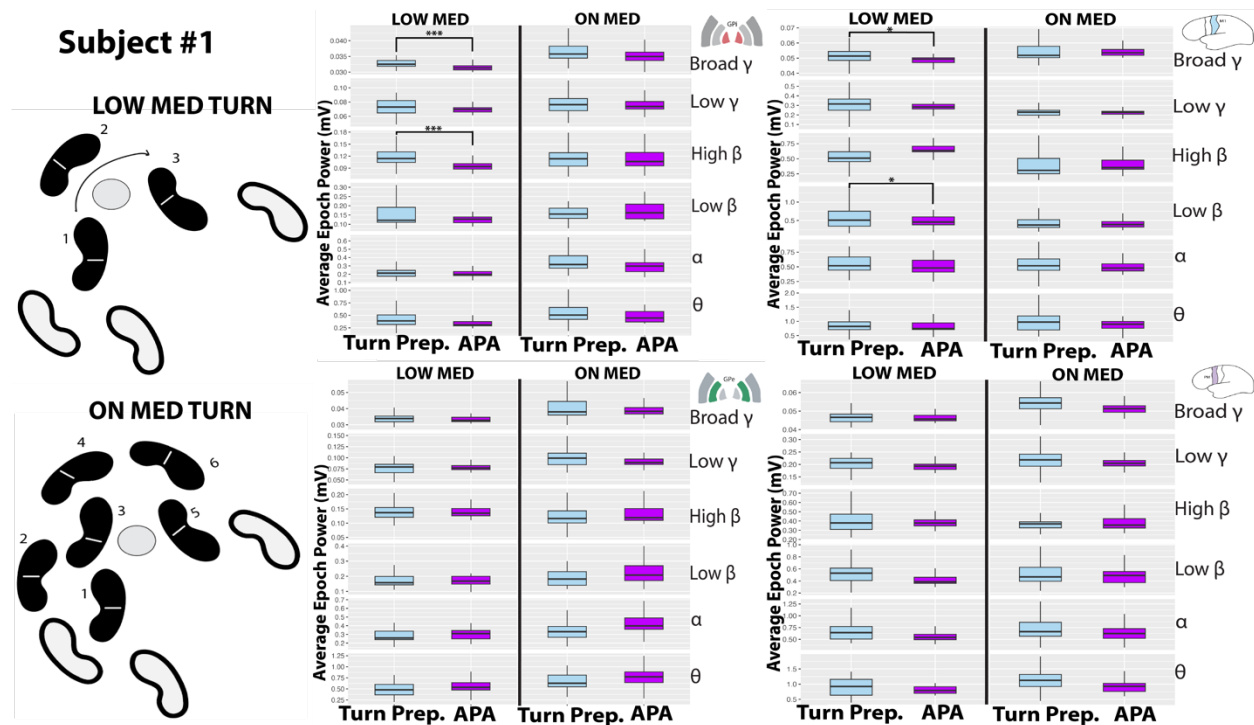


**Figure 4.2 Subject #1 turn types and power modulation**

Figure footnotes: Subject #1 dominant turn types under “LOW” and “ON” medication conditions and contact average power for both turn epochs using the “spectrogram” function. Boxplots created with upper whisker representing  $1.5 * \text{IQR}$  past the  $3^{\text{rd}}$  quartile and lower whisker representing  $1.5 * \text{IQR}$  below the  $1^{\text{st}}$  quartile. Significance between epochs is denoted with \*  $p < 0.05$ , \*\*  $p < 0.01$ , \*\*\*  $p < 0.001$  following Wilcoxon rank-sum testing and multiple corrections. Significant power modulation is exhibited at  $\beta$  and broadband  $\gamma$  frequencies while “LOW” medication at GPi and M1 for this individual. Abbreviations: GPi = globus pallidus internus, GPe = globus pallidus externus, M1 = primary motor cortex, PMC = premotor cortex;  $\theta$  = theta,  $\alpha$  = alpha,  $\beta$  = beta,  $\gamma$  = gamma.



**Table 4.2 Subject #1 optimized model comparisons**

Table footnotes: Subject #1 multiple linear regression model statistics reflecting data from each turn epoch and corresponding turn metrics. VIF = variance inflation factor. Model with the highest adjusted R<sup>2</sup> value used data from the “turn preparation” epoch to describe turn duration.

Turn Epoch	Metric Analyzed	Number of predictors in model (& if medication state is included)	Adjusted model R <sup>2</sup>	Normality of residuals using Shapiro-Wilk’s (p-value)	VIF range
Turn preparation	Turn duration	13 (Yes)	0.51	0.63	1.4-4.3
Turn preparation	Number of steps to turn	7 (No)	0.24	0.70	1.2-2.0
Turn	Turn duration	11 (Yes)	0.34	0.14	1.3-4.5
Turn	Number of steps to turn	6 (No)	0.30	0.65	1.3-2.1

**Subject #2**

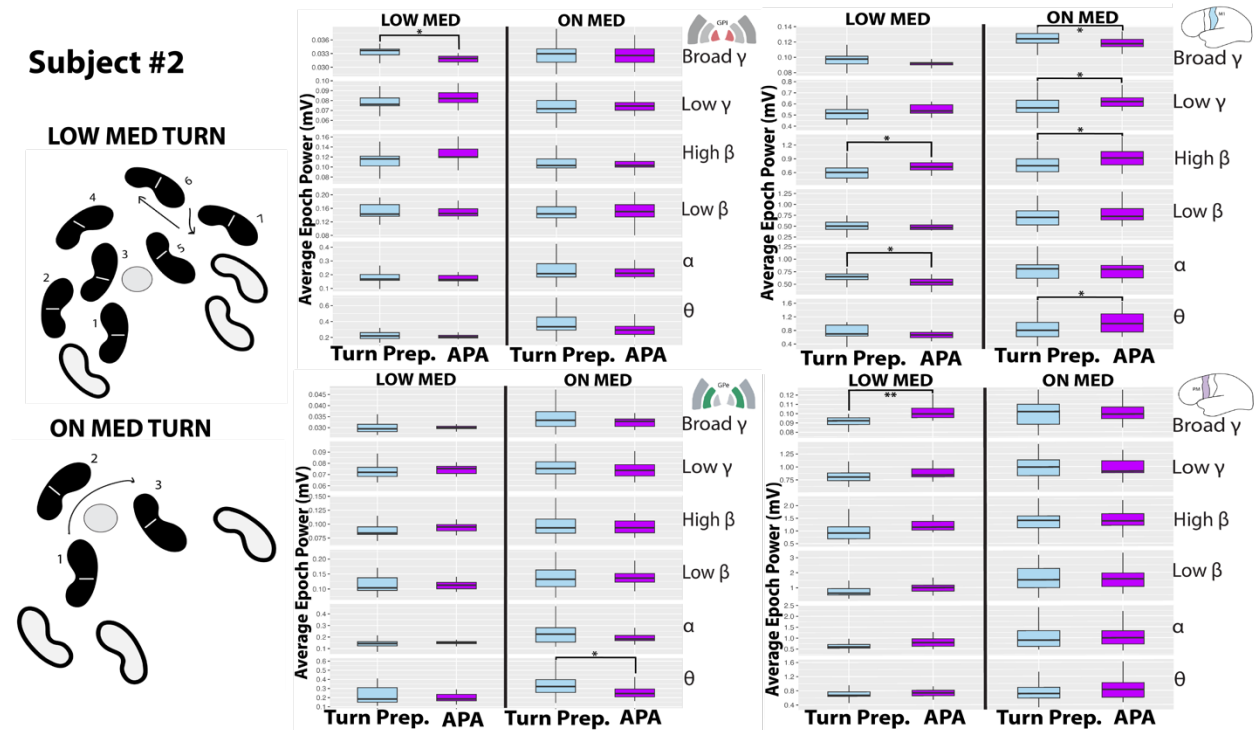


**Figure 4.3 Subject #2 turn types and power modulation**

Figure footnotes: Subject #2 dominant turn types under “LOW” and “ON” medication conditions and contact average power for both turn epochs using the “spectrogram” function. (Figure caption continued on the next page).

(Figure caption continued from the previous page). Boxplots created with upper whisker representing 1.5 \* the interquartile ratio (IQR) past the 3<sup>rd</sup> quartile and lower whisker representing 1.5 \* IQR below the 1<sup>st</sup> quartile. Significance between epochs is denoted with \*  $p < 0.05$  and \*\*  $p < 0.01$  following Wilcoxon rank-sum testing and multiple corrections. Significant power modulation is exhibited at GPi and PMC for broadband  $\gamma$  frequencies while “LOW” medication and at GPe for  $\theta$  while “ON” medication. M1 displayed significant modulation at  $\beta$  frequencies under both medication states and  $\gamma$  while “ON” medication only, as well as at additional lower frequencies. Abbreviations: GPi = globus pallidus internus, GPe = globus pallidus externus, M1= primary motor cortex, PMC = premotor cortex;  $\theta$  = theta,  $\alpha$  = alpha,  $\beta$  = beta,  $\gamma$  = gamma.

### Table 4.3 Subject #2 optimized model comparisons

Table footnotes: Subject #2 multiple linear regression model statistics reflecting data from each turn epoch and corresponding turn metrics. VIF = variance inflation factor. Model with the highest adjusted  $R^2$  value used data from the “turn” epoch to describe turn duration.

Turn Epoch	Metric Analyzed	Number of predictors in model (& if medication state is included)	Adjusted model $R^2$	Normality of residuals using Shapiro-Wilk's (p-value)	VIF range
Turn preparation	Turn duration	14 (Yes)	0.84	0.84	1.3-6.2
Turn preparation	Number of steps to turn	13 (No)	0.72	0.72	1.4-5.2
Turn	Turn duration	14 (Yes)	0.85	0.14	2.2-11.6
Turn	Number of steps to turn	11 (Yes)	0.68	0.53	1.5-7.8

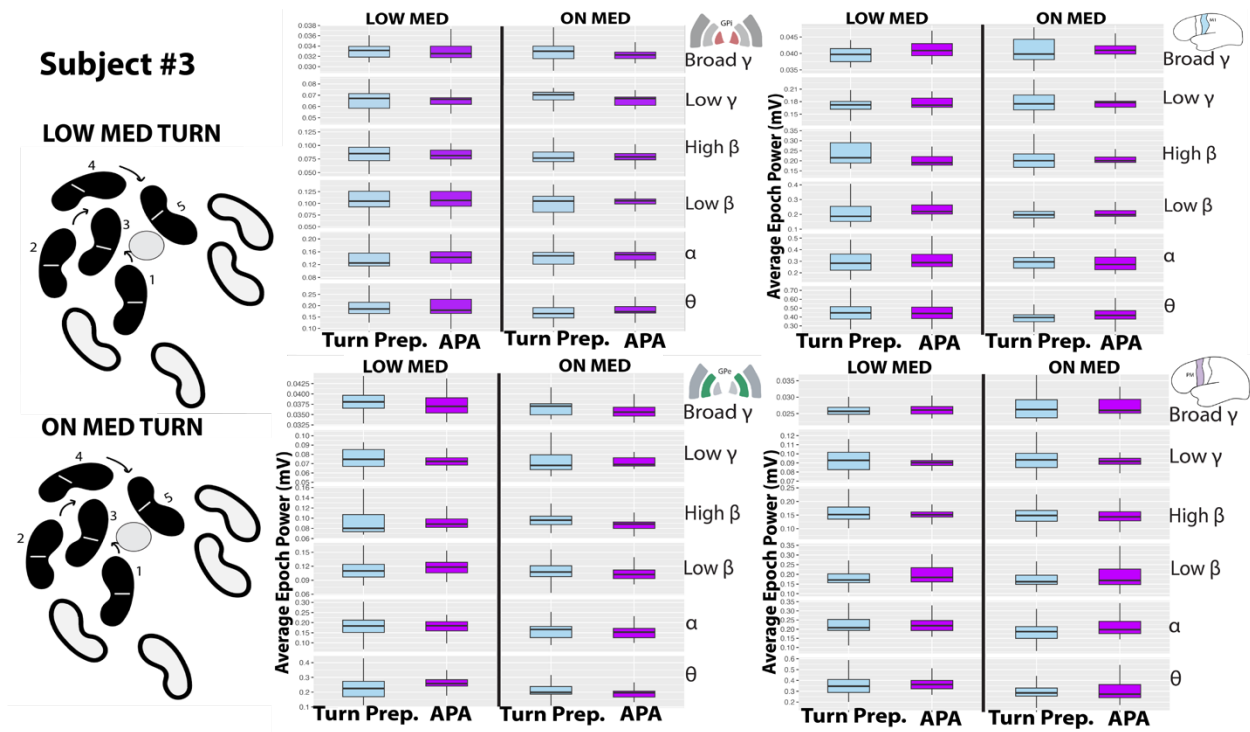


**Figure 4.4 Subject #3 turn types and power modulation**

Figure footnotes: Subject #3 dominant turn types under “LOW” and “ON” medication conditions and contact average power for both turn epochs using the “spectrogram” function. Boxplots created with upper whisker representing  $1.5 \times$  the interquartile ratio (IQR) past the 3<sup>rd</sup> quartile and lower whisker representing  $1.5 \times$  IQR below the 1<sup>st</sup> quartile. No significance was seen among power modulation between turn epochs. Abbreviations: GPi = globus pallidus internus, GPe = globus pallidus externus, M1= primary motor cortex, PMC = premotor cortex;  $\theta$  = theta,  $\alpha$  = alpha,  $\beta$  = beta,  $\gamma$  = gamma.

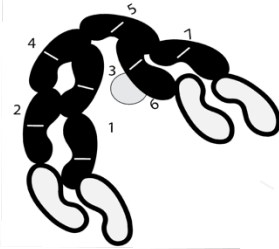
**Table 4.4 Subject #3 optimized model comparisons**

Table footnotes: Subject #3 multiple linear regression model statistics reflecting data from each turn epoch and corresponding turn metrics. VIF = variance inflation factor. Model with the highest adjusted R<sup>2</sup> value used data from the “turn preparation” epoch to describe “number of steps to turn”.

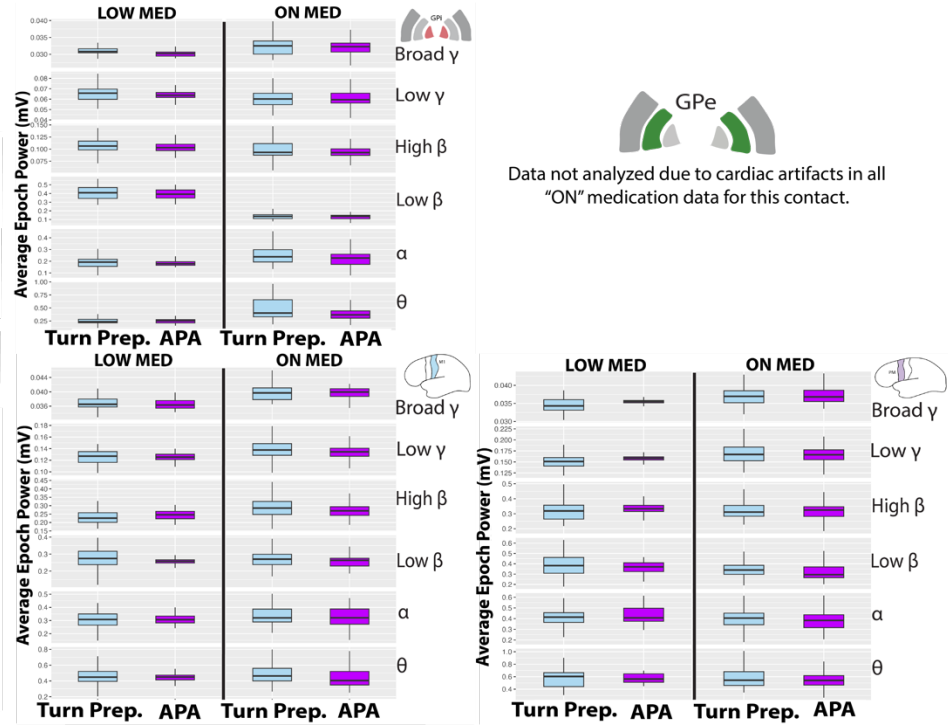
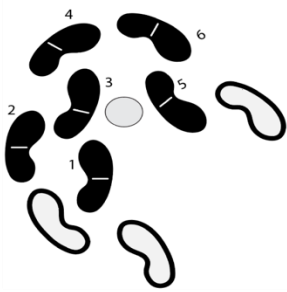
Turn Epoch	Metric Analyzed	Number of predictors in model (& if medication state is included)	Adjusted model R <sup>2</sup>	Normality of residuals using Shapiro-Wilk's (p-value)	VIF range
Turn preparation	Turn duration	13 (No)	0.50	0.48	1.3-2.6
Turn preparation	Number of steps to turn	14 (Yes)	0.54	0.79	1.4-3.5
Turn	Turn duration	7 (No)	0.09	0.05	1.1-2.2
Turn	Number of steps to turn	7 (Yes)	0.27	0.35	1.0-2.4

## Subject #4

### LOW MED TURN



### ON MED TURN



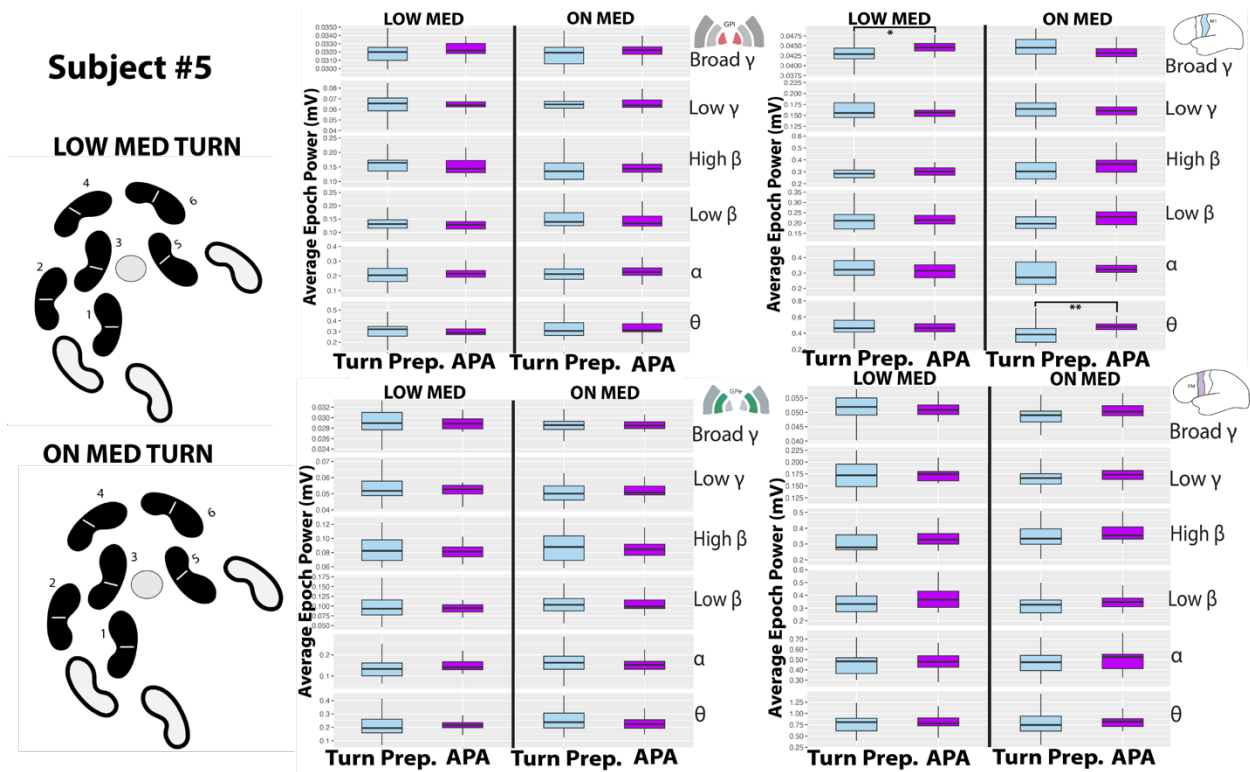
**Figure 4.5 Subject #4 turn types and power modulation**

Figure footnotes: Subject #4 dominant turn types under “LOW” and “ON” medication conditions and contact average power for both turn epochs using the “spectrogram” function. Boxplots created with upper whisker representing  $1.5 \times$  the interquartile ratio (IQR) past the 3<sup>rd</sup> quartile and lower whisker representing  $1.5 \times$  IQR below the 1<sup>st</sup> quartile. No significance was seen among power modulation between turn epochs. GPe data not shown due to the presence of widespread cardiac artifacts in this channel. Abbreviations: GPi = globus pallidus internus, GPe = globus pallidus externus, M1= primary motor cortex, PMC = premotor cortex;  $\theta$  = theta,  $\alpha$  = alpha,  $\beta$  = beta,  $\gamma$  = gamma.

**Table 4.5 Subject #4 optimized model comparisons**

Table footnotes: Subject #4 multiple linear regression model statistics reflecting data from each turn epoch and corresponding turn metrics. VIF = variance inflation factor. Model with the highest adjusted R<sup>2</sup> value used data from the “turn” epoch to describe “number of steps to turn,” however, the model shows a non-normal distribution of residuals, suggesting model representation may not be valid for this combination. Models were constructed without data from the GPe contacts; logic provided in methods section.

Turn Epoch	Metric Analyzed	Number of predictors in model (& if medication state is included)	Adjusted model R <sup>2</sup>	Normality of residuals using Shapiro-Wilk's (p-value)	VIF range
Turn preparation	Turn duration	4 (Yes)	0.28	0.59	1.1-1.5
Turn preparation	Number of steps to turn	3 (Yes)	0.45	0.34	1.1-1.4
Turn	Turn duration	3 (No)	0.37	0.36	1.2-1.3
Turn	Number of steps to turn	2 (No)	0.49	0.03	1.2



**Figure 4.6 Subject #5 turn types and power modulation**

Figure footnotes: Subject #5 dominant turn types under “LOW” and “ON” medication conditions and contact average power for both turn epochs using the “spectrogram” function. Boxplots created with upper whisker representing 1.5 \* the interquartile ratio (IQR) past the 3<sup>rd</sup> quartile and lower whisker representing 1.5 \* IQR below the 1<sup>st</sup> quartile. Task-related power modulation was seen for broadband  $\gamma$  power at M1 while “LOW” medication ( $p < 0.05$ ) and  $\theta$  while “ON” medication ( $p < 0.01$ ). Abbreviations: GPI = globus pallidus internus, GPe = globus pallidus externus, M1= primary motor cortex, PMC = premotor cortex;  $\theta$  = theta,  $\alpha$  = alpha,  $\beta$  = beta,  $\gamma$  = gamma.

### Table 4.6 Subject #5 optimized model comparisons

Table footnotes: Subject #5 multiple linear regression model statistics reflecting data from each turn epoch and corresponding turn metrics. VIF = variance inflation factor. Model with the highest adjusted R<sup>2</sup> value used data from the “turn” epoch to describe “turn duration”.

Turn Epoch	Metric Analyzed	Number of predictors in model (& if medication state is included)	Adjusted model R <sup>2</sup>	Normality of residuals using Shapiro-Wilk’s (p-value)	VIF range
Turn preparation	Turn duration	14 (Yes)	0.50	0.24	1.1-3.3
Turn preparation	Number of steps to turn	9 (No)	0.48	0.06	1.1-1.9
Turn	Turn duration	15 (Yes)	0.63	0.44	1.1-3.3
Turn	Number of steps to turn	13 (No)	0.55	0.13	1.2-2.4

### 4.4 180-degree turning discussion

While it is somewhat difficult to compare model results and quality aggregated between subjects due to the heterogeneity among turn types, medication state, turn direction, and individual subject disease progression and pathophysiology, general trends among the data offer potential insights into the underlying mechanisms of turn quality in people with PD.

Across subjects, levodopa medication did not have a consistent effect on turn classification and strategy. While Subjects #1, 2, and 4 demonstrated differences in dominant turn type, they did not necessarily become more “effective” while “ON” medication (specifically, for Subject #1, who turned using a greater number of steps to turn while in this state). Subjects #3 and 5 did not demonstrate appreciable changes in their dominant turn type between medication states. Subjects #2, 3, and 4 also exhibited significant medication-related changes in turn duration and “number of steps to turn,” with



the “LOW” medication state featuring longer turns and greater number of steps. This result was also reinforced by the varying effects medication had (positive or negative) on the turn metrics in individual subjects, as reflected in the multiple linear regressions. This result is relatively consistent with literature suggesting levodopa to change some metrics of turns in people with PD (i.e. turning distance), but not others (body rotation or turn strategy), while resulting in continued turning impairments compared to controls<sup>118</sup>. These results also reinforce the hypothesis that levodopa may have variable effects in individuals on postural control aspects, with some subjects experiencing improvement, worsening, or no change. This is again thought to be driven by the diversity of the circuits underlying various aspects of postural control and their relative dopaminergic responsiveness and/or state of dysfunction or disease progression in individual patients. Turning 180-degrees, like gait initiation, requires a series of weight shifts prior to, during, and after the turn, as well as repeated motor execution (stepping) for effective completion. Thus, again we posit that there are likely various implicated motor circuits relating to the stepping and postural control components of this task which are comprised of a diverse group of synapses in addition to levodopa.

Relating to dynamic power modulation across the task, Subjects #1, 2, and 5 demonstrated significant power changes between the “turn preparation” and “turn” epochs. Interestingly, Subjects #1 and 5 exhibited these significant differences in their neural modulation, however, similar changes were not reflected among their turn metrics. An interesting pattern shared among the subjects demonstrating significant power modulation is the finding that broadband  $\gamma$  power significantly decreased at the pallidum and cortex (for two subjects) between turn preparation and the turn. Complicating this

finding is the trend among subjects in model data where cortical broadband  $\gamma$  power was often a significant predictor and inversely related to the turning metrics (i.e. greater power was associated with faster turning featuring less steps). This finding suggests that perhaps individuals with PD may exhibit faulty gross “pro-kinetic” signaling during turning which could be mediating turning dysfunction in this population. Another explanation is perhaps broadband  $\gamma$  power modulation largely occurs prior to the turn, with other neural processes driving the turn besides cortical broadband  $\gamma$  signaling.

Similar to Aim 1, another explanation could also be that this modulation reflects a control mechanism where movement is tempered as one turns, to facilitate the processing and integration of much sensory information and limb coordination relative to other motor activities such as overground walking. Thus, this signal could act as a beneficial mechanism for subjects to maintain greater safety and stability during the turn, with greater broadband  $\gamma$  power associated with turns of increased vigor but less sensory integration (suggesting perhaps safety or stability concerns here).

Other power modulation commonalities were exhibited among subjects for  $\beta$  signaling. Of note, Subjects #2, 4, and 5 demonstrated little or no significant  $\beta$  modulation across the turn epochs, mostly overlapping with those subjects who did not demonstrate more “effective” turning with medication. These results suggest there may be a levodopa-mediated effect on  $\beta$  modulation in the circuits underlying turning, with breakdown occurring in this relationship for these individuals as seen in the resulting turn performance. When significant changes in  $\beta$  modulation were exhibited across the turn epochs, pallidal  $\beta$  power trends were mixed, with cortical  $\beta$  generally increasing. Model results were consistent with these trends, with Subjects #1 and #3 displaying shared

predictors from the “turn preparation” epoch of pallidal and cortical  $\beta$  signaling positively correlated to the turn metric (either by increasing turn duration or the number of steps to turn). These findings suggest  $\beta$  involvement in broadband  $\gamma$  signaling which may be facilitating a turn “scaling” or “quality” window prior to turning to maintain the “status-quo” and improve turn stability or integrate necessary motor programs.

In others,  $\beta$  modulation during the turn itself appeared more nuanced or complex, with fewer shared trends among  $\beta$  model predictors. For the number of steps to turn metric, Subjects #4 and 5 demonstrated a positive relationship with M1  $\beta$  power modulation, however, Subject #5 exhibited the opposite relationship for PMC  $\beta$  signaling. This was similar to Subject #2’s cortical data for the turn duration metric, with the  $\beta$  bands exhibiting opposing effects on the metric at M1 and PMC. These data support hypotheses that broadly, cortical  $\beta$  power has a role in pallidal disinhibition within movement circuits, however, these regions may serve different purposes in this mechanism during turning, with additional control mechanisms for turn performance mediated by sub- $\beta$  frequency bands, as well as modulatory windows. Consistent with these ideas, fMRI data from individuals with PD experiencing FoG displayed increased activation during turning at the caudate, with the opposite at PMC, suggesting dysfunction during turning is likely at least partially mediated by signaling breakdown at these areas<sup>119</sup>.

Regarding trends across model performance, subjects were relatively split between which metric was better represented (“number of steps to turn” vs turn duration), as well as which epoch surrounding the turn was most predictive of this metric. This suggests that perhaps the relationships between neural modulation and postural control strategy or the timing and planning associated with these may be highly individualized. It

can be reasoned that if an individual with PD has difficulty with postural control during turning (e.g. such as performing a substantial weight shift which considerably displaces the CoM to execute a pivot turn), they may have to continue to spend greater amounts of attentional or motor resources to modulate their turn strategy within the turn itself, compared to doing this with automatic, pre-planning. Conversely, if another individual perhaps assumes turning will be difficult or prepares to turn with less prominent weight shifts and smaller steps to facilitate minimal instability, they may have greater relative neural modulation in the preparation phase of the turn instead. This explanation is consistent with previous research suggesting the turn preparation phase of turning (particularly, the anticipatory step length) is correlated with overall turn performance (e.g., velocity and turning radius), suggesting an individual's pre-planning and biomechanical set-up are highly influential in the success of the turn, with breakdown leading to dysfunction<sup>116</sup>.

To summarize, the widespread variability present between subjects regarding turn performance metrics, turn strategy, dynamic neural modulation, and response to levodopa, suggest that continued focus robustly characterizing turn performance in this population is warranted for the development of effective therapeutics to treat problematic turning dysfunction. Furthermore, this variability and lack of consistent and clear-cut "improvements" between and within subjects in turn metrics also lends itself to continued attention spent towards developing individualized adaptive neuromodulatory interventions to treat turning dysfunction.

## Chapter 5. Discussion

### 5.1 Key findings

Overall, the results of this exploratory work validate continued research spent on the investigation of the neural circuitry underlying postural control and balance in PD, both to improve current therapeutic offerings and quality of life, as well as improve the understanding of these fundamental motor tasks. Collectively, these results suggest that: 1) Levodopa's effects on postural transitions are nuanced and therapy does not result in straightforward, uniform benefit (e.g., for amplitude and timing aspects) relating to performance; 2) Neural modulation within and across pallidal-cortical regions (particularly, pallidal-cortical coherence for gait initiation) appears highly influential on postural transition performance and quality in PD, and changes significantly between different postural transitions (i.e. from quiet standing to weight shift and stepping); and 3) The continued validation of  $\beta$  and broadband  $\gamma$  modulation's importance in motor circuits, including during postural transitions, perhaps by facilitating an appropriate "window" for sensory integration, motor planning, and/or scaling to occur prior to the postural transition. Data from the two postural transitions suggest further investigation is warranted for untangling these processes, especially due to the lack of consistent modulation (in direction, magnitude, and timing) for these frequencies across medication states and regions, and in association with metrics of task performance.

While there were some inconsistencies, particularly among pallidal broadband  $\gamma$  power modulation seen between the two tasks, analysis approaches and task components make it difficult to discern whether these differences relate to the diversity of circuitry underlying these tasks or more nuance in modulation than was captured. APAs

during gait initiation are likely more straightforward for analysis, by consisting of (typically) a single APA and step. Conversely, turns feature multiple steps and APAs which were included in the averaged neural power as analyzed in Aim 2. Furthermore, it is assumed that subjects may have to continue to modulate their performance during the turn due to the variety of turning options and components, whereas during gait initiation there is probably limited within-task modulation, due to its highly stereotyped nature and relatively short epoch durations.

The multitude of subject responses exhibited to levodopa and related neural modulation, regardless of the postural transition task, suggest that continued consideration of individualized neuromodulatory interventions is likely indicated following further research into characterizing these processes under greater task conditions and postural control domains. Intervention should be done carefully however, as it is apparent that the various spatiotemporal aspects of postural transition tasks performance, quality, and safety are likely interwoven, with overlapping neural circuitry. While treatment of one APA aspect may produce benefit, it may have resulting effects on other APA aspects which could have severely detrimental results for the safety or overall mobility of the individual.

## **5.2 Limitations of the study**

There are quite a few limitations in this project which warrant discussion. One primary limitation in this work is the relatively small sample size of the subjects due to the invasive and investigational nature of this work, which could limit the generalizability of these results. Similarly, a potential limitation may pertain to the number of trials included

for both aims, and whether there were enough repetitions to gain an accurate proxy for the neural state and motor performance of that individual while accounting for assumed neurophysiological variation. For example, a recent review and meta-analysis suggested that FoG during turning most often occurs at the end of a turn and at the inner leg of a turn cycle<sup>115</sup>, suggesting that data with these events may offer increased insight into the breakdown of neural circuitry while turning in this population. However, since the neural data during turning were collected from the L-hemisphere only, with bilateral turn directions, the data likely reflects both circuit breakdown as well as physiological modulation mediating turning in the aggregated data, with each's respective influence on the turning metrics recorded unknown.

Another important limitation includes differences in the time since diagnosis, LEDD dosing, and baseline motor function. Since there was much variation in this cohort's time since diagnosis (disease duration), it is highly probable that their symptoms of postural instability are quite variable, both in severity as well as in levodopa-responsiveness. For example, previous research has suggested levodopa to have some benefit on various turn metrics (i.e. turning duration), while worsening postural sway, however these changes were found in people with severe PD only<sup>74</sup>. Thus, grouped subject data likely reflects much variation in the responses to levodopa simply from this variance in symptom severity and disease progression. Other sources of assumed variation within the data include individual neurophysiology data (e.g., the electrode positioning within the target, impedance levels, and other sources of physiological and anatomical variance). These were all attempted to be accounted for by the handling of neural data (i.e. establishing subject-specific artifact removal thresholds, blanking of one subject's data where artifact

bands were present across all time points, keeping turns data analyzed individually), as well as including the potential random effects of subjects in the linear mixed models.

### **5.3 Future Directions**

There are many future directions from these data which should receive consideration. A logical next step is to analyze these data and postural tasks while “ON” DBS and medication, as this would be a required step for the potential integration and/or development of adaptive neuromodulatory interventions. Another necessary step would be to further characterize the neural modulation associated with postural transitions across a greater variety of PD presentations and disease durations to facilitate the development of neuromodulatory interventions able to effectively assist with postural instability and balance dysfunction in people with a range of functional statuses and levodopa-responsiveness.

Due to the nuanced and stepwise nature of the neural modulation seen across the tasks here, it also appears likely that much additional work will need to be done in characterizing these responses during a variety of different balance tasks across multiple balance domains, allowing for greater specificity in the identification of biomarkers for adaptive therapies which may be fruitful in improving postural instability under many task and environmental demands versus other gross motor activities likely associated with profound neural modulation such as walking. Lastly, these data would also benefit from the addition of neural data and task metrics recorded from individuals without a diagnosed movement disorder (such as is possible in those implanted with a DBS device for the treatment of non-motor diagnoses), allowing for investigation of neural modulation which is more physiological versus that which may represent circuit breakdown due to PD.



## References

1. Lo RY, Tanner CM, Albers KB, et al. Clinical features in early Parkinson disease and survival. *Arch Neurol*. Nov 2009;66(11):1353-8. doi:10.1001/archneurol.2009.221
2. Aleksovski D, Miljkovic D, Bravi D, Antonini A. Disease progression in Parkinson subtypes: the PPMI dataset. *Neurol Sci*. Nov 2018;39(11):1971-1976. doi:10.1007/s10072-018-3522-z
3. Hely MA, Morris JG, Reid WG, Trafficante R. Sydney Multicenter Study of Parkinson's disease: non-L-dopa-responsive problems dominate at 15 years. *Mov Disord*. Feb 2005;20(2):190-9. doi:10.1002/mds.20324
4. Rajput AH, Pahwa R, Pahwa P, Rajput A. Prognostic significance of the onset mode in parkinsonism. *Neurology*. Apr 1993;43(4):829-30. doi:10.1212/wnl.43.4.829
5. Bath JE, Wang DD. Unraveling the threads of stability: A review of the neurophysiology of postural control in Parkinson's disease. *Neurotherapeutics*. Apr 2024;21(3):e00354. doi:10.1016/j.neurot.2024.e00354
6. Jankovic J, McDermott M, Carter J, et al. Variable expression of Parkinson's disease: a base-line analysis of the DATATOP cohort. The Parkinson Study Group. *Neurology*. Oct 1990;40(10):1529-34. doi:10.1212/wnl.40.10.1529
7. Viseux FJF, Delval A, Defebvre L, Simoneau M. Postural instability in Parkinson's disease: Review and bottom-up rehabilitative approaches. *Neurophysiol Clin*. Nov 2020;50(6):479-487. doi:10.1016/j.neucli.2020.10.013
8. Mancini M, Rocchi L, Horak FB, Chiari L. Effects of Parkinson's disease and levodopa on functional limits of stability. *Clin Biomech (Bristol, Avon)*. May 2008;23(4):450-8. doi:10.1016/j.clinbiomech.2007.11.007

9. Horak FB, Nutt JG, Nashner LM. Postural inflexibility in parkinsonian subjects. *J Neurol Sci.* Aug 1992;111(1):46-58. doi:10.1016/0022-510x(92)90111-w
10. Crouse JJ, Phillips JR, Jahanshahi M, Moustafa AA. Postural instability and falls in Parkinson's disease. *Rev Neurosci.* Jul 1 2016;27(5):549-55. doi:10.1515/revneuro-2016-0002
11. Bekkers EMJ, Dijkstra BW, Heremans E, Verschueren SMP, Bloem BR, Nieuwboer A. Balancing between the two: Are freezing of gait and postural instability in Parkinson's disease connected? *Neurosci Biobehav Rev.* Nov 2018;94:113-125. doi:10.1016/j.neubiorev.2018.08.008
12. Muller M, Marusic U, van Emde Boas M, Weiss D, Bohnen NI. Treatment options for postural instability and gait difficulties in Parkinson's disease. *Expert Rev Neurother.* Dec 2019;19(12):1229-1251. doi:10.1080/14737175.2019.1656067
13. Gu Q, Huang P, Xuan M, et al. Greater loss of white matter integrity in postural instability and gait difficulty subtype of Parkinson's disease. *Can J Neurol Sci.* Nov 2014;41(6):763-8. doi:10.1017/cjn.2014.34
14. Herman T, Rosenberg-Katz K, Jacob Y, Giladi N, Hausdorff JM. Gray matter atrophy and freezing of gait in Parkinson's disease: Is the evidence black-on-white? *Mov Disord.* Jan 2014;29(1):134-9. doi:10.1002/mds.25697
15. Seuthe J, Heinzel A, Hulzinga F, et al. Towards a better understanding of anticipatory postural adjustments in people with Parkinson's disease. *PLoS One.* 2024;19(3):e0300465. doi:10.1371/journal.pone.0300465

16. Collomb-Clerc A, Welter ML. Effects of deep brain stimulation on balance and gait in patients with Parkinson's disease: A systematic neurophysiological review. *Neurophysiol Clin*. Nov 2015;45(4-5):371-88. doi:10.1016/j.neucli.2015.07.001
17. Hall LM, Brauer SG, Horak F, Hodges PW. The effect of Parkinson's disease and levodopa on adaptation of anticipatory postural adjustments. *Neuroscience*. Oct 10 2013;250:483-92. doi:10.1016/j.neuroscience.2013.07.006
18. Horak FB, Frank J, Nutt J. Effects of dopamine on postural control in parkinsonian subjects: scaling, set, and tone. *J Neurophysiol*. Jun 1996;75(6):2380-96. doi:10.1152/jn.1996.75.6.2380
19. Rocchi L, Carlson-Kuhta P, Chiari L, Burchiel KJ, Hogarth P, Horak FB. Effects of deep brain stimulation in the subthalamic nucleus or globus pallidus internus on step initiation in Parkinson disease: laboratory investigation. *J Neurosurg*. Dec 2012;117(6):1141-9. doi:10.3171/2012.8.JNS112006
20. Mancini M, Zampieri C, Carlson-Kuhta P, Chiari L, Horak FB. Anticipatory postural adjustments prior to step initiation are hypometric in untreated Parkinson's disease: an accelerometer-based approach. *Eur J Neurol*. Sep 2009;16(9):1028-34. doi:10.1111/j.1468-1331.2009.02641.x
21. Nutt JG, Bloem BR, Giladi N, Hallett M, Horak FB, Nieuwboer A. Freezing of gait: moving forward on a mysterious clinical phenomenon. *Lancet Neurol*. Aug 2011;10(8):734-44. doi:10.1016/S1474-4422(11)70143-0
22. Mancini M, Horak FB, Zampieri C, Carlson-Kuhta P, Nutt JG, Chiari L. Trunk accelerometry reveals postural instability in untreated Parkinson's disease. *Parkinsonism Relat Disord*. Aug 2011;17(7):557-62. doi:10.1016/j.parkreldis.2011.05.010

23. Mellone S, Mancini M, King LA, Horak FB, Chiari L. The quality of turning in Parkinson's disease: a compensatory strategy to prevent postural instability? *J Neuroeng Rehabil*. Apr 19 2016;13:39. doi:10.1186/s12984-016-0147-4
24. Mancini M, El-Gohary M, Pearson S, et al. Continuous monitoring of turning in Parkinson's disease: Rehabilitation potential. *NeuroRehabilitation*. 2015;37(1):3-10. doi:10.3233/NRE-151236
25. Bonora G, Mancini M, Carpinella I, Chiari L, Horak FB, Ferrarin M. Gait initiation is impaired in subjects with Parkinson's disease in the OFF state: Evidence from the analysis of the anticipatory postural adjustments through wearable inertial sensors. *Gait Posture*. Jan 2017;51:218-221. doi:10.1016/j.gaitpost.2016.10.017
26. Horak FB, Dimitrova D, Nutt JG. Direction-specific postural instability in subjects with Parkinson's disease. *Exp Neurol*. Jun 2005;193(2):504-21. doi:10.1016/j.expneurol.2004.12.008
27. Jacobs JV, Dimitrova DM, Nutt JG, Horak FB. Can stooped posture explain multidirectional postural instability in patients with Parkinson's disease? *Exp Brain Res*. Sep 2005;166(1):78-88. doi:10.1007/s00221-005-2346-2
28. King LA, St George RJ, Carlson-Kuhta P, Nutt JG, Horak FB. Preparation for compensatory forward stepping in Parkinson's disease. *Arch Phys Med Rehabil*. Sep 2010;91(9):1332-8. doi:10.1016/j.apmr.2010.05.013
29. St George RJ, Carlson-Kuhta P, King LA, Burchiel KJ, Horak FB. Compensatory stepping in Parkinson's disease is still a problem after deep brain stimulation randomized to STN or GPi. *J Neurophysiol*. Sep 2015;114(3):1417-23. doi:10.1152/jn.01052.2014

30. Visser M, Marinus J, Bloem BR, Kisjes H, van den Berg BM, van Hilten JJ. Clinical tests for the evaluation of postural instability in patients with parkinson's disease. *Arch Phys Med Rehabil*. Nov 2003;84(11):1669-74. doi:10.1053/s0003-9993(03)00348-4
31. Lizarraga KJ, Fasano A. Effects of Deep Brain Stimulation on Postural Trunk Deformities: A Systematic Review. *Mov Disord Clin Pract*. Nov 2019;6(8):627-638. doi:10.1002/mdc3.12829
32. Mancini M, Horak, F., Nutt., J. *Balance dysfunction in parkinson's disease: Basic mechanisms to clinical management*. Elsevier; 2019.
33. Kim SM, Kim DH, Yang Y, Ha SW, Han JH. Gait Patterns in Parkinson's Disease with or without Cognitive Impairment. *Dement Neurocogn Disord*. Jun 2018;17(2):57-65. doi:10.12779/dnd.2018.17.2.57
34. Schoneburg B, Mancini M, Horak F, Nutt JG. Framework for understanding balance dysfunction in Parkinson's disease. *Mov Disord*. Sep 15 2013;28(11):1474-82. doi:10.1002/mds.25613
35. Morris ME, Iansek R, Galna B. Gait festination and freezing in Parkinson's disease: pathogenesis and rehabilitation. *Mov Disord*. 2008;23 Suppl 2:S451-60. doi:10.1002/mds.21974
36. Winter DA. Human balance and posture control during standing and walking. *Gait & Posture*. 1995;3(4):193-214. doi:10.1016/0966-6362(96)82849-9
37. Lin CC, Creath RA, Rogers MW. Variability of Anticipatory Postural Adjustments During Gait Initiation in Individuals With Parkinson Disease. *J Neurol Phys Ther*. Jan 2016;40(1):40-6. doi:10.1097/NPT.0000000000000112

38. Lencioni T, Meloni M, Bowman T, et al. Events Detection of Anticipatory Postural Adjustments through a Wearable Accelerometer Sensor Is Comparable to That Measured by the Force Platform in Subjects with Parkinson's Disease. *Sensors*. Mar 30 2022;22(7)doi:10.3390/s22072668
39. Mancini M, Chiari L, Holmstrom L, Salarian A, Horak FB. Validity and reliability of an IMU-based method to detect APAs prior to gait initiation. *Gait Posture*. Jan 2016;43:125-31. doi:10.1016/j.gaitpost.2015.08.015
40. Xu D, Carlton LG, Rosengren KS. Anticipatory postural adjustments for altering direction during walking. *J Mot Behav*. Sep 2004;36(3):316-26. doi:10.3200/JMBR.36.3.316-326
41. El-Gohary M, Pearson S, McNames J, et al. Continuous monitoring of turning in patients with movement disability. *Sensors*. Dec 27 2013;14(1):356-69. doi:10.3390/s140100356
42. Krzyszton K, Stolarski J, Kochanowski J. Evaluation of Balance Disorders in Parkinson's Disease Using Simple Diagnostic Tests-Not So Simple to Choose. *Front Neurol*. 2018;9:932. doi:10.3389/fneur.2018.00932
43. Stebbins GT, Goetz CG, Burn DJ, Jankovic J, Khoo TK, Tilley BC. How to identify tremor dominant and postural instability/gait difficulty groups with the movement disorder society unified Parkinson's disease rating scale: comparison with the unified Parkinson's disease rating scale. *Mov Disord*. May 2013;28(5):668-70. doi:10.1002/mds.25383
44. Kotagal V. Is PIGD a legitimate motor subtype in Parkinson disease? *Ann Clin Transl Neurol*. Jun 2016;3(6):473-7. doi:10.1002/acn3.312

45. Takakusaki K. Functional Neuroanatomy for Posture and Gait Control. *J Mov Disord.* Jan 2017;10(1):1-17. doi:10.14802/jmd.16062
46. Takakusaki K, Takahashi M, Noguchi T, Chiba R. Neurophysiological mechanisms of gait disturbance in advanced Parkinson's disease patients. *Neurology and Clinical Neuroscience.* 2022;11(4):201-217. doi:10.1111/ncn3.12683
47. Visser JE, Bloem BR. Role of the basal ganglia in balance control. *Neural Plast.* 2005;12(2-3):161-74; discussion 263-72. doi:10.1155/NP.2005.161
48. Ivanenko Y, Gurfinkel VS. Human Postural Control. *Front Neurosci.* 2018;12:171. doi:10.3389/fnins.2018.00171
49. Ganguly J, Kulshreshtha D, Almotiri M, Jog M. Muscle Tone Physiology and Abnormalities. *Toxins (Basel).* Apr 16 2021;13(4)doi:10.3390/toxins13040282
50. Horak FB. Postural orientation and equilibrium: what do we need to know about neural control of balance to prevent falls? *Age Ageing.* Sep 2006;35 Suppl 2:ii7-ii11. doi:10.1093/ageing/afl077
51. Jacobs JV, Horak FB. Cortical control of postural responses. *J Neural Transm* 2007;114(10):1339-48. doi:10.1007/s00702-007-0657-0
52. Anson E, Bigelow RT, Studenski S, Deshpande N, Agrawal Y. Failure on the Foam Eyes Closed Test of Standing Balance Associated With Reduced Semicircular Canal Function in Healthy Older Adults. *Ear Hear.* Mar/Apr 2019;40(2):340-344. doi:10.1097/AUD.0000000000000619
53. Bosch TJ, Kammermeier S, Groth C, et al. Cortical and Cerebellar Oscillatory Responses to Postural Instability in Parkinson's Disease. *Front Neurol.* 2021;12:752271. doi:10.3389/fneur.2021.752271

54. Araujo-Silva F, Santinelli FB, Felipe ILL, et al. Temporal dynamics of cortical activity and postural control in response to the first levodopa dose of the day in people with Parkinson's disease. *Brain Res.* Jan 15 2022;1775:147727. doi:10.1016/j.brainres.2021.147727
55. Shoushtarian M, Murphy A, Iansek R. Examination of central gait control mechanisms in Parkinson's disease using movement-related potentials. *Mov Disord.* Nov 2011;26(13):2347-53. doi:10.1002/mds.23844
56. Mustile M, Kourtis D, Edwards MG, et al. Characterizing neurocognitive impairments in Parkinson's disease with mobile EEG when walking and stepping over obstacles. *Brain Commun.* 2023;5(6):fcad326. doi:10.1093/braincomms/fcad326
57. Payne AM, McKay JL, Ting LH. The cortical N1 response to balance perturbation is associated with balance and cognitive function in different ways between older adults with and without Parkinson's disease. *Cereb Cortex Commun.* 2022;3(3):tgac030. doi:10.1093/texcom/tgac030
58. Bekkers EMJ, Dijkstra BW, Dockx K, Heremans E, Verschueren SMP, Nieuwboer A. Clinical balance scales indicate worse postural control in people with Parkinson's disease who exhibit freezing of gait compared to those who do not: A meta-analysis. *Gait Posture.* Jul 2017;56:134-140. doi:10.1016/j.gaitpost.2017.05.009
59. Nieuwboer A, Giladi N. Characterizing freezing of gait in Parkinson's disease: models of an episodic phenomenon. *Mov Disord.* Sep 15 2013;28(11):1509-19. doi:10.1002/mds.25683



60. Chen CC, Yeh CH, Chan HL, et al. Subthalamic nucleus oscillations correlate with vulnerability to freezing of gait in patients with Parkinson's disease. *Neurobiol Dis*. Dec 2019;132:104605. doi:10.1016/j.nbd.2019.104605
61. Pozzi NG, Canessa A, Palmisano C, et al. Freezing of gait in Parkinson's disease reflects a sudden derangement of locomotor network dynamics. *Brain*. Jul 1 2019;142(7):2037-2050. doi:10.1093/brain/awz141
62. Nwogo RO, Kammermeier S, Singh A. Abnormal neural oscillations during gait and dual-task in Parkinson's disease. *Front Syst Neurosci*. 2022;16:995375. doi:10.3389/fnsys.2022.995375
63. Syrkin-Nikolau J, Koop MM, Prieto T, et al. Subthalamic neural entropy is a feature of freezing of gait in freely moving people with Parkinson's disease. *Neurobiol Dis*. Dec 2017;108:288-297. doi:10.1016/j.nbd.2017.09.002
64. Singh A, Plate A, Kammermeier S, Mehrkens JH, Ilmberger J, Bötzel K. Freezing of gait-related oscillatory activity in the human subthalamic nucleus. *Basal Ganglia*. 2013;3(1):25-32. doi:10.1016/j.baga.2012.10.002
65. Anidi C, O'Day JJ, Anderson RW, et al. Neuromodulation targets pathological not physiological beta bursts during gait in Parkinson's disease. *Neurobiol Dis*. Dec 2018;120:107-117. doi:10.1016/j.nbd.2018.09.004
66. de Lima-Pardini AC, Coelho DB, Nucci MP, et al. Brain networks associated with anticipatory postural adjustments in Parkinson's disease patients with freezing of gait. *Neuroimage Clin*. 2020;28:102461. doi:10.1016/j.nicl.2020.102461
67. Ragothaman A, Mancini M, Nutt JG, Fair DA, Miranda-Dominguez O, Horak FB. Resting state functional networks predict different aspects of postural control in

Parkinson's disease. *Gait Posture*. Sep 2022;97:122-129.  
doi:10.1016/j.gaitpost.2022.07.003

68. Stocchi F, Tagliati M, Olanow CW. Treatment of levodopa-induced motor complications. *Mov Disord*. 2008;23 Suppl 3:S599-612. doi:10.1002/mds.22052

69. Leodori G, Santilli M, Modugno N, et al. Postural Instability and Risk of Falls in Patients with Parkinson's Disease Treated with Deep Brain Stimulation: A Stabilometric Platform Study. *Brain Sci*. Aug 25 2023;13(9)doi:10.3390/brainsci13091243

70. Bloem BR, Beckley DJ, van Dijk JG, Zwiderman AH, Remler MP, Roos RA. Influence of dopaminergic medication on automatic postural responses and balance impairment in Parkinson's disease. *Mov Disord*. Sep 1996;11(5):509-21. doi:10.1002/mds.870110506

71. Nantel J, McDonald JC, Bronte-Stewart H. Effect of medication and STN-DBS on postural control in subjects with Parkinson's disease. *Parkinsonism Relat Disord*. Mar 2012;18(3):285-9. doi:10.1016/j.parkreldis.2011.11.005

72. Rocchi L, Chiari L, Horak FB. Effects of deep brain stimulation and levodopa on postural sway in Parkinson's disease. *J Neurol Neurosurg Psychiatry*. Sep 2002;73(3):267-74. doi:10.1136/jnnp.73.3.267

73. Leroy T, Baggen RJ, Lefebvre N, et al. Effects of Oral Levodopa on Balance in People with Idiopathic Parkinson's Disease. *J Parkinsons Dis*. 2023;13(1):3-23. doi:10.3233/JPD-223536

74. Curtze C, Nutt JG, Carlson-Kuhta P, Mancini M, Horak FB. Levodopa Is a Double-Edged Sword for Balance and Gait in People With Parkinson's Disease. *Mov Disord*. Sep 2015;30(10):1361-70. doi:10.1002/mds.26269

75. Adamson MB, Gilmore G, Stratton TW, Baktash N, Jog MS. Medication status and dual-tasking on turning strategies in Parkinson disease. *J Neurol Sci.* Jan 15 2019;396:206-212. doi:10.1016/j.jns.2018.11.028
76. Schaafsma JD, Balash Y, Gurevich T, Bartels AL, Hausdorff JM, Giladi N. Characterization of freezing of gait subtypes and the response of each to levodopa in Parkinson's disease. *Eur J Neurol.* Jul 2003;10(4):391-8. doi:10.1046/j.1468-1331.2003.00611.x
77. Osborne JA, Botkin R, Colon-Semenza C, et al. Physical Therapist Management of Parkinson Disease: A Clinical Practice Guideline From the American Physical Therapy Association. *Phys Ther.* Apr 1 2022;102(4)doi:10.1093/ptj/pzab302
78. Cossu G, Pau M. Subthalamic nucleus stimulation and gait in Parkinson's Disease: a not always fruitful relationship. *Gait Posture.* Feb 2017;52:205-210. doi:10.1016/j.gaitpost.2016.11.039
79. Potter-Nerger M, Volkman J. Deep brain stimulation for gait and postural symptoms in Parkinson's disease. *Mov Disord.* Sep 15 2013;28(11):1609-15. doi:10.1002/mds.25677
80. Ramirez-Zamora A, Ostrem JL. Globus Pallidus Interna or Subthalamic Nucleus Deep Brain Stimulation for Parkinson Disease: A Review. *JAMA Neurol.* Mar 1 2018;75(3):367-372. doi:10.1001/jamaneurol.2017.4321
81. Rocchi L, Chiari L, Cappello A, Gross A, Horak FB. Comparison between subthalamic nucleus and globus pallidus internus stimulation for postural performance in Parkinson's disease. *Gait Posture.* Apr 2004;19(2):172-83. doi:10.1016/S0966-6362(03)00059-6

82. Colnat-Coulbois S, Gauchard GC, Maillard L, et al. Bilateral subthalamic nucleus stimulation improves balance control in Parkinson's disease. *J Neurol Neurosurg Psychiatry*. Jun 2005;76(6):780-7. doi:10.1136/jnnp.2004.047829
83. Heß T, Oehlwein C, Milani TL. Anticipatory Postural Adjustments and Compensatory Postural Responses to Multidirectional Perturbations-Effects of Medication and Subthalamic Nucleus Deep Brain Stimulation in Parkinson's Disease. *Brain Sci*. Mar 7 2023;13(3)doi:10.3390/brainsci13030454
84. St George RJ, Carlson-Kuhta P, Burchiel KJ, Hogarth P, Frank N, Horak FB. The effects of subthalamic and pallidal deep brain stimulation on postural responses in patients with Parkinson disease. *J Neurosurg*. Jun 2012;116(6):1347-56. doi:10.3171/2012.2.JNS11847
85. Shin HW, Kim MS, Kim SR, Jeon SR, Chung SJ. Long-term Effects of Bilateral Subthalamic Deep Brain Stimulation on Postural Instability and Gait Difficulty in Patients with Parkinson's Disease. *J Mov Disord*. May 2020;13(2):127-132. doi:10.14802/jmd.19081
86. Shivitz N, Koop MM, Fahimi J, Heit G, Bronte-Stewart HM. Bilateral subthalamic nucleus deep brain stimulation improves certain aspects of postural control in Parkinson's disease, whereas medication does not. *Mov Disord*. Aug 2006;21(8):1088-97. doi:10.1002/mds.20905
87. Patel M, Nilsson MH, Rehncrona S, et al. Strategic alterations of posture are delayed in Parkinson's disease patients during deep brain stimulation. *Sci Rep*. Dec 7 2021;11(1):23550. doi:10.1038/s41598-021-02813-y

88. Limousin P, Foltynie T. Long-term outcomes of deep brain stimulation in Parkinson disease. *Nat Rev Neurol*. Apr 2019;15(4):234-242. doi:10.1038/s41582-019-0145-9
89. Castrioto A, Lozano AM, Poon YY, Lang AE, Fallis M, Moro E. Ten-year outcome of subthalamic stimulation in Parkinson disease: a blinded evaluation. *Arch Neurol*. Dec 2011;68(12):1550-6. doi:10.1001/archneurol.2011.182
90. Szlufik S, Kloda M, Friedman A, et al. The Neuromodulatory Impact of Subthalamic Nucleus Deep Brain Stimulation on Gait and Postural Instability in Parkinson's Disease Patients: A Prospective Case Controlled Study. *Front Neurol*. 2018;9:906. doi:10.3389/fneur.2018.00906
91. St George RJ, Nutt JG, Burchiel KJ, Horak FB. A meta-regression of the long-term effects of deep brain stimulation on balance and gait in PD. *Neurology*. Oct 5 2010;75(14):1292-9. doi:10.1212/WNL.0b013e3181f61329
92. Tsuboi T, Lemos Melo Lobo Jofili Lopes J, Moore K, et al. Long-term clinical outcomes of bilateral GPi deep brain stimulation in advanced Parkinson's disease: 5 years and beyond. *J Neurosurg*. Oct 9 2020:1-10. doi:10.3171/2020.6.JNS20617
93. Johnson L, Rodrigues J, Teo WP, et al. Interactive effects of GPi stimulation and levodopa on postural control in Parkinson's disease. *Gait Posture*. May 2015;41(4):929-34. doi:10.1016/j.gaitpost.2015.03.346
94. Sirica D, Hewitt AL, Tarolli CG, et al. Neurophysiological biomarkers to optimize deep brain stimulation in movement disorders. *Neurodegener Dis Manag*. Aug 2021;11(4):315-328. doi:10.2217/nmt-2021-0002

95. Gilron R, Little S, Perrone R, et al. Long-term wireless streaming of neural recordings for circuit discovery and adaptive stimulation in individuals with Parkinson's disease. *Nat Biotechnol.* Sep 2021;39(9):1078-1085. doi:10.1038/s41587-021-00897-5
96. Louie KH, Gilron R, Yaroshinsky MS, et al. Cortico-Subthalamic Field Potentials Support Classification of the Natural Gait Cycle in Parkinson's Disease and Reveal Individualized Spectral Signatures. *eNeuro.* Nov-Dec 2022;9(6)doi:10.1523/ENEURO.0325-22.2022
97. Olaru M, Cernera S, Hahn A, et al. Motor network gamma oscillations in chronic home recordings predict dyskinesia in Parkinson's disease. *Brain.* Jun 3 2024;147(6):2038-2052. doi:10.1093/brain/awae004
98. Sellers KK, Gilron R, Anso J, et al. Analysis-rcs-data: Open-Source Toolbox for the Ingestion, Time-Alignment, and Visualization of Sense and Stimulation Data From the Medtronic Summit RC+S System. *Front Hum Neurosci.* 2021;15:714256. doi:10.3389/fnhum.2021.714256
99. Riedel K, Sidorenko, A. Minimum Bias Multiple Taper Spectral Estimation. *IEEE Transactions on Signal Processing.* 1995;43(1):188–95. doi:10.1109/78.365298
100. McCoy EJ, Walden, A.T., Percival, D.B. Multitaper spectral estimation of power law processes. *IEEE Transactions on Signal Processing.* 1998;46(3):655 - 668. doi:10.1109/78.661333
101. Nijmeijer EM, Heuvelmans P, Bolt R, Gokeler A, Otten E, Benjaminse A. Concurrent validation of the Xsens IMU system of lower-body kinematics in jump-landing and change-of-direction tasks. *J Biomech.* Jun 2023;154:111637. doi:10.1016/j.jbiomech.2023.111637

102. Yiou E, Caderby T, Delafontaine A, Fourcade P, Honeine JL. Balance control during gait initiation: State-of-the-art and research perspectives. *World J Orthop*. Nov 18 2017;8(11):815-828. doi:10.5312/wjo.v8.i11.815
103. Uemura K, Yamada M, Nagai K, Ichihashi N. Older adults at high risk of falling need more time for anticipatory postural adjustment in the precrossing phase of obstacle negotiation. *J Gerontol A Biol Sci Med Sci*. Aug 2011;66(8):904-9. doi:10.1093/gerona/qlr081
104. Lu C, Amundsen Huffmaster SL, Tuite PJ, Vachon JM, MacKinnon CD. Effect of Cue Timing and Modality on Gait Initiation in Parkinson Disease With Freezing of Gait. *Arch Phys Med Rehabil*. Jul 2017;98(7):1291-1299 e1. doi:10.1016/j.apmr.2017.01.009
105. Mahmoodi R, Olyaei GR, Talebian S, Shadmehr A, Ghotbi N, Hadian MR. Postural Stability in Individuals with and without Sacroiliac Joint Dysfunction Before and After Pelvic Belt Application. *Archives of Neuroscience*. 2021;8(1)doi:10.5812/ans.106242
106. Bates D, Mächler M, Bolker B, Walker S. Fitting Linear Mixed-Effects Models Using lme4. *Journal of Statistical Software*. 2015;67(1)doi:10.18637/jss.v067.i01
107. Takakusaki K, Takahashi M, Obara K, Chiba R. Neural substrates involved in the control of posture. *Advanced Robotics*. 2016;31(1-2):2-23. doi:10.1080/01691864.2016.1252690
108. Litvak V, Eusebio A, Jha A, et al. Movement-related changes in local and long-range synchronization in Parkinson's disease revealed by simultaneous magnetoencephalography and intracranial recordings. *J Neurosci*. Aug 1 2012;32(31):10541-53. doi:10.1523/JNEUROSCI.0767-12.2012

109. Lofredi R, Neumann W., Bock, A., Horn A., Huebl J., Siegert S., Schneider G., Krauss, JK., Kühn AA. Dopamine-dependent scaling of subthalamic gamma bursts with movement velocity in patients with Parkinson's disease. *eLife*. 2018;7(7:e31895)doi:10.7554/eLife.31895.001
110. Crone NE, Miglioretti DL, Gordon B, et al. Functional mapping of human sensorimotor cortex with electrocorticographic spectral analysis. I. Alpha and beta event-related desynchronization. *Brain*. Dec 1998;121 ( Pt 12):2271-99. doi:10.1093/brain/121.12.2271
111. Delval A, Braquet A, Dirhoussi N, et al. Motor Preparation of Step Initiation: Error-related Cortical Oscillations. *Neuroscience*. Nov 21 2018;393:12-23. doi:10.1016/j.neuroscience.2018.09.046
112. Hell F, Plate A, Mehrkens JH, Botzel K. Subthalamic oscillatory activity and connectivity during gait in Parkinson's disease. *Neuroimage Clin*. 2018;19:396-405. doi:10.1016/j.nicl.2018.05.001
113. Asher EE, Plotnik M, Gunther M, et al. Connectivity of EEG synchronization networks increases for Parkinson's disease patients with freezing of gait. *Commun Biol*. Aug 30 2021;4(1):1017. doi:10.1038/s42003-021-02544-w
114. Burleigh-Jacobs A, Horak FB, Nutt JG, Obeso JA. Step initiation in Parkinson's disease: influence of levodopa and external sensory triggers. *Mov Disord*. Mar 1997;12(2):206-15. doi:10.1002/mds.870120211
115. Spildooren J, Vinken C, Van Baekel L, Nieuwboer A. Turning problems and freezing of gait in Parkinson's disease: a systematic review and meta-analysis. *Disabil Rehabil*. Dec 2019;41(25):2994-3004. doi:10.1080/09638288.2018.1483429



116. Miri AL, Laskovski L, Bueno MEB, Rodrigues DC, Moura FA, Smaili SM. A biomechanical analysis of turning during gait in individuals with different subtypes of Parkinson's disease. *Clin Biomech (Bristol, Avon)*. Feb 2024;112:106166. doi:10.1016/j.clinbiomech.2023.106166
117. Jozová. S, Nagy, I. Use of Linear Regression to Discrete Data. presented at: 2021 Smart City Symposium Prague; 2021;
118. Conradsson D, Paquette C, Lökk J, Franzen E. Pre- and unplanned walking turns in Parkinson's disease - Effects of dopaminergic medication. *Neuroscience*. Jan 26 2017;341:18-26. doi:10.1016/j.neuroscience.2016.11.016
119. Gilat M, Shine JM, Walton CC, O'Callaghan C, Hall JM, Lewis SJG. Brain activation underlying turning in Parkinson's disease patients with and without freezing of gait: a virtual reality fMRI study. *NPJ Parkinsons Dis*. 2015;1:15020. doi:10.1038/npjparkd.2015.20

## Publishing Agreement

It is the policy of the University to encourage open access and broad distribution of all theses, dissertations, and manuscripts. The Graduate Division will facilitate the distribution of UCSF theses, dissertations, and manuscripts to the UCSF Library for open access and distribution. UCSF will make such theses, dissertations, and manuscripts accessible to the public and will take reasonable steps to preserve these works in perpetuity.

I hereby grant the non-exclusive, perpetual right to The Regents of the University of California to reproduce, publicly display, distribute, preserve, and publish copies of my thesis, dissertation, or manuscript in any form or media, now existing or later derived, including access online for teaching, research, and public service purposes.

DocuSigned by:

*Jessica Bath*

987983955023496...

\_\_\_\_\_  
Author Signature

7/14/2024

\_\_\_\_\_  
Date